



FACULTY OF SCIENCE

Department of Biochemistry, Physiology and Microbiology
Laboratory for Protein Biochemistry and Biomolecular Engineering

Towards unveiling the Photoactive Yellow Proteins: characterization of a halophilic member and a proteomic approach to study light responses

Samy Memmi

Thesis submitted to fulfill the requirements for the degree of 'Doctor in Biochemistry'

May 2008

Promotor: Prof. Dr. Jozef Van Beeumen

Co-promotor: Prof. Dr. Bart Devreese

Table of contents

List of publications	i
List of abbreviations	ii
Abstract	iv
Chapter one	
1 Principles in photobiology	1
1.1 Introduction	1
1.2 The nature of light	1
1.3 Fundamentals in protein photochemistry	3
1.4 References	3
Chapter two	
2 Biological photosensors	4
2.1 Light as a source of energy	4
2.2 Light as a source of information	5
2.2.1 Red-/green-light photoperception	7
2.2.1.1 Sensory rhodopsins	7
2.2.1.2 (Bacterio)phytochromes	9
2.2.2 Blue-light sensing	11
2.2.2.1 Cryptochromes	11
2.2.2.2 LOV proteins	12
2.2.2.3 BLUF domain proteins	14
2.3 References	16
Chapter three	
3 Photoactive Yellow Proteins	22

3.1	History	22
3.2	Photochemical reactions	23
3.3	PYP properties	26
3.3.1	Structural features	26
3.3.2	Mutational analysis	28
3.4	Phylogenetic distribution	33
3.5	Biosynthesis	38
3.6	<i>Pyp</i> genes as molecular scouts in search of potential TAL biocatalysts?	40
3.7	Genetic context	43
3.7.1	<i>Rhodobacter</i> gene context	44
3.8	References	46

Chapter four

4	Photoactive Yellow Protein from the halophilic bacterium <i>Salinibacter ruber</i>	53
---	---	----

Chapter five

5	PYP-phytochrome-related proteins	77
5.1	Introduction	77
5.2	Properties	78
5.3	Function	81
5.4	References	84

Chapter six

6	A proteomic study of Ppr-mediated photoresponses in <i>Rhodospirillum centenum</i> reveals a role as regulator of polyketide synthesis	86
---	--	----

Abstracts of other publications	111
Summary (Dutch)	114
Dankwoord	117

List of publications

Memmi, S.; Kyndt, J.A.; Meyer, T.E.; Devreese, B.; Cusanovich, M.; Van Beeumen, J. (2008) Photoactive Yellow Protein from the halophilic bacterium *Salinibacter ruber*. *Biochemistry* 47, 2014 - 2024.

Cardol, P.; Boutaffala, L.; **Memmi, S.;** Devreese, B.; Matagne, R.F.; Remacle, C. (2008) In *Chlamydomonas*, the loss of ND5 subunit prevents the assembly of whole mitochondrial complex I and leads to the formation of a low-abundant 700 kD subcomplex. *Biochimica et Biophysica Acta – Bioenergetics* 1777, 388-96

Scharlaken, B.; De Graaf, D.C.; **Memmi, S.;** Devreese, B.; Van Beeumen, J.; Jacobs, F.J. (2007) Differential protein expression in the honey bee head after a bacterial challenge. *Archives of Insect Biochemistry and Physiology* 65, 223-37.

Kyndt, J.A.; Savvides, S.N.; **Memmi, S.;** Koh, M.; Fitch, J.C.; Meyer, T.E.; Heyn, M.P.; Van Beeumen, J.; Cusanovich, M.A. (2007) Structural role of tyrosine 98 in Photoactive Yellow Protein: effects on fluorescence, gateway, and photocycle recovery. *Biochemistry* 46, 95-105.

Samyn, B.; Sergeant, K.; **Memmi, S.;** Debysen, G.; Devreese, B.; Van Beeumen, J. (2006) MALDI-TOF/TOF *de novo* sequence analysis of 2D-PAGE-separated proteins from *Halorhodospira halophila*, a bacterium with unsequenced genome. *Electrophoresis* 27, 2702-11.

Abbreviations

2-DE	Two-dimensional electrophoresis
ATP	Adenosine triphosphate
ACN	Acetonitril
Bph	Bacteriophytochrome
BLUF	Blue-light sensing using FAD
BR	Bacteriorhodopsin
BV	Biliverdin
CA	Cinnamic acid
CBB	Coomassie brilliant blue
CHS	Chalcone synthase
CoA	Co-enzyme A
CRY	Cryptochrome
CTAS	<i>p</i> -coumaroyltriatic acid synthase
CV	Coefficient of variation
dH ₂ O	Distilled H ₂ O
DTT	Dithiothreitol
ESI	Electrospray ionization
FAD	Flavin adenine dinucleotide
FMN	Flavin mononucleotide
GAF	Domain homologues originally found in cGMP-binding phosphodiesterase, <i>Anabaena</i> adenylate cyclase, and <i>E. coli</i> FhlA
GGDEF/EAL	Signature amino acid sequence for phosphodiesterase and/or diguanylate cyclase activity
HAL	Histidine ammonia-lyase
HemO	Heme oxygenase
HK	Histidine kinase
IPG	Immobilized pH gradient
IR	Infrared
LOV	Protein domain involved in sensing light-oxygen-voltage
MALDI	Matrix-assisted laser desorption/ionization
MCP	Methyl-accepting chemotaxis protein
MIO	3,5-dihydro-5-methylidene-4H-imidazol-4-one
nLC	Nano liquid chromatography
PΦB	Phytochromobilin
PAL	Phenylalanine ammonia-lyase
PAC	Photoactivated adenylyl cyclase
PAS	Acronym based upon periodic clock protein, aryl hydrocarbon receptor nuclear translocator and, single minded protein
PAGE	Polyacrylamide gel electrophoresis
PCB	Phycocyanobilin
pCL	<i>p</i> -coumaryl CoA-ligase
pHCA	<i>p</i> -hydroxycinnamic acid
PHB	Poly-β-hydroxybutyrate
PHY	Phytochrome
PKS	Polyketide synthase
Ppr	PYP-phytochrome-related
Ppd	PYP-bacteriophytochrome-diguanylate cyclase/phosphodiesterase
PYP	Photoactive yellow protein

Q	Quadrupole
SD	Standard deviation
SDS	Sodium dodecyl sulfate
SR	Sensory rhodopsin
STS	Stilbene synthase
TAL	Tyrosine ammonia-lyase
TEMED	Tetramethylethylenediamine
THN	1,3,6,8-tetrahydroxynaphtalene
TOF	Time-of-flight
UV	Ultraviolet
WT	Wild-type
XR	Xanthorhodopsin

Abstract

The response of living matter to the environmental light climate requires the conversion of light energy into biological signals, and is studied through the science of photobiology, for which some related terms and principles are briefly described in [Chapter one](#). Light can be used as a source of free energy to facilitate a process that otherwise would be thermodynamically unfeasible, such as photosynthesis. Alternatively, light can be used as a source of information allowing organisms to optimally exploit the existing light conditions for growth and development and/or to permit protection from light damage. The molecular basis is provided by a number of specialized photoreceptor proteins which interact with a specific chromophore to initiate a photochemical reaction or signaling event. As described in [Chapter two](#), nature has developed several types of light-sensitive photoreceptors, functioning in energy conversion or signaling, and varying widely in their chromophore composition, photochemistry and photocycle kinetics. Among them, the family of blue-light absorbing [Photoactive Yellow Proteins](#) (PYPs) has become an attractive model system to study the molecular events related to light perception. PYP is a small, water-soluble and cytoplasmic protein that covalently binds a *p*-hydroxycinnamic acid chromophore, which is fine-tuned for efficient light absorption and initiates a photocycle by a *trans* to *cis* isomerization ([Chapter three](#)). PYPs were originally discovered in a number of halophilic proteobacteria, but the *pyp* gene distribution actually spans a wider spectrum of both phototrophic as well as non-photosynthetic bacteria. The very first representative of the latter class has been characterized from *Salinibacter ruber*, as described in [Chapter four](#) in which we demonstrated the first example of a truly halophilic PYP that is stabilized by ionic strength. Furthermore, illumination with blue light ignites a cyclic series of dark reactions including the typical intermediates I₁, I₂ and I₂'₂, which suggests that it is functional although the recovery to the dark-adapted state was observed to be the slowest of any PYP. More interestingly, PYP from *Salinibacter ruber* contains an unusual 31-residue N-terminal extension which appears to be disordered relative to the remainder of the protein and which induces a unique dimerization of the photosensor with no precedents described before with any of the other published PYPs. Truncation of the N-terminal extension does not seem to influence the photochemical properties, and no structural motif or functional relevance towards signaling could thus far be established.

PYP can also be part of multi-domain proteins where it forms the N-terminal domain that is followed by a bacteriophytochrome (Bph) central domain and by a C-terminal enzymatic output domain related to histidine kinases or diguanylate cyclases. [Chapter five](#) describes such a

hybrid photosensor kinase from the purple phototroph *Rhodospirillum rubrum*, called Ppr (PYP-phytochrome-related). Here, the PYP domain acts as a blue-light switch reversing the effects of red light on the Bph domain, resulting in a light-regulated histidine kinase activity of Ppr and the concomitant light-regulated phosphorylation of a yet unknown response regulator. Its environmental significance was explored through comparative 2-DE, as presented in Chapter six in which we analyzed the protein expression changes in wild-type *Rb. rubrum* relative to a *ppr*-disrupted strain in response to actinic blue- (390 - 510 nm) and red- (>600 nm) light conditions during photosynthetic growth. Differentially regulated proteins provided indications that the Ppr-mediated photoresponse involves an increased acetyl-CoA pool causing a shift in the lipid metabolism in favor of polyketide biosynthesis to adapt the cell against the exposed light conditions. However, the nature of this adaptation remains unclear and requires further study.

Chapter one

1 Principles in photobiology

1.1 Introduction

Life on earth has developed appropriate responses to the existing light conditions for its competition for survival. The effects of light on living organisms and biological processes is studied through the science of photobiology, which is currently divided into 5 subspecialty areas by the American Society for Photobiology [1], including (i) photochemistry, photophysics and phototechnology, (ii) photosensory and circadian biology, (iii) photosynthesis, bio- and chemiluminescence, (iv) photomedicine and (v) environmental photobiology and ultraviolet (UV) radiation effects. Individual light-mediated processes are examined starting from the molecular basis of light perception (photochemistry) to the final effects on the whole organism in the ecosystem (environmental photobiology). How radiation is absorbed, what wavelengths are utilized, and what action or effect the radiation elicits in biological systems are questions of primary concern.

Also in this work, the absorption of light constitutes the connecting thread of the investigations. However, this research is not confined to one of the distinct fields in photobiology mentioned earlier, but rather contains interdisciplinary elements to study the biochemical implications of light absorption, particularly in two specialized photosensor proteins (Chapters four and five) and in bacterial cells (Chapter six).

For readers that are not familiar with the science of photobiology, the following two paragraphs are intended to provide a short description of some fundamental terms and principles that could be of relevant help in the further reading of this work. For a broader overview as well as more detailed information, the reader is referred to the major sources of specialized literature and information, *e. g.* [2].

1.2 The nature of light [2]

Light is a form of electromagnetic radiation. The nominal wavelengths of *visible light* are 400-760 nm. This is a very small region of the overall electromagnetic spectrum, which ranges from short-wavelength γ -rays to long-wavelength radio waves (**Table 1-1**). The *ultraviolet* (UV) radiations important in photobiology lie in the wavelength band from approximately 160 nm, below which oxygen is strongly absorbing, up to the threshold of violet light at 400 nm. *Infrared*

(IR) radiation begins at the long-wavelength limit of red light at 760 nm. Wavelengths longer than 1 μm are essentially ‘heat waves’, of which the biological effects are initiated by temperature elevation.

Table 1-1. Electromagnetic spectrum ^a							
Spectral band ^b	Wavelength range			Photon energy (eV)			
Microwave	100	-	0.1	cm	10 ⁻⁶	-	10 ⁻³
IR-C	1000	-	3	μm	0.001	-	0.4
IR-B	3	-	1.4	μm	0.4	-	0.9
IR-A	1.4	-	0.76	μm	0.9	-	1.6
Visible	760	-	400	nm	1.6	-	3.1
UV-A	400	-	320	nm	3.1	-	3.9
UV-B	320	-	280	nm	3.9	-	4.4
UV-C	280	-	100	nm	4.4	-	12.4
Vacuum UV	100	-	10	nm	12.4	-	124
X-rays	10	-	0.01	nm	10 ²	-	10 ⁵
γ -rays	0.1	-	0.0001	nm	10 ⁵	-	10 ⁷

^aTable taken from [2]

^bIR = infrared radiation; UV = ultraviolet radiation

Electromagnetic radiation is propagated in the form of waves. A perfectly monochromatic light wave is characterized by a single wavelength (λ) and a single frequency (ν). The wave propagates at a wave velocity (v) that depends on the refractive index of the medium (n) according to the fundamental relationship:

$$v = \lambda\nu = c/n$$

where c is the speed of light in vacuum (3.0×10^8 m/s). Polychromatic light contains a distribution of wavelengths, *e.g.* the spectrum of sunlight. An electromagnetic wave carries with it coupled electric and magnetic fields, which are responsible for its interactions with matter. According to the classical electromagnetic theory of Maxwell, the electric and magnetic fields lie in the plane transverse to the direction of wave motion. The electric and magnetic fields of electromagnetic radiation are mutually perpendicular, and their amplitudes oscillate with the frequency of the light. With the advent of quantum optics in the late 19th and 20th centuries, it was deduced that certain properties of electromagnetic radiation may be described more accurately by considering the radiation to be composed of small energy packets or *quanta*. The energy content of a light quantum, which is also known as a photon, is related to the frequency by the equation:

$$E = h\nu = hc/\lambda$$

where h is Planck’s constant (6.63×10^{-34} J s⁻¹). The quantum energy associated with different wavelengths of electromagnetic radiations are given in **Table 1-1** in units of eV, where 1 eV = 1.60×10^{-19} J. When electromagnetic radiation interacts with matter, the microscopic transfer of energy is limited by the photon energy, *e.g.* X-rays can eject strongly bound inner-shell electrons from atoms, while visible light interacts only with the less strongly bound valence electrons.

1.3 Fundamentals in protein photochemistry

The central principle in photochemistry is that chemical changes occur when the light is effectively absorbed by molecular compounds. However, the amino acids making up the backbone of a protein do not absorb visible radiation. The latter requires interaction with a specific molecule, called a chromophore, to initiate a photochemical reaction. The protein with its bound chromophore is generally referred to as holoprotein (versus apoprotein without the chromophore). The absorption of a single photon by the chromophore produces an excited state in which one electron of the absorbing molecule is raised to a higher energy level. In the excited state, various reaction pathways, such as isomerization (if a double bond is present) or electron and/or proton transfer can be initiated [3, 4], depending on the molecular structure, the wavelength of the light, and the specific reaction conditions. Through a sequence of relaxation processes, the holoprotein returns to its dark-adapted state with the original unexcited chromophore, completing a photocycle and thus priming the photoreceptor for catching a new light photon. Photoactivation is often accompanied by a structural change of the protein, caused by subtle changes of the H-bonding interactions in the chromophore-binding pocket upon light absorption. The quantum yield of a given photochemical product is the probability that the absorption of one photon by the system leads to one molecule of that product [2], which can *e.g.* be a signaling state in the case of photosensory proteins. As described in Chapter two, nature has developed several types of light-sensitive holoproteins, functioning in energy conversion or signaling, and varying widely in their chromophore composition, photochemistry and photocycle kinetics. Overall, a photobiological process takes place in stages, starting with very fast processes at the physical level (light absorption), followed by dark chemical reactions (*e.g.* signal transduction, ATP synthesis), and terminating with relatively slow events at the biological level (*e.g.* phototaxis, cell growth).

1.4 References

1. http://www.pol-us.net/ASP_Home/whatis.html.
2. Smith, K.C., The science of photobiology - 2nd edition. *Plenum Press*, 1989.
3. Hellingwerf, K.J., The molecular basis of sensing and responding to light in microorganisms. *Antonie Van Leeuwenhoek*, 2002. **81**(1-4): p. 51-9.
4. Hellingwerf, K.J., Hendriks, J., and Gensch, T., Photoactive Yellow Protein, a new type of photoreceptor protein: Will this "yellow lab" bring us where we want to go? *Journal of Physical Chemistry A*, 2003. **107**(8): p. 1082-1094.

Chapter two

2 Biological photosensors

2.1 Light as a source of energy

The energy from sunlight is converted into ATP, the chemical energy used by all living organisms, through the action of H⁺-translocating ATP synthases, which harnesses the free energy of the electrochemical membrane potential that is generated upon the absorption of light. There are two known photochemical mechanisms for phototrophic energy conversion. In plants, algae and some bacteria, active proton transport is concomitant with a transmembrane electron flow, which is initiated by photo-oxidation of protein-(bacterio)chlorophyll complexes that are associated with specialized membrane systems. Light-harvesting (bacterio)-chlorophylls efficiently funnel the energy of the broad solar spectrum into specific reaction center (bacterio)chlorophylls, which, in turn, elicits sequential electron transfer from the excited chlorophyll to an electron acceptor, accompanied by secondary proton extrusion across the photosynthetic membranes.

Alternatively, H⁺ are directly transported across the cytoplasmic membrane to the extracellular side by light-driven proton pumps [1], which have seven membrane-spanning helical segments forming a polar channel and a retinal chromophore at a conserved lysine residue. Thus, ejecting protons out of the cell generates an inwardly directed proton motive force needed for ATP synthesis, active transport and motility. This simple way of light energy conversion was first discovered nearly three decades ago in the halophile *Halobacterium salinarum* in the form of the light-driven proton pump bacteriorhodopsin (BR) [1]. The BR ($\lambda_{\max} = 568$ nm) reaction cycle drives electrogenic proton translocation through photoisomerization of the all-*trans* retinal chromophore to the 13-*cis* configuration, and offers the organism an alternative for the respiratory chain when oxygen levels are low, as often emerges in the naturally hypersaline environments (>20% NaCl) where this haloarchaeal organism prevails. Several BR variations have been discovered in the Archaea, capable of light-induced Cl⁻ transport (halorhodopsin, HR) [2], and control of cell motility (sensory rhodopsin (SR) I [3] and II [4]). HR ($\lambda_{\max} = 576$ nm) is coexpressed with BR in semianaerobic conditions and transports Cl⁻ into the cell, hyperpolarizing the membrane positive-outside. The inward transport of Cl⁻ by HR contributes to the membrane potential and also helps to maintain pH homeostasis by avoiding cytoplasmic alkalization [5]. The two SR provide the cells with the ability to respond to light as an attractant or repellent, depending on its color and the stage of growth of the cells (as described further below). BR, HR

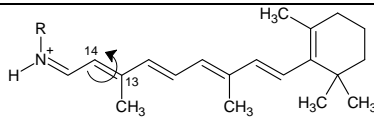
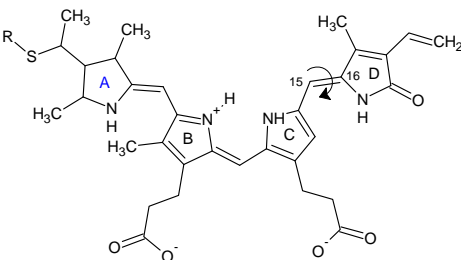
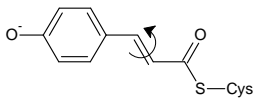
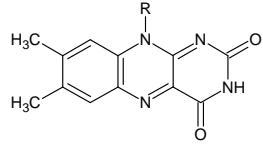
and SR are classified as type 1 (microbial) rhodopsins, according to conserved residues in the retinal binding pocket, that distinguish them from the type 2 rhodopsins found in the eyes of animals. Until recent findings, it was generally thought that rhodopsin-based phototrophy was restricted to Archaea and extreme conditions of high light intensity and high salt. However, in an uncultivated marine γ -proteobacterium (the Sar86 lineage), a gene homologous to BR was discovered, of which the expression in *E. coli* produced a retinal protein, named proteorhodopsin (PR), capable of transmembrane proton transport [6, 7]. Further analyses of marine bacterioplankton established that PR functionality is widespread in the oceans both phylogenetically and biogeographically [6, 8], a finding also supported by the large number of rhodopsin homologs (~800) found during the Sargasso Sea metagenome study [9]. Moreover, retinal proteins with homology to BR and bearing all-*trans* retinal as a chromophore have subsequently also been discovered in different groups of eukaryotes, fungi and algae. Some of them are apparently proton pumps, as *Leptosphaeria* rhodopsin [10], while others are sensors, such as the rhodopsins of *Chlamydomonas* [11-14]. However, the most unusual retinal protein, xanthorhodopsin (XR), was recently found in the extreme halophilic eubacterium *Salinibacter ruber*, and represents a novel pigment complex combining a carotenoid antenna, salinixanthin, with the retinal proton pump in order to increase the spectral range of light-harvesting by about two-fold [15]. Energy transfer from light-harvesting carotenoids is common in chlorophyll-based photosynthetic systems [16], but has not been shown before in retinal-based pumps or receptors. To date, little is known about *Salinibacter's* photobiology, but it might turn out to be quite complex as, in addition to xanthorhodopsin, genes encoding a halorhodopsin-like protein [17], two sensory rhodopsins related to haloarchaeal SRI [17] and a Photoactive Yellow Protein (PYP) homologue have been found in the genome. Although only expression of xanthorhodopsin was detected so far [15], the spectral and photokinetic properties of the *pyp* gene product described in Chapter 4 shows that it is a genuine PYP and is likely to be functional.

2.2 Light as a source of information

Besides the photoreceptors specialized in light energy transduction, living organisms also possess a class of light-sensitive proteins, called photosensors, which have evolved to monitor the ambient light environment and allow organisms to optimally use the existing light conditions for growth and development and/or to permit protection from light damage. Several families of photosensors exist, according to the type of chromophore they carry. An overview of these families is given in **Table 2.1**, and shows that nature has foreseen a relatively small number of chromophore variants to provide photoactivity. This observation is supported by the recent

discoveries of chimeric proteins composed of a combination of known chromophore binding domains, including xanthorhodopsin [15] (retinal/carotenoid), PYP-phytochrome-related protein [18] and PYP-bacteriophytochrome diguanylate cyclase/phosphodiesterase [19] (*p*-coumaric acid/linear tetrapyrrole), and phy3 [20] and neochrome [21] (linear tetrapyrrole/flavin). Consequently, each resulting family may contain members with strongly divergent biological function(s).

Table 2.1 Photosensor families

Photosensor family	Chromophore class	Basic chromophore structure	Primary photochemistry
Rhodopsin	Linear polyene (retinal)		<i>Trans-cis</i> isomerization
Phytochromes (PΦB, PCB, BV)	Linear tetrapyrrole		<i>Trans-cis</i> isomerization
PYPs	<i>p</i> -coumaric acid (4-OH-cinnamic acid)		<i>Trans-cis</i> isomerization
Cryptochromes	Flavin (FAD), pterin (MTHF)		Oxidized FAD
LOV	Flavin (FMN)		FMN-cysteinylyl adduct formation
BLUF	Flavin (FAD)		FAD-tyrosine H-bond strengthening

The arrow indicates in each case the isomerized double bond.

Initially, the best studied photoreceptors all absorb in the green/red light spectrum, although blue light was long known to regulate several responses in plants, such as phototropism, stomatal opening, inhibition of hypocotyls' growth, induction of flowering, circadian rhythms and light-dependent transcriptional regulation. Moreover, in aquatic ecosystems, blue light is predominant because of the attenuating properties of the water column. The molecular identification of blue-light detecting photosensors in plants and micro-organisms, including bacteria and fungi, revealed exciting new progresses in this field of photobiology over the past 15 years. However, with the advent of genome sequencing, new and different candidate

photosensors are likely to appear, and much work waits ahead to understand their physiological roles and molecular mechanisms of light perception and signal transduction. A brief overview on the current knowledge of the different photosensor families and their unique features, with emphasis on microbial photosensing, is presented in the following sections.

2.2.1 Red-/green-light photoperception

2.2.1.1 Sensory rhodopsins

Sensory rhodopsins (SR) are photoactive, membrane-embedded, retinylidene proteins that are structurally similar to the proton pump BR, and are widespread in the microbial world in each of the three domains of life: Archaea, Bacteria and Eukarya. They relay environmental light stimuli *via* varying modes of signaling in different organisms, including interactions with other membrane proteins or cytoplasmic transducers and light-controlled Ca^{2+} channel activity.

In Archaea like *Halobacterium salinarum* or *Natronomonas pharaonis*, SRI and SRII mediate opposing photomotility responses in complex with their cognate transducer proteins HtrI and HtrII, through control of a phosphorylation cascade which modulates the cell's flagellar motors (**Figure 2.1**) [22, 23]. When oxygen and respiratory substrates are plentiful, the cells grow chemoheterotrophically and synthesize the repellent photosensor SRII ($\lambda_{\text{max}} = 487$ nm) as their only rhodopsin, strategically seeking the dark to escape from potential photo-oxidative damage. A drop in oxygen tension suppresses SRII production and induces synthesis of SRI along with the structurally similar BR and HR, which are used to generate a proton motive force for ATP synthesis (as described in section 2.1). SRI ($\lambda_{\text{max}} = 587$ nm) mediates an attractant migration into illuminated areas where ion pumping by BR and HR will be maximally activated. However, a long-lived photo-intermediate of SRI, called S_{373} , absorbs near-UV photons and mediates a strong repellent response [22]. Therefore, the color-sensitive signals from SRI attract the cells into regions containing orange light only if this region is relatively free of near-UV photons.

The primary photoprocess is all-*trans* to 13-*cis* isomerization of the C13-C14 double bond in the retinal chromophore, identical to that occurring in BR, yet different from the type 2 rhodopsins found in the photoreceptor cells of animal eyes which involves 11-*cis* to all-*trans* photoisomerization, and controls the activation of hetero-trimeric G-proteins leading to visual reception [24]. Photoisomerization alters the structure of the receptors at the SR-Htr interface, thereby communicating the signal to the Htr proteins [5]. Moreover, the signaling process is dependent on interaction of SR with the transducer proteins, as transducer-free *H. salinarum* SRI [25, 26] and *N. pharaonis* SRII [5] have been observed to carry out light-driven proton transport like BR.

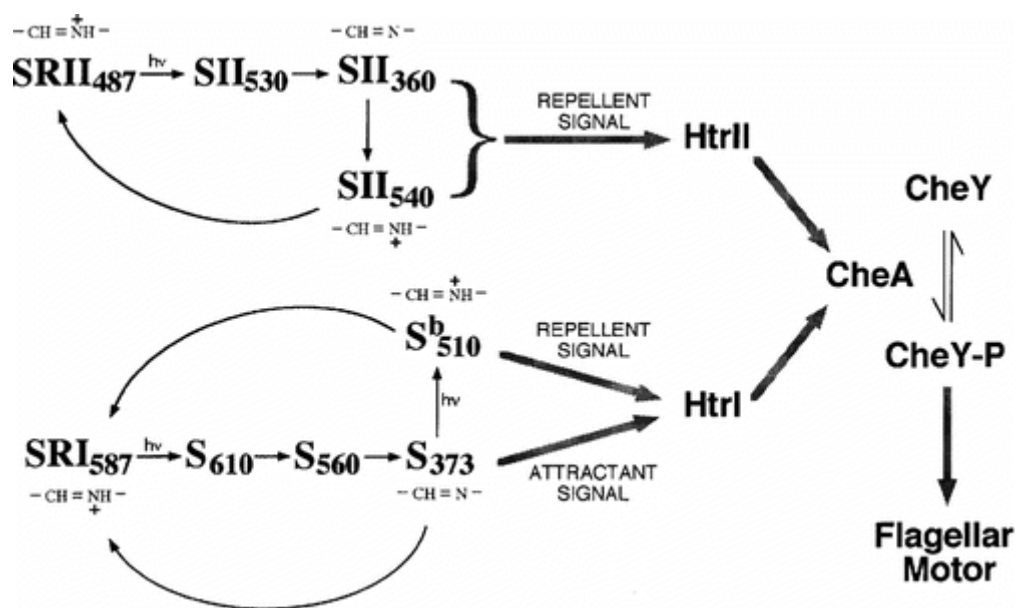


Figure 2.1

Photocycles of *H. salinarum* SRI and SRII and their coupling to the flagellar motor. Photon absorption in the dark initiates a cyclic chain of transitions involving several intermediates which could be distinguished based on their spectral (denoted by respective subscripts in the figure) and temporal changes. Approximate first order half-lives at room temperature for SRI intermediates S_{610} , S_{560} , S_{373} , and S_{b510} are 90 μ s, 270 μ s, 800 ms, and 80 ms, respectively. For SII $_{530}$, SII $_{360}$, and SII $_{540}$, they are respectively 160 μ s, 120 ms, and 330 ms [22]. The indicated signaling states (see text) in each photocycle transmit signals *via* HtrI and HtrII to CheA. CheA controls the extent of phosphorylation of CheY, which in turn modulates the flagellar motor. Arrows with $h\nu$ indicate light reactions and the state of protonation of the Schiff base is indicated. The picture is taken from [22].

The first eubacterial sensory rhodopsin to be identified was *Anabaena* sensory rhodopsin (ASR) from the freshwater cyanobacterium *Anabaena* sp. PCC7120 [27, 28]. ASR interacts with a tetrameric transducer, which is encoded in an operon along with ASR and accelerates the ASR photocycle [28, 29]. Surprisingly, the results from the crystal structure, chromophore extraction and spectroscopic analysis indicate that ASR exists as a mixture of stable *all-trans* ($\lambda_{\max} = 550$ nm) and *13-cis* ($\lambda_{\max} = 537$ nm) isomeric configurations. Moreover, one spectral form can be efficiently photoconverted to the other, characterizing ASR as a photochromic pigment [30, 31]. Thus, the ratio of the *cis* and *trans* chromophore forms depends on the wavelength of illumination, providing a mechanism for single-pigment color sensing. The thermal half-lives of the *trans* (~ 100 min) and *cis* (~ 300 min) ground-state forms are similar to the red and far-red photochromic states of plant phytochrome (as described in the next section), and suggests that this protein in *Anabaena* might analogously be responsible for modulating chromatic adaptation (triggering differential biosynthesis of light-absorbing pigments based on the quality of light), although this remains to be proven [28, 32, 33].

Eukaryotic SRs for which a function in the cell has been established are exemplified by CSRA and CSRB from the green alga *Chlamydomonas reinhardtii*, which were identified by genomic analysis and shown to mediate light-dependent cellular motility [12-14, 34, 35]. Moreover, the photobehavior in *C. reinhardtii* and other algal species, which involves motility responses towards the direction (phototaxis) as well as the intensity (photophobic response) of light, results from the generation of Ca^{2+} currents in the plasma membrane, as characterized by electrophysiological measurements [36]. CSRA and CSRB, each consisting of a rhodopsin domain as part of a larger protein, were demonstrated to mediate a fast and slow current, at high and low light intensities respectively, for phototaxis orientation and photophobic response [33]. In addition, the 300 N-terminal residues have been shown to exhibit light-gated channel activity for protons (CSRA) or other cations (CSRB), when expressed in *Xenopus* oocytes [34, 35], although the relation with their activities in *Chlamydomonas* is not yet clear. Three additional sensory rhodopsin genes (cop5, cop6 and cop7) were predicted from *Chlamydomonas* genome sequencing [37], each showing a seven-transmembrane rhodopsin domain fused to other domains with high homology to well-studied signal-transducing proteins, *i.e.* histidinyl kinases, phosphor-acceptor regulators and adenylyl or guanylyl cyclases [33]. Although expected to be sensory in function, it remains to be determined as how these proteins are expressed and just what their biological roles are in the cell.

2.2.1.2 (Bacterio)phytochromes

Phytochromes are photochromic photosensors which use a covalently attached bilin-type chromophore that enables reversible photoconversion between two stable conformations, a red-light absorbing form (P_r) and a far-red-light absorbing form (P_{fr}). Phytochromes were initially discovered in higher plants [38], mediating many aspects of growth and development in response to near infrared light. However, accumulating genetic and genomic analysis show that they are also widely distributed among micro-organisms, including cyanobacteria (Cphs), proteobacteria (Bphs) and fungi (Fphs) [39]. Moreover, all phytochromes and phytochrome-related proteins contain a modular domain architecture, typified by a conserved N-terminal photosensory core domain (PCD), consisting of PAS¹, GAF² and PHY³ subdomains, and a C-terminal regulatory histidine kinase or histidine kinase-related domain [39, 41]. In contrast, a GGDEF/EAL⁴ type of diguanylate cyclase/phosphodiesterase domain has been identified instead of a histidine kinase

¹ PAS; Acronym based upon periodic clock protein, aryl hydrocarbon receptor nuclear translocator and, single minded protein

² GAF; domain homologues originally found in cGMP-binding phosphodiesterase, *Anabaena* adenylylate cyclase, and *E. coli* EhlA [40]

³ PHY; photosensory domains specific to phytochromes

⁴ GGDEF/EAL, signature amino acid sequence for phosphodiesterase and/or diguanylate cyclase activity

domain in the Bphs from *Rhodobacter sphaeroides* and *Thermochromatium tepidum*, while one of the six Bphs of *Rhodospseudomonas palustris* contains an additional CheY phosphate receiver domain at the C-terminus [19]. The PCD autocatalytically binds a linear tetrapyrrole (bilin), of which the exact nature varies between species. Plant phytochromes carry a phytochromobilin (PΦB), while Cph1s and Cph2s (numbers refer to specific subclasses within the Cph family) use phycocyanobilin (PCB) as chromophore, both *via* covalent attachment to a conserved Cys in the GAF domain of the PCD [42]. PCB has a ring D ethyl instead of a vinyl side chain in PΦB, and is produced by cyanobacteria as a component of phycobiliproteins, which serve as accessory pigments for photosynthetic light collection. In contrast, Bphs and Fphs preferably incorporate biliverdin (BV), which is a precursor in the PCB and PΦB biosynthesis pathway and is synthesized from heme by a heme oxygenase [43]. The vinyl A side chain of BV forms a covalent thioether bound with a Cys residue upstream of the PAS domain [44, 45]. Moreover, phytochromes with a proposed BV chromophore all lack the GAF cysteine, while the PAS cysteine is conserved [44].

Phytochromes can be reversibly interconverted by red (R) or far-red (FR) light (**Figure 2.2**), and act as light-regulated molecular switches, in which one of the two forms is biologically active. While photoconversion between P_r and P_{fr} can be rapid, dark recovery can take a few minutes to several hours or days. Nevertheless, the quantum efficiency is remarkably low, typically less than 10% which suggests that strong illumination is necessary to switch from one state to the other. The primary process is a *cis-trans* isomerization of the exocyclic C15-C16 double bond, inducing conformational changes in the protein, which eventually leads to an altered phosphorylation state for signal transduction. The biological outputs from phytochromes reflects the ratio of P_r and P_{fr} forms, and this ratio is determined by the light environment, by the forward and reverse rate of photoconversion, and by the rates for thermal interconversion between these forms [41].

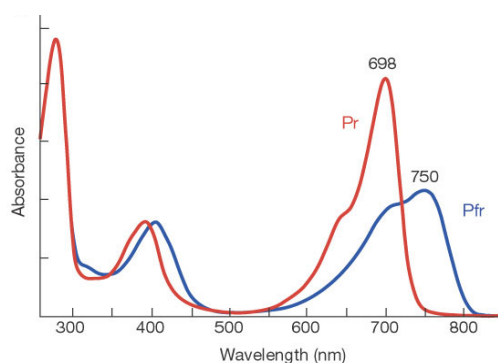


Figure 2.2

Absorbance spectra after saturation with red and far-red light of *Deinococcus radiodurans* Bph. The biliverdin chromophore was attached to the apoprotein in *E. coli* by co-expression of a heme oxygenase. Figure from [43].

Signal transfer by prokaryotic phytochromes most frequently utilizes the two-component signaling paradigm, *i.e.* ligand-dependent histidine kinase activation and phosphotransfer to a response regulator that further regulates transcription or motility. For example, RcaE from the

cyanobacterium *Fremyella diplosiphon* is associated with its cognate response regulator RcaF in a two-membered operon and acts as a photosensor for the complementary chromatic adaptation (CCA) *via* a possible five-step phosphorelay [46, 47]. CCA involves variation of the biliprotein composition of the phycobilisomes that comprise the light-harvesting antenna system in response to red and green light, using the photochromicity of RcaE [48]. Similarly, an associated response regulator has been identified in the Bph operon of *Deinococcus radiodurans* [49], which regulates the synthesis of carotenoids, possibly to protect against harmful UV-light.

2.2.2 Blue-light sensing

To date, blue light is known to be monitored by a number of photosensor families which can be classified into two main categories, *i.e.* the flavin-based photosensors, comprising cryptochromes, LOV (Light, Oxygen, Voltage) and BLUF (Blue Light sensing Using EAD) proteins, and the Photoactive Yellow Proteins (PYPs), binding *p*-coumaric acid as chromophore. The PYP family will be extensively described in Chapter three, to situate the biochemical characterization of a newly discovered *pyp* gene in *Salinibacter ruber*, discussed in Chapter four. Members of the photosensory proteins binding riboflavin derivatives are described below and are characterized by the non-covalent binding of flavin mononucleotide (FMN) or flavin adenine dinucleotide (FAD), contrary to the covalently bound cofactors of phytochromes, rhodopsins and PYPs.

2.2.2.1 Cryptochromes

The cryptochromes (*cry*) owe their name to the long-hidden nature of the chemical structure of their chromophore(s) and their presumed prevalence in lower plants and fungi (cryptogams⁵) [50]. However, *cry* proteins have been identified in several plant species as well as in animals and bacteria. They contain two non-covalently bound prosthetic groups, a photoactive FAD and a pterin antenna (5,10-methenyltetrahydrofolate, MTHF - a heterocyclic chromophore resembling a flavin but with only two rings instead of three), and are very similar to microbial DNA photolyases, especially within the chromophore binding region. However, *cry* proteins contain a distinctive C-terminal extension that is absent in the photolyases. The latter possess a redox active FAD as primary chromophore and either a pterin, a deazaflavin (8-hydroxy-8-dimethyl-5-deazariboflavin, 8-HDF) [51] or even FMN or FAD [52, 53] as an antenna, and are considered to be the evolutionary precursors of the cryptochromes. Found in both prokaryotes

⁵ Cryptogams is a name referring to plants and fungi that do not reproduce by seeds. The term is sometimes used as a term of convenience but since the organisms in question are not regarded as a coherent group by contemporary plant systematics, the word is considered obsolete in taxonomy.

and eukaryotes, they catalyze the light-dependent repair of damaged DNA produced from exposure to UV-B irradiation (280-320 nm). Photolyases type I and II mediate the repair of cyclobutane pyrimidine dimers (CPD), whereas (6-4) photolyases catalyze the repair of pyrimidine (6-4) pyrimidone photoproducts. Therefore, the catalytically active chromophore is FADH⁻, the double electron-reduced form of FAD that transfers an electron from the excited state to the DNA lesion [54].

Despite their homology to photolyases, cryptochromes lack DNA repair activity, with the exception of the so-called cry-DASH proteins (*Drosophila*, *Arabidopsis*, *Synechocystis* and *Homo* cryptochromes) [55] which are able to split CPD, with high specificity towards single stranded DNA [56]. As yet, no definite evidence for their role as photosensor has been presented, the cry-DASH might solely constitute specialized photolyases [54]. The functional form of cry proteins in the dark state is presumably the fully oxidized FAD, acting as blue-light sensors to regulate processes ranging from circadian regulation in plants and animals to plant growth and development. In *Arabidopsis thaliana* there are now three known cryptochromes, *At-cry1*, 2 and 3. *At-cry3* is a member of the Cry-DASH family, while *At-cry1* and *At-cry2* have been found to mediate the blue light inhibition of hypocotyl elongation [57] and developmental changes during transition of plant seedlings from darkness into the light, such as anthocyanin formation [58]. However, *At-cry2* is rapidly degraded at high light intensities [59, 60], indicating that *At-cry2* functions under low light intensities, whereas *At-cry1* functions mainly under high light intensities.

2.2.2.2 LOV proteins

The LOV family of blue-light photoreceptor domains constitutes a subclass of proteins within the PAS domain superfamily, and is named after their significant homology with domains in a number of proteins that are involved in sensing light, oxygen, or voltage. LOV domains contain a highly conserved key sequence, *i.e.* QXNCRFLQ [61] and commonly bind FMN as cofactor. They were first identified in two membrane associated phototropins in *A. thaliana* (phot1 and phot2) during studies on phototropism [61, 62], the adaptive process whereby plants bend toward a light source to maximize light capture for photosynthesis, and which is most effectively induced by blue and UV-A light. Phototropins bind two oxidized FMN chromophores within a pair of LOV domains arranged in tandem (LOV1 and LOV2), and undergo blue-light induced autophosphorylation via the serine/threonine kinase in the C-terminal half. They are now known to be the photosensors for phototropism, chloroplast movement, leaf expansion, rapid growth inhibition, and stomatal opening [63].

In the dark, phot-LOV domains absorb maximally at ~ 450 nm (LOV_{447}) [64, 65] and, upon blue light illumination, enter a photocycle (**Figure 2.3**) involving the reversible formation of a covalent bond between the 4a carbon of the flavin isoalloxazine ring and the sulfur atom of the nearby cysteine residue that is part of the conserved LOV key sequence. The resulting cysteinyl adduct has a single absorption band centered near 390 nm (LOV_{390}), and is normally formed *via* the μs decay of the red-shifted FMN triplet state (LOV_{660}) [66] that arises from an excited FMN singlet [67]. However, direct formation of the adduct from the singlet state has also been reported [68]. The adduct then slowly reverts back to the dark state within seconds or minutes (LOV_{447}) [64]. Detailed structural information, both in the dark and in the photoactivated state, are available for the LOV2 domain of phy3 [69, 70] (a phytochrome-phototropin hybrid photoreceptor from the fern *Adiantum capillus-veneris*) and for *C. reinhardtii* phot-LOV1 [71], which show that the FMN chromophore is tightly bound to the protein through hydrogen bonding and hydrophobic interactions. Cysteinyl adduct formation produces major conformational changes, involving the loss of α -helical structure, which activate the kinase function [72-75].

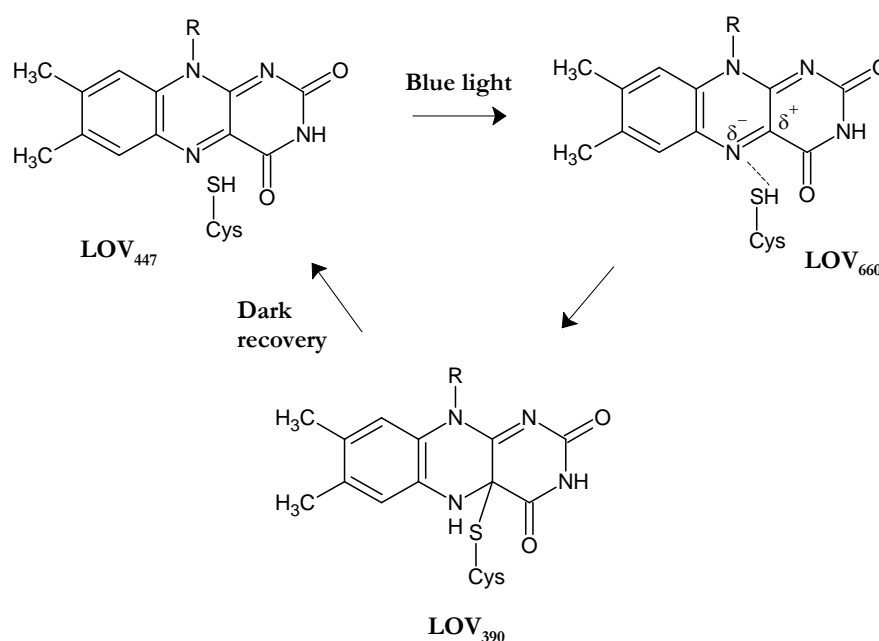


Figure 2.3

Schematic representation of LOV domain photochemistry. In darkness, the FMN chromophore is non-covalently bound within the LOV domain, forming a species that absorbs maximally at 447 nm (LOV_{447}). Light drives the production of a highly reactive triplet-state flavin (LOV_{660}) that leads to the formation of a covalent bond between the C(4a) carbon of the FMN chromophore and a conserved cysteine residue within the LOV domain (LOV_{390}). The photoreaction process is fully reversible in the dark.

On the basis of sequence analysis, as much as 91 LOV proteins have been identified in eubacteria, cyanobacteria, archaea and fungi [76-78], bearing a single LOV domain with the canonical QXNCRFLQ amino acid motif, and being associated with a variety of effector domains. As more prokaryote sequences will become available *via* ongoing genome projects, this number will almost certainly increase. Examples of bacterial LOV photosensors include histidine kinases (LOV-HK), regulators of stress sigma factors (LOV-STAS⁶), DNA-binding transcription factors (LOV-HTH⁷), response regulators (LOV-RR) and phosphodiesterases (LOV-GGDEF/EAL). However, to date, phot-LOV-like photochemistry in bacterial LOV proteins, *i.e.* binding of FMN, a typical absorption in the dark around 450 nm and the appearance of a 390 nm absorbing photoproduct upon blue-light irradiation indicative for cysteinyl adduct formation, has only been demonstrated in a few cases: YvtA from *Bacillus subtilis* [79], LovK from *Caulobacter crescentus* [77], and the LOV-HK from *Pseudomonas putida* [80], *Brucella melitensis*, *Brucella abortus*, *Erythrobacter litoralis* (2) and *Pseudomonas syringae* [81]. Information about their functional role(s) in the biology of the bacterial cell is even less evident. YvtA from *B. subtilis*, in which the N-terminal LOV domain is followed by a STAS, is known to act as a positive regulator of the general stress transcription factor σ^B [82, 83], while the LOV-HK from the mammalian pathogen *B. abortus* mediates the visible-light increased virulence [81]. In the differentiating bacterium *C. crescentus*, the LOV-HK LovK is part of a two-component signaling system and is required for the light-dependent enhancement of intercellular attachment [84].

An example of a fungal LOV protein is given by the transcription factor ‘white collar-1’ (WC-1) from *Neurospora crassa*, in which the LOV domain is upstream of a PAS domain and a zinc-finger domain, and functions as a blue-light activated transcriptional regulator, mediating the circadian clock and other light responses in this ascomycete [85, 86]. Homologs of WC-1 have been reported in several other fungal groups, both phycomycetes and basidiomycetes [87-89].

2.2.2.3 BLUF domain proteins

A third type of flavin photosensor has been identified in the N-terminal BLUF domains of AppA (activation of photopigment and puc expression) from *Rhodobacter spaeroides* and PAC (photoactivated adenyl cyclase) from the flagellate *Euglena gracilis*. The BLUF domain also occurs in several other bacterial proteins, mainly in cyanobacteria and α -proteobacteria [90], but their function has not yet been elucidated, with the exception of Slr1694 from *Synechocystis* PCC6803 [91].

⁶ STAS, sulfate transporter/anti-sigma factor antagonist

⁷ HTH, helix-turn-helix

AppA from *R. sphaeroides* is a light and redox regulator of the expression of photosynthesis genes, build of a light-sensing BLUF module and a redox-sensing C-terminal domain [92-94]. Moreover, transcription of *R. sphaeroides puc* and *puf* operons, which encodes for the photosynthetic machinery, is dependent on oxygen tension and light *via* interaction of AppA with the repressor protein PpsR. At low oxygen tension, reduced AppA and PpsR form a complex and repression is released, whereas under fully aerobic growth conditions, oxidized AppA releases PpsR, allowing the latter to bind to the promoter of photosynthesis genes and repress their transcription. However, at intermediate oxygen concentration ($\sim 100 \mu\text{M}$ dissolved oxygen), light determines whether AppA acts as a transcriptional anti-repressor of PpsR. Moreover, blue light has been shown to repress *puc* and *puf* transcription, most likely to avoid production of singlet oxygen during photosynthesis [95].

AppA light-sensing is catalyzed by its N-terminal BLUF domain through the reversible formation of a ~ 10 nm red-shifted intermediate (BLUF_{RED}) upon blue-light absorption ($\lambda_{\text{max}} = 460$ nm). This transient ground state intermediate, formed after ~ 400 ps, is presumed to be the signaling state and recovers in ~ 900 s. However, unlike in LOV proteins, the signaling state BLUF_{RED} occurs from the electronically excited singlet state of the FAD chromophore (within 1 ns), whereas the triplet state is formed *via* a side reaction with very low efficiency [96, 97]. Two conserved amino acids are considered essential for the accomplishment of the BLUF photocycle, referred to as Tyr21 and Gln63 from the AppA numbering. It is thought that the light-induced red-shift in the absorption spectrum is caused by rearrangements of hydrogen bonds around the flavin chromophore, mainly strengthening H-bonds at the C(4)=O position with Tyr21 and Gln63, leading to a stable local conformational change.

Similar photocycle characteristics have been reported for other members of the BLUF family, like PAC from *E. gracilis* [98], for Slr1694 from *Synechocystis* PCC6803 and Tll0078 of *Thermosynechococcus elongatus* BP-1 [91], and for YcgF from *E. coli* [99], albeit with some differences in the dark state absorption maxima, the magnitude of the red-shift interval, or the recovery lifetime, ranging from a few seconds to several minutes. The Slr1694 protein is involved in the regulation of phototaxis, as shown in the *slr1694* disruptant [91], and PAC from *E. gracilis* contains four BLUF domains, forming a heterotetramer composed of two FAD-binding subunits ($\text{PAC}\alpha$ and $\text{PAC}\beta$). PAC mediates a step-up photophobic response, in which the swimming direction of the unicellular flagellate is abruptly altered after a sudden increase in incident blue light intensity, resulting in photoavoidance of the protist [100].

2.3 References

1. Oesterhelt, D. and Stoeckenius, W., Functions of a new photoreceptor membrane. *Proceedings of the National Academy of Sciences of the United States of America*, 1973. **70**(10): p. 2853-2857.
2. Schobert, B. and Lanyi, J.K., Halorhodopsin is a light-driven chloride pump. *Journal of Biological Chemistry*, 1982. **257**(17): p. 306-313.
3. Bogomolni, R.A. and Spudich, J.L., Identification of a third rhodopsin-like pigment in phototactic *Halobacterium Halobium*. *Proceedings of the National Academy of Sciences of the United States of America-Biological Sciences*, 1982. **79**(20): p. 6250-6254.
4. Takahashi, T., Tomioka, H., Kamo, N., and Kobatake, Y., A photosystem other than Ps370 also mediates the negative phototaxis of *Halobacterium halobium*. *FEMS Microbiology Letters*, 1985. **28**(2): p. 161-164.
5. Spudich, J.L., Variations on a molecular switch: transport and sensory signalling by archaeal rhodopsins. *Molecular Microbiology*, 1998. **28**(6): p. 1051-1058.
6. Beja, O., Spudich, E.N., Spudich, J.L., Leclerc, M., and DeLong, E.F., Proteorhodopsin phototrophy in the ocean. *Nature*, 2001. **411**(6839): p. 786-789.
7. Beja, O., Aravind, L., Koonin, E.V., Suzuki, M.T., Hadd, A., Nguyen, L.P., Jovanovich, S., Gates, C.M., Feldman, R.A., Spudich, J.L., Spudich, E.N., and DeLong, E.F., Bacterial rhodopsin: Evidence for a new type of phototrophy in the sea. *Science*, 2000. **289**(5486): p. 1902-1906.
8. de la Torre, J.R., Christianson, L.M., Beja, O., Suzuki, M.T., Karl, D.M., Heidelberg, J., and DeLong, E.F., Proteorhodopsin genes are distributed among divergent marine bacterial taxa. *Proceedings of the National Academy of Sciences of the United States of America*, 2003. **100**(22): p. 12830-12835.
9. Venter, J.C., Remington, K., Heidelberg, J.F., Halpern, A.L., Rusch, D., Eisen, J.A., Wu, D.Y., Paulsen, I., Nelson, K.E., Nelson, W., Fouts, D.E., Levy, S., Knap, A.H., Lomas, M.W., Nealson, K., White, O., Peterson, J., Hoffman, J., Parsons, R., Baden-Tillson, H., Pfannkoch, C., Rogers, Y.H., and Smith, H.O., Environmental genome shotgun sequencing of the Sargasso Sea. *Science*, 2004. **304**(5667): p. 66-74.
10. Waschuk, S.A., Bezerra, A.G., Shi, L., and Brown, L.S., *Leptosphaeria* rhodopsin: Bacteriorhodopsin-like proton pump from a eukaryote. *Proceedings of the National Academy of Sciences of the United States of America*, 2005. **102**(19): p. 6879-6883.
11. Foster, K.W., Saranak, J., Patel, N., Zarilli, G., Okabe, M., Kline, T., and Nakanishi, K., A rhodopsin is the functional photoreceptor for phototaxis in the unicellular eukaryote *Chlamydomonas*. *Nature*, 1984. **311**(5988): p. 756-759.
12. Govorunova, E.G., Jung, K.H., Sineshchekov, O.A., and Spudich, J.L., *Chlamydomonas* sensory Rhodopsins A and B: Cellular content and role in photophobic responses. *Biophysical Journal*, 2004. **86**(4): p. 2342-2349.
13. Sineshchekov, O.A., Govorunova, E.G., Jung, K.H., Zauner, S., Maier, U.G., and Spudich, J.L., Rhodopsin-mediated photoreception in cryptophyte flagellates. *Biophysical Journal*, 2005. **89**(6): p. 4310-4319.
14. Sineshchekov, O.A., Jung, K.H., and Spudich, J.L., Two rhodopsins mediate phototaxis to low- and high-intensity light in *Chlamydomonas reinhardtii*. *Proceedings of the National Academy of Sciences of the United States of America*, 2002. **99**(13): p. 8689-8694.
15. Balashov, S.P., Imasheva, E.S., Boichenko, V.A., Anton, J., Wang, J.M., and Lanyi, J.K., Xanthorhodopsin: a proton pump with a light-harvesting carotenoid antenna. *Science*, 2005. **309**(5743): p. 2061-4.
16. Polivka, T. and Sundstrom, V., Ultrafast dynamics of carotenoid excited states - From solution to natural and artificial systems. *Chemical Reviews*, 2004. **104**(4): p. 2021-2071.
17. Mongodin, E.F., Nelson, K.E., Daugherty, S., Deboy, R.T., Wister, J., Khouri, H., Weidman, J., Walsh, D.A., Papke, R.T., Sanchez Perez, G., Sharma, A.K., Nesbo, C.L.,

- MacLeod, D., Bapteste, E., Doolittle, W.F., Charlebois, R.L., Legault, B., and Rodriguez-Valera, F., The genome of *Salinibacter ruber*: convergence and gene exchange among hyperhalophilic bacteria and archaea. *Proceedings of the National Academy of Sciences of the United States of America*, 2005. **102**(50): p. 18147-52.
18. Jiang, Z.Y., Swem, L.R., Rushing, B.G., Devanathan, S., Tollin, G., and Bauer, C.E., Bacterial photoreceptor with similarity to photoactive yellow protein and plant phytochromes. *Science*, 1999. **285**(5426): p. 406-409.
 19. Kyndt, J.A., Meyer, T.E., and Cusanovich, M.A., Photoactive yellow protein, bacteriophytochrome, and sensory rhodopsin in purple phototrophic bacteria. *Photochemical & Photobiological Sciences*, 2004. **3**(6): p. 519-30.
 20. Nozue, K., Kanegae, T., Imaizumi, T., Fukuda, S., Okamoto, H., Yeh, K.C., Lagarias, J.C., and Wada, M., A phytochrome from the fern *Adiantum* with features of the putative photoreceptor NPH1. *Proceedings of the National Academy of Sciences of the United States of America*, 1998. **95**(26): p. 15826-15830.
 21. Suetsugu, N., Mittmann, F., Wagner, G., Hughes, J., and Wada, M., A chimeric photoreceptor gene, NEOCHROME, has arisen twice during plant evolution. *Proceedings of the National Academy of Sciences of the United States of America*, 2005. **102**(38): p. 13705-13709.
 22. Hoff, W.D., Jung, K.H., and Spudich, J.L., Molecular mechanism of photosignaling by archaeal sensory rhodopsins. *Annual Review of Biophysics and Biomolecular Structure*, 1997. **26**: p. 223-258.
 23. Klare, J.P., Gordeliy, V.I., Labahn, J., Buldt, G., Steinhoff, H.J., and Engelhard, M., The archaeal sensory rhodopsin II/transducer complex: a model for transmembrane signal transfer. *FEBS Letters*, 2004. **564**(3): p. 219-224.
 24. Sakmar, T.P., Menon, S.T., Marin, E.P., and Awad, E.S., Rhodopsin: Insights from recent structural studies. *Annual Review of Biophysics and Biomolecular Structure*, 2002. **31**: p. 443-484.
 25. Bogomolni, R.A., Stoeckenius, W., Szundi, I., Perozo, E., Olson, K.D., and Spudich, J.L., Removal of Transducer Htri Allows Electrogenic Proton Translocation by Sensory Rhodopsin-I. *Proceedings of the National Academy of Sciences of the United States of America*, 1994. **91**(21): p. 10188-10192.
 26. Spudich, J.L., Protein-Protein Interaction Converts a Proton Pump into a Sensory Receptor. *Cell*, 1994. **79**(5): p. 747-750.
 27. Gartner, W. and Losi, A., Crossing the borders: archaeal rhodopsins go bacterial. *Trends in Microbiology*, 2003. **11**(9): p. 405-407.
 28. Jung, K.H., Trivedi, V.D., and Spudich, J.L., Demonstration of a sensory rhodopsin in eubacteria. *Molecular Microbiology*, 2003. **47**(6): p. 1513-1522.
 29. Vogeley, L. and Luecke, H., Crystallization, X-ray diffraction analysis and SIRAS/molecular-replacement phasing of three crystal forms of *Anabaena* sensory rhodopsin transducer. *Acta Crystallographica Section F-Structural Biology and Crystallization Communications*, 2006. **62**: p. 388-391.
 30. Vogeley, L., Sineshchekov, O.A., Trivedi, V.D., Sasaki, J., Spudich, J.L., and Luecke, H., *Anabaena* sensory rhodopsin: A photochromic color 0 sensor at 2.0 angstrom. *Science*, 2004. **306**(5700): p. 1390-1393.
 31. Sineshchekov, O.A., Trivedi, V.D., Sasaki, J., and Spudich, J.L., Photochromicity of *Anabaena* sensory rhodopsin, an atypical microbial receptor with a cis-retinal light-adapted form. *Journal of Biological Chemistry*, 2005. **280**(15): p. 14663-14668.
 32. Jung, K.H., The distinct signaling mechanisms of microbial sensory rhodopsins in Archaea, Eubacteria and Eukarya. *Photochemistry and Photobiology*, 2007. **83**(1): p. 63-69.
 33. Spudich, J.L., The multitasking microbial sensory rhodopsins. *Trends in Microbiology*, 2006. **14**(11): p. 480-7.

34. Nagel, G., Ollig, D., Fuhrmann, M., Kateriya, S., Mustl, A.M., Bamberg, E., and Hegemann, P., Channelrhodopsin-1: A light-gated proton channel in green algae. *Science*, 2002. **296**(5577): p. 2395-2398.
35. Nagel, G., Szellas, T., Huhn, W., Kateriya, S., Adeishvili, N., Berthold, P., Ollig, D., Hegemann, P., and Bamberg, E., Channelrhodopsin-2, a directly light-gated cation-selective membrane channel. *Proceedings of the National Academy of Sciences of the United States of America*, 2003. **100**(24): p. 13940-13945.
36. Sineshchekov, O.A. and Govorunova, E.G., Rhodopsin-mediated photosensing in green flagellated algae. *Trends in Plant Science*, 1999. **4**(2): p. 58-63.
37. Kateriya, S., Nagel, G., Bamberg, E., and Hegemann, P., "Vision" in single-celled algae. *News in Physiological Sciences*, 2004. **19**: p. 133-137.
38. Butler, W.L., Norris, K.H., Siegelman, H.W., and Hendricks, S.B., Detection, Assay, and Preliminary Purification of the Pigment Controlling Photoresponsive Development of Plants. *Proceedings of the National Academy of Sciences of the United States of America*, 1959. **45**(12): p. 1703-1708.
39. Karniol, B., Wagner, J.R., Walker, J.M., and Vierstra, R.D., Phylogenetic analysis of the phytochrome superfamily reveals distinct microbial subfamilies of photoreceptors. *Biochemical Journal*, 2005. **392**: p. 103-116.
40. Aravind, L. and Ponting, C.P., The GAF domain: an evolutionary link between diverse phototransducing proteins. *Trends in Biochemical Sciences*, 1997. **22**(12): p. 458-459.
41. Rockwell, N.C., Su, Y.S., and Lagarias, J.C., Phytochrome structure and signaling mechanisms. *Annual Review of Plant Biology*, 2006. **57**: p. 837-858.
42. Wu, S.H. and Lagarias, J.C., Defining the bilin lyase domain: Lessons from the extended phytochrome superfamily. *Biochemistry*, 2000. **39**(44): p. 13487-13495.
43. Bhoo, S.H., Davis, S.J., Walker, J., Karniol, B., and Vierstra, R.D., Bacteriophytochromes are photochromic histidine kinases using a biliverdin chromophore. *Nature*, 2001. **414**(6865): p. 776-779.
44. Lamparter, T., Evolution of cyanobacterial and plant phytochromes. *FEBS Letters*, 2004. **573**(1-3): p. 1-5.
45. Lamparter, T., Carrascal, M., Michael, N., Martinez, E., Rottwinkel, G., and Abian, J., The biliverdin chromophore binds covalently to a conserved cysteine residue in the N-terminus of *Agrobacterium phytochrome* Agp1. *Biochemistry*, 2004. **43**(12): p. 3659-3669.
46. Kehoe, D.M. and Grossman, A.R., New classes of mutants in complementary chromatic adaptation provide evidence for a novel four-step phosphorelay system. *Journal of Bacteriology*, 1997. **179**(12): p. 3914-3921.
47. Vierstra, R.D. and Davis, S.J., Bacteriophytochromes: new tools for understanding phytochrome signal transduction. *Seminars in Cell and Developmental Biology*, 2000. **11**(6): p. 511-21.
48. Terauchi, K., Montgomery, B.L., Grossman, A.R., Lagarias, J.C., and Kehoe, D.M., RcaE is a complementary chromatic adaptation photoreceptor required for green and red light responsiveness. *Molecular Microbiology*, 2004. **51**(2): p. 567-577.
49. Davis, S.J., Vener, A.V., and Vierstra, R.D., Bacteriophytochromes: Phytochrome-like photoreceptors from nonphotosynthetic eubacteria. *Science*, 1999. **286**(5449): p. 2517-2520.
50. Gressel, J., Blue-Light Photoreception. *Photochemistry and Photobiology*, 1979. **30**(6): p. 749-754.
51. Weber, S., Light-driven enzymatic catalysis of DNA repair: a review of recent biophysical studies on photolyase. *Biochimica et Biophysica Acta-Bioenergetics*, 2005. **1707**(1): p. 1-23.
52. Fujihashi, M., Numoto, N., Kobayashi, Y., Mizushima, A., Tsujimura, M., Nakamura, A., Kawarabayashi, Y., and Miki, K., Crystal structure of archaeal photolyase from *Sulfolobus*

- tokodaii* with two FAD molecules: Implication of a novel light-harvesting cofactor. *Journal of Molecular Biology*, 2007. **365**(4): p. 903-910.
53. Ueda, T., Kato, A., Kuramitsu, S., Terasawa, H., and Shimada, I., Identification and characterization of a second chromophore of DNA photolyase from *Thermus thermophilus* HB27. *Journal of Biological Chemistry*, 2005. **280**(43): p. 36237-36243.
 54. Losi, A., Flavin-based blue-light photosensors: A photobiophysics update. *Photochemistry and Photobiology*, 2007. **83**(6): p. 1283-1300.
 55. Brudler, R., Hitomi, K., Daiyasu, H., Toh, H., Kucho, K., Ishiura, M., Kanehisa, M., Roberts, V.A., Todo, T., Tainer, J.A., and Getzoff, E.D., Identification of a new cryptochrome class: Structure, function, and evolution. *Molecular Cell*, 2003. **11**(1): p. 59-67.
 56. Selby, C.P. and Sancar, A., A cryptochrome/photolyase class of enzymes with single-stranded DNA-specific photolyase activity. *Proceedings of the National Academy of Sciences of the United States of America*, 2006. **103**(47): p. 17696-17700.
 57. Ahmad, M. and Cashmore, A.R., Hy4 Gene of a *Thaliana* Encodes a Protein with Characteristics of a Blue-Light Photoreceptor. *Nature*, 1993. **366**(6451): p. 162-166.
 58. Jenkins, G.I., Christie, J.M., Fuglevand, G., Long, J.C., and Jackson, J.A., Plant responses to UV and blue light: Biochemical and genetic approaches. *Plant Science*, 1995. **112**(2): p. 117-138.
 59. Ahmad, M., Jarillo, J.A., and Cashmore, A.R., Chimeric proteins between cry1 and cry2 *Arabidopsis* blue light photoreceptors indicate overlapping functions and varying protein stability. *Plant Cell*, 1998. **10**(2): p. 197-207.
 60. Lin, C.T., Yang, H.Y., Guo, H.W., Mockler, T., Chen, J., and Cashmore, A.R., Enhancement of blue-light sensitivity of *Arabidopsis* seedlings by a blue light receptor cryptochrome 2. *Proceedings of the National Academy of Sciences of the United States of America*, 1998. **95**(5): p. 2686-2690.
 61. Huala, E., Oeller, P.W., Liscum, E., Han, I.S., Larsen, E., and Briggs, W.R., *Arabidopsis* NPH1: A protein kinase with a putative redox-sensing domain. *Science*, 1997. **278**(5346): p. 2120-2123.
 62. Briggs, W.R., Christie, J.M., and Salomon, M., Phototropins: A new family of flavin-binding blue light receptors in plants. *Antioxidants & Redox Signaling*, 2001. **3**(5): p. 775-788.
 63. Briggs, W.R. and Christie, J.M., Phototropins 1 and 2: versatile plant blue-light receptors. *Trends in Plant Science*, 2002. **7**(5): p. 204-210.
 64. Kasahara, M., Swartz, T.E., Olney, M.A., Onodera, A., Mochizuki, N., Fukuzawa, H., Asamizu, E., Tabata, S., Kanegae, H., Takano, M., Christie, J.M., Nagatani, A., and Briggs, W.R., Photochemical properties of the flavin mononucleotide-binding domains of the phototropins from *Arabidopsis*, rice, and *Chlamydomonas reinhardtii*. *Plant Physiology*, 2002. **129**(2): p. 762-773.
 65. Salomon, M., Christie, J.M., Knieb, E., Lempert, U., and Briggs, W.R., Photochemical and mutational analysis of the FMN-binding domains of the plant blue light receptor, phototropin. *Biochemistry*, 2000. **39**(31): p. 9401-9410.
 66. Swartz, T.E., Corchnoy, S.B., Christie, J.M., Lewis, J.W., Szundi, I., Briggs, W.R., and Bogomolni, R.A., The photocycle of a flavin-binding domain of the blue light photoreceptor phototropin. *Journal of Biological Chemistry*, 2001. **276**(39): p. 36493-36500.
 67. Kennis, J.T.M., Crosson, S., Gauden, M., van Stokkum, I.H.M., Moffat, K., and van Grondelle, R., Primary reactions of the LOV2 domain of phototropin, a plant blue-light photoreceptor. *Biochemistry*, 2003. **42**(12): p. 3385-3392.
 68. Penzkofer, A., Endres, L., Schiereis, T., and Hegemann, P., Yield of photo-adduct formation of LOV domains from *Chlamydomonas reinhardtii* by picosecond laser excitation. *Chemical Physics*, 2005. **316**(1-3): p. 185-194.

69. Crosson, S. and Moffat, K., Structure of a flavin-binding plant photoreceptor domain: Insights into light-mediated signal transduction. *Proceedings of the National Academy of Sciences of the United States of America*, 2001. **98**(6): p. 2995-3000.
70. Crosson, S. and Moffat, K., Photoexcited structure of a plant photoreceptor domain reveals a light-driven molecular switch. *Plant Cell*, 2002. **14**(5): p. 1067-1075.
71. Fedorov, R., Schlichting, I., Hartmann, E., Domratcheva, T., Fuhrmann, M., and Hegemann, P., Crystal structures and molecular mechanism of a light-induced signaling switch: The Phot-LOV1 domain from *Chlamydomonas reinhardtii*. *Biophysical Journal*, 2003. **84**(4): p. 2474-2482.
72. Corchnoy, S.B., Swartz, T.E., Lewis, J.W., Szundi, I., Briggs, W.R., and Bogomolni, R.A., Intramolecular proton transfers and structural changes during the photocycle of the LOV2 domain of phototropin 1. *Journal of Biological Chemistry*, 2003. **278**(2): p. 724-731.
73. Swartz, T.E., Wenzel, P.J., Corchnoy, S.B., Briggs, W.R., and Bogomolni, R.A., Vibration spectroscopy reveals light-induced chromophore and protein structural changes in the LOV2 domain of the plant blue-light receptor phototropin 1. *Biochemistry*, 2002. **41**(23): p. 7183-7189.
74. Harper, S.M., Christie, J.M., and Gardner, K.H., Disruption of the LOV-J alpha helix interaction activates phototropin kinase activity. *Biochemistry*, 2004. **43**(51): p. 16184-16192.
75. Harper, S.M., Neil, L.C., and Gardner, K.H., Structural basis of a phototropin light switch. *Science*, 2003. **301**(5639): p. 1541-1544.
76. Crosson, S., Rajagopal, S., and Moffat, K., The LOV domain family: Photoresponsive signaling modules coupled to diverse output domains. *Biochemistry*, 2003. **42**(1): p. 2-10.
77. Losi, A., The bacterial counterparts of plant phototropins. *Photochemical & Photobiological Sciences*, 2004. **3**(6): p. 566-574.
78. Briggs, W.R., The LOV domain: a chromophore module servicing multiple photoreceptors. *Journal of Biomedical Science*, 2007. **14**(4): p. 499-504.
79. Losi, A., Polverini, E., Quest, B., and Gartner, W., First evidence for phototropin-related blue-light receptors in prokaryotes. *Biophysical Journal*, 2002. **82**(5): p. 2627-2634.
80. Krauss, U., Losi, A., Gartner, W., Jaeger, K.E., and Eggert, T., Initial characterization of a blue-light sensing, phototropin-related protein from *Pseudomonas putida*: a paradigm for an extended LOV construct. *Physical Chemistry Chemical Physics*, 2005. **7**(14): p. 2804-2811.
81. Swartz, T.E., Tseng, T.S., Frederickson, M.A., Paris, G., Comerci, D.J., Rajashekar, G., Kim, J.G., Mudgett, M.B., Splitter, G.A., Ugalde, R.A., Goldbaum, F.A., Briggs, W.R., and Bogomolni, R.A., Blue-light-activated histidine kinases: Two-component sensors in bacteria. *Science*, 2007. **317**(5841): p. 1090-1093.
82. Avila-Perez, M., Hellingwerf, K.J., and Kort, R., Blue light activates the sigma(B)-dependent stress response of *Bacillus subtilis* via YtvA. *Journal of Bacteriology*, 2006. **188**(17): p. 6411-6414.
83. Gaidenko, T.A., Kim, T.J., Weigel, A.L., Brody, M.S., and Price, C.W., The blue-light receptor YtvA acts in the environmental stress signaling pathway of *Bacillus subtilis*. *Journal of Bacteriology*, 2006. **188**(17): p. 6387-6395.
84. Purcell, E.B., Siegal-Gaskins, D., Rawling, D.C., Fiebig, A., and Crosson, S., A photosensory two-component system regulates bacterial cell attachment. *Proceedings of the National Academy of Sciences of the United States of America*, 2007. **104**(46): p. 18241-18246.
85. Froehlich, A.C., Liu, Y., Loros, J.J., and Dunlap, J.C., White collar-1, a circadian blue light photoreceptor, binding to the frequency promoter. *Science*, 2002. **297**(5582): p. 815-819.
86. He, Q.Y., Cheng, P., Yang, Y.H., Wang, L.X., Gardner, K.H., and Liu, Y., White collar-1, a DNA binding transcription factor and a light sensor. *Science*, 2002. **297**(5582): p. 840-843.

87. Idnurm, A. and Heitman, J., Light controls growth and development via a conserved pathway in the fungal kingdom. *Plos Biology*, 2005. **3**(4): p. 615-626.
88. Idnurm, A., Rodriguez-Romero, J., Corrochano, L.M., Sanz, C., Iturriaga, E.A., Eslava, A.P., and Heitman, J., The *Phycomyces* madA gene encodes a blue-light photoreceptor for phototropism and other light responses. *Proceedings of the National Academy of Sciences of the United States of America*, 2006. **103**(12): p. 4546-4551.
89. Silva, F., Torres-Martinez, S., and Garre, V., Distinct white collar-1 genes control specific light responses in *Mucor circinelloides*. *Molecular Microbiology*, 2006. **61**(4): p. 1023-1037.
90. Gomelsky, M. and Klug, G., BLUF: a novel FAD-binding domain involved in sensory transduction in microorganisms. *Trends in Biochemical Sciences*, 2002. **27**(10): p. 497-500.
91. Okajima, K., Yoshihara, S., Fukushima, Y., Geng, X.X., Katayama, M., Higashi, S., Watanabe, M., Sato, S., Tabata, S., Shibata, Y., Itoh, S., and Ikeuchi, M., Biochemical and functional characterization of BLUF-type flavin-binding proteins of two species of cyanobacteria. *Journal of Biochemistry*, 2005. **137**(6): p. 741-750.
92. Gomelsky, M. and Kaplan, S., AppA, a Novel Gene Encoding a Trans-Acting Factor Involved in the Regulation of Photosynthesis Gene-Expression in *Rhodobacter sphaeroides* 2.4.1. *Journal of Bacteriology*, 1995. **177**(16): p. 4609-4618.
93. Gomelsky, M. and Kaplan, S., Molecular genetic analysis suggesting interactions between AppA and PpsR in regulation of photosynthesis gene expression in *Rhodobacter sphaeroides* 2.4.1. *Journal of Bacteriology*, 1997. **179**(1): p. 128-134.
94. Gomelsky, M. and Kaplan, S., AppA, a redox regulator of photosystem formation in *Rhodobacter sphaeroides* 2.4.1, is a flavoprotein - Identification of a novel FAD binding domain. *Journal of Biological Chemistry*, 1998. **273**(52): p. 35319-35325.
95. Braatsch, S., Gomelsky, M., Kuphal, S., and Klug, G., A single flavoprotein, AppA, integrates both redox and light signals in *Rhodobacter sphaeroides*. *Molecular Microbiology*, 2002. **45**(3): p. 827-36.
96. Dragnea, V., Waegle, M., Balascuta, S., Bauer, C., and Dragnea, B., Time-resolved spectroscopic studies of the AppA blue-light receptor BLUF domain from *Rhodobacter sphaeroides*. *Biochemistry*, 2005. **44**(49): p. 15978-15985.
97. Gauden, M., Yeremenko, S., Laan, W., van Stokkum, I.H.M., Ihalainen, J.A., van Grondelle, R., Hellingwerf, K.J., and Kennis, J.T.M., Photocycle of the flavin-binding photoreceptor AppA, a bacterial transcriptional antirepressor of photosynthesis genes. *Biochemistry*, 2005. **44**(10): p. 3653-3662.
98. Ito, S., Murakami, A., Sato, K., Nishina, Y., Shiga, K., Takahashi, T., Higashi, S., Iseki, M., and Watanabe, M., Photocycle features of heterologously expressed and assembled eukaryotic flavin-binding BLUF domains of photoactivated adenylyl cyclase (PAC), a blue-light receptor in *Euglena gracilis*. *Photochemical & Photobiological Sciences*, 2005. **4**(9): p. 762-769.
99. Rajagopal, S., Key, J.M., Purcell, E.B., Boerema, D.J., and Moffat, K., Purification and initial characterization of a putative blue light-regulated phosphodiesterase from *Escherichia coli*. *Photochemistry and Photobiology*, 2004. **80**(3): p. 542-547.
100. Iseki, M., Matsunaga, S., Murakami, A., Ohno, K., Shiga, K., Yoshida, K., Sugai, M., Takahashi, T., Hori, T., and Watanabe, M., A blue-light-activated adenylyl cyclase mediates photoavoidance in *Euglena gracilis*. *Nature*, 2002. **415**(6875): p. 1047-1051.

Chapter three

3 Photoactive Yellow Proteins

3.1 History

In 1985, a small yellow-colored protein was isolated during a search for soluble electron-transport proteins in the extreme halophilic and phototrophic bacterium *Halorhodospira*[†] *halophila* (Hhal) strain BN9626 [2]. The yellow protein was not identical to any protein previously reported but the UV-visible absorption spectrum ($\lambda_{\max} = 446$ nm) suggested a chromophore similar to flavins, which have an oxygen, nitrogen or sulfur substitution of the 8-methyl group. Two years later, the protein was shown to be photoactive as the color could be reversibly bleached by a pulse of 445 nm laser light, and was hence referred to as Photoactive Yellow Protein (PYP) [3]. In fact, the photochemical properties strongly resembled the retinal-containing sensory rhodopsins from *Halobacterium halobium* [4], although no retinal could be extracted from PYP after acid treatment [3]. The amino acid sequence of PYP from *H. halophila* BN9626 was determined in 1993 through automated sequence analysis, and showed that the protein consists of a single peptide chain of 125 amino acid residues [5]. The molecular weight of the pure protein (14,021.4 Da) was assessed by electrospray mass spectrometry, and revealed a mass difference of 146.9 Da compared to the calculated mass. This was due to the presence of the unidentified chromophore, which was shown to be covalently linked to cysteine 69 [5]. That same year, a first implication about PYP's biological function arose, when the absorption spectrum of PYP was shown to be similar to the wavelength dependence of *H. halophila* cells reverting their swimming direction upon a sudden increase in light intensity, which is also called a step-up 'photophobic' ('fear of light) response [6]. Consequently, PYP was suggested to function as the primary photoreceptor for a negative photoresponse towards blue light, as a way of protection against harmful UV-light. However, this hypothesis has never been verified genetically, for example through knock-out mutants, and it is still unknown how the PYP might affect the direction of swimming if involved at all. In 1994, two research groups independently resolved the chemical structure of the chromophore [7, 8]. From measurements of molecular weight, UV-absorbance, NMR-spectra, capillary electrophoresis, chemical cleavage and high resolution mass spectrometry, the prosthetic group was unambiguously identified as 4-hydroxycinnamic acid (also known as *p*-hydroxycinnamic acid or *p*-coumaric acid), linked to C69 via a thiol ester. This was the first

[†] In 1996, the purple bacterium was removed from the genus *Ectothiorhodospira*, based on 16S rRNA sequences, and reassigned to the new genus *Halorhodospira* gen. nov [1].

example ever reported of *p*-hydroxycinnamic acid (pHCA) to occur as a cofactor in Eubacteria. The three-dimensional structure, resolved in 1995 by X-ray crystallography at 1.4 Å resolution, indicated that PYP contains a central β -sheet flanked on either side by short loops and helices [8, 9]. This α/β -fold, previously unrecognized in prokaryotes, showed similarities with the eukaryotic signal transduction domains SH2 and profilin. Key amino acid residues were observed to interact with the chromophore, thus creating an active site suited for photon-induced conformational changes and subsequent signal transduction.

The *pyp* gene sequence from *H. halophila* BN9626 was cloned by Baca *et al.* in 1994 [8] and Kort *et al.* in 1996 [10]. The translated amino acid sequence matched the previously published protein sequence [5] with one exception: Gln56 replaced Glu56. When the genome sequence of *Halorhodospira halophila* SL-1 (type strain) was released in 2006 (Joint Genome Institute), the *pyp* gene was found to be organized in an operon with two enzymes that catalyze the activation and biosynthesis of the *p*-coumaric acid chromophore, respectively (see section 3.5) [11]. Moreover, the amino acid sequences of *H. halophila* PYP from strains BN9626 and SL-1 differ in eight positions, but none of the substitutions are situated in the active site. Interestingly, the genome of *H. halophila* SL-1 contains a second *pyp* gene, encoding for a 130 amino acid containing protein that shares 60% sequence identity with the previously characterized PYP. Although its heterologously reconstituted protein product was shown to be photoactive ($\lambda_{\max} = 443$ nm) [12], PYP(B) has never been observed in *H. halophila* extracts, which suggests that it is not very abundant or that its expression is itself regulated, unlike the prototypic PYP which appears to be constitutively expressed. Since its discovery more than two decades ago, many other PYP homologues have been identified in various bacterial species (as further described in section 3.4), and many more are expected to be discovered. PYP from *H. halophila*, however, is by far the best characterized Photoactive Yellow Protein in terms of structure and physico-chemical properties. Moreover, it has become the structural prototype for a large and diverse family of sensory proteins generally known as PAS¹ domains that are found in virtually all forms of life.

3.2 Photochemical reactions

Upon blue light illumination, PYP undergoes a cyclic series of dark reactions [3], and several intermediates of the Hhal PYP solution photocycle could be distinguished based on their spectral and temporal changes, as shown in **Figure 3.1**. In the dark or ground state form P ($\lambda_{\max} = 446$ nm), the anionic form of the chromophore is stabilized by hydrogen bonds to E46 and

¹ PAS; Acronym based upon periodic clock protein, aryl hydrocarbon receptor nuclear translocator and, single minded protein

Y42. Absorption of a blue light photon ($\lambda_{\text{max}} = 446 \text{ nm}$) results in an electronically excited state P^* , followed by rapid *trans-to-cis* isomerization around the 7-8 double bond of the *p*-hydroxycinnamoyl chromophore. Accompanying chromophore isomerization, the dark-adapted state P is rapidly converted into I_0 (1.9 ps) and subsequently into I_0^\ddagger (220 ps), both absorbing at 510 nm [13, 14]. In about 3 ns, I_0^\ddagger decays into the red-shifted intermediate I_1 ($\lambda_{\text{max}} = 465 \text{ nm}$) [15, 16]. I_1 decays in $\sim 500 \mu\text{s}$ to I_1' , in which the deprotonated chromophore becomes exposed to the solvent [17]. Fast protonation of the phenolic oxygen by the solvent results in the blue-shifted I_2 intermediate ($\lambda_{\text{max}} = 355 \text{ nm}$), in which the hydrogen bonds to E46 and Y42 are broken. Since the formation of the I_2 intermediate is accompanied by a loss of visible color, the I_1 to I_2 transition is therefore also referred to as the '(photo)bleaching reaction'. Then, a major conformational change, occurring in about 1.5 ms and which involves exposure of a significant part of the hydrophobic protein interior, forms the I_2' intermediate. The I_2 and I_2' intermediates are in equilibrium [18], and this equilibrium is pH-dependent, with a pK_a of 6.4 [19, 20]. Finally, I_2' recovers back to the dark state P in about 160 milliseconds [21], and this step is referred to as the 'recovery reaction'. Since the I_2' intermediate is the longest living species and the only one with a significant conformational change (see below), it is generally believed to be the signaling state that allows interaction with an unknown signal transducer in the case of *H. halophila* PYP.

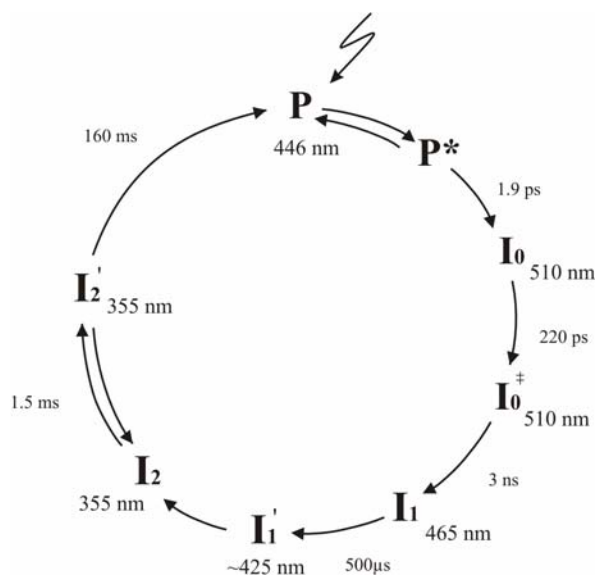


Figure 3.1

Schematic representation of the solution photocycle of Hhal PYP at room temperature and neutral pH, initiated by the absorption of a blue-light photon. Each intermediate is followed by its half-life. Subscripts refer to the absorption maxima. Additional intermediates may be present, especially under frozen, crystalline, or dehydrated states.

The PYP photocycle shows different properties when the protein is in some way restrained, such as in crystals [22], at low-temperature [23, 24] or in a dehydrated state [25], and may involve additional intermediates.

By comparison with the formation of the triplet state of chlorophyll by laser flash excitation, the quantum yield of the photobleaching reaction of Hhal PYP was calculated to be ~ 0.6 [26], which was later confirmed during a study of the early intermediates obtained by photobleaching experiments [14, 27]. Although independent reports have determined it to be lower (~ 0.35 , [28]), the quantum yield is still large enough to be biologically significant. The quantum yield for fluorescence, on the other hand, is very small (0.0014 – 0.0035, [23, 25, 29]).

The effects of temperature, hydrophobicity, viscosity and pH of the solvent on the photocycle kinetics of Hhal PYP have been extensively studied [26, 30, 31]. The effect of temperature follows normal Arrhenius behavior for the bleaching reaction, while the kinetics of recovery has a bell-shaped dependence on temperature [26]: the reaction becomes twice as fast between 5°C and 35°C, and then slows down threefold when the temperature is raised to 62°C, indicating alternate conformations with differing kinetics [26]. This deviation has been quantitatively described by a thermodynamic model as a change in heat capacity of the protein, resulting from the bleached state being more hydrophobic than the ground state [31].

By verifying the kinetics in various alcohol-water mixtures, it was demonstrated that the rate constant for the bleaching reaction increases with the hydrophobicity of the solvent, which at the same time decreases the rate constant for dark state recovery. Moreover, the photobleached I_2' state binds to lipid bilayers [32] and to dyes [21]. This suggests that formation of I_2' is accompanied by a conformational change which exposes hydrophobic residues to the solvent, consistent with the thermodynamic model [31], and may be important for binding to a hydrophobic site of a yet unknown signal transduction partner [26].

The Hhal PYP photocycle is affected by ionic strength and solution pH. With increasing salt concentration up to 600 mM the recovery rate decreases and the I_2/I_2' equilibrium shifts in the direction of I_2' due to screening of the ion pair E12/K110, while at higher ionic strength both effects reverse [33]. Over the pH range 5-10, the rate constant for photobleaching decreases about threefold with a pKa of approximately 5.7 [30], and is consistent with a protonation event during the formation of I_2 [34]. The dark recovery is maximal at pH 8, which is 16 times faster than at pH 5 [30], and shows a bell-shaped dependence on pH, controlled by the pK_a values of 6.4 and 9.4. The pK_a values of 5.7 and 6.4 are believed to represent the ionization of the E46 carboxylic acid, while the pKa at 9.4 would reflect the deprotonation of the chromophore hydroxyl [34], when these functional groups are exposed to solvent following flash photolysis. They fit the model in which the recovery reaction will be slow when both groups are protonated or ionized at low pH or high pH respectively, but will be fastest at neutral pH where presumably only E46 is ionized during $I_2 - I_2'$ transition [35]. There is evidence from FTIR that a proton can

be transferred from E46 to the chromophore during photobleaching [36]. However, kinetics of proton uptake and release are perfectly synchronized with transient absorption changes in WT and E46Q and E46A mutants, suggesting that protons are taken up from the solvent rather than being transferred from E46 [17, 37]. Upon recovery, the chromophore is deprotonated through hydroxide uptake from the solvent [17, 37].

3.3 PYP properties

PYP has become the structural prototype for the large family of signaling proteins containing the PAS domain sequence motif [25]. Moreover, as a result of some of its intrinsic features (*i.e.* small size, water-soluble, stable along a broad pH and temperature range, and known photocycle), and the access to high-resolution structural information for the PYP ground state [9] and some of the photocycle intermediates [15, 38, 39], in combination with the feasibility of site-directed mutagenesis [13, 30, 40] and reconstitution of chromophore variants [41, 42], this blue-light photoreceptor has become an attractive model system to study the molecular events related to the conversion of light energy into a biological signal.

3.3.1 Structural features

The crystal structures of two wild-type PYP species, *i.e.* of the prototypic PYP from *H. halophila* [9] and the PYP domain from *Rhodospirillum centenum* Ppr [43], and several Hhal PYP mutants, such as Y98Q and E46Q [44, 45] among others, have been determined. PYP adopts an α/β -fold composed of a central anti-parallel β -sheet flanked by helices, as shown in **Figure 3.2**.



Figure 3.2

Structure of Hhal PYP. Key structural elements include the N-terminal cap or first two helices, the β -scaffold (green), the chromophore binding loop and the connecting helix. Note that, upon illumination, the global conformational change is believed to occur mainly in the N-terminal domain (see Section 3.3.2), which is however located on the other side of the β -scaffold relative to the chromophore binding pocket where the initial structural perturbation is localized. (A) View with the N-terminal cap at the back, the chromophore to the left, the β -scaffold in the middle and the connecting helix in the upper left corner. (B) End-on view of the β -scaffold, with the N-terminus on the left, the chromophore on the right, and the connecting helix at the right rear. Image taken from [25].

There are two hydrophobic cores located on either side of the central β -sheet, and the chromophore itself is covalently

bound via a thioester to C69 in the major hydrophobic cavity where it interacts with a number of key amino acids by a network of hydrogen bonds. The three-dimensional structure of Hhal PYP in the dark state [9] shows that the protonated carboxylate of E46 and the hydroxyl of Y42 are hydrogen-bonded to the phenolic oxygen of the chromophore (**Figure 3.3**). The chromophore carbonyl oxygen atom hydrogen binds to the main-chain amide group of C69. The T50 side chain is hydrogen-bonded to the hydroxyl of Y42 and to the E46 backbone. The chromophore is shielded from the solvent by R52, which forms hydrogen bonds with the carbonyls of T50 and Y98, although the NMR solution structure suggests an interaction between R52 and the ring structure of Y98 [46]. In addition, the chromophore is surrounded by a number of hydrophobic residues (F62, A67, F75 and F96 [25]), which stabilize it in the native conformation.

These binding properties of the pHCA chromophore contribute to the characteristic absorption peak (color) of the protein at 446 nm. Free protonated *trans-p*-coumaric acid absorbs at 284 nm and has a minor band at 310 nm (at neutral pH) [47]. Upon formation of the thioester bond with C69, the absorption maximum is shifted to 335 nm. A shift in the pK_a value of pHCA, resulting from the stabilizing effect of the hydrogen bonds in the native conformation, leads to deprotonation and a red-shift in the absorbance spectrum to around 410. The remaining 410 to 446 nm shift is attributed to specific interactions with the protein environment [48].

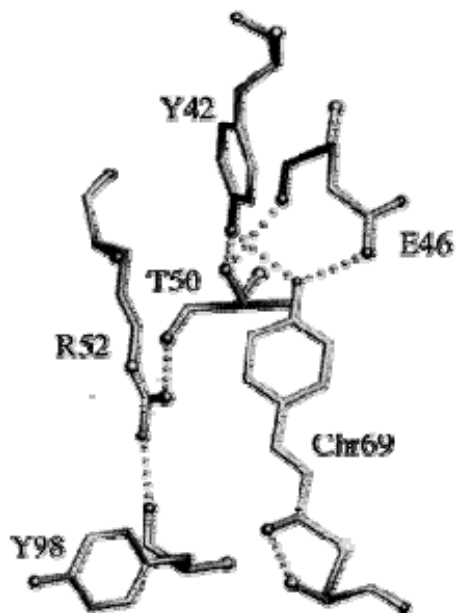


Figure 3.3

Detailed structure of the active site of Hhal PYP in the dark state [9]. Hydrogen bonds are indicated by dotted lines. Image was taken from [48].

Using time-resolved Von Laue crystallography, also the structure of a long-lived intermediate, presumed to be equivalent to I_2 , was determined [38]. When photobleached, the chromophore undergoes *trans* to *cis* isomerization, and becomes more exposed to the solvent, whereby the interaction with the nearby amino acid side chains is altered. The major movement involves R52, which is repositioned and makes a new hydrogen bond with the chromophore hydroxyl and presumably contributes to stabilization of the signaling state. E46, T50 and Y42 only move over a small distance, while C69 shows no repositioning in the bleached state [37]. These same changes are likely to occur in solution, while additional, more dynamic changes may be hampered due to crystal constraints, [25].

The structural change that arises at the chromophore double bond upon light absorption is thus relayed to the remainder of the protein, which results in a significant exposure of hydrophobic residues in the protein interior [26, 31], at least in solution. Consequently, this creates a signaling state with a new molecular surface which could interact with a specific, yet unknown, transducer, thus initiating a signal transduction cascade. Significant structural changes involving the protein backbone were not observed in the crystal structure of the two states of PYP, most likely due to crystal lattice constraints [37].

3.3.2 Mutational analysis

From crystallographic work, a number of key amino acid residues have been identified in Hhal PYP that are most likely to affect the properties of the chromophore, *i.e.* Y42, E46, T50, R52, P68, Y98 and M100. Their roles have been explored through site-directed mutagenesis, and are further discussed below.

In the dark state, **E46** forms hydrogen bonds to the chromophore's phenolate oxygen, and plays an important role in spectral tuning by lowering the pK_a for ionization of the chromophore hydroxyl in the folded protein to 2.8 or less, and is supported by the increased pK_a for pHCA ionization in the mutants E46Q (5.0), E46A (7.9) and E46D (8.6), the latter of which approaches that of the chromophore in solution (~ 9.0) [13]. Alteration of the hydrogen-bonding network like in E46Q, creates a red-shift (to 462 nm) of the absorption maximum, which is ascribed to an increased negative charge density on the chromophore [30]. However, the major effect of E46Q resides on the photocycle kinetics, in which both the formation and recovery of the I_2' intermediate are dramatically accelerated with increasing pH [25, 30]. The rate constant for dark recovery has a sigmoidal dependence on pH ($pK_a = 8$) and is increased 700-fold upon a change in pH from 5 to 10.

In Hhal PYP, **M100** partially shields the chromophore from solvent and is implicated to mediate the *cis-trans* reisomerization as a result of the polarizability of the M100 sulfur and its location above the aromatic ring of the chromophore [37, 40]. Moreover, the recovery of the photocycle is slowed down by as much as 1000-fold in the single mutants M100A, M100L and M100K, which is sufficient for ambient light to produce a steady-state bleach. The case in which the recovery rate is only decreased 20-fold in mutant M100E, is attributed to the ability of E100 to stabilize a transient positive charge on the aromatic ring during the isomerization [37, 49]. Photoreversal studies with M100A indeed show that reisomerization of the chromophore is the rate-limiting step in the recovery [40, 44]. However, PYP homologues from *Rhodobacter capsulatus* (Rcap) and *Rhodobacter sphaeroides* (Rsph) (see section 3.4) have natural M100G substitutions

(**Figure 3.7**), yet recovery is accelerated by 100-fold relative to wild-type Hhal PYP. The G100M mutant of Rcap PYP has a minimal effect on recovery, which implies that M100 interacts differently with the chromophore as a result of an altered conformation of the peptide segment containing M100 [50]. This would be analogous to what has been observed in the crystal structure of the PYP domain of the hybrid photoreceptor protein Ppr from *Rhodospirillum centenum* (Rcen) (see Section 3.4). In the latter, the $\beta 4$ - $\beta 5$ loop that contains M100 assumes a conformation unlike that in Hhal PYP, as shown in **Figure 3.4**, thereby preventing M100 to interact with the chromophore while solvent access is increased [43]. This may partially explain the more than 300-fold slower recovery of the Rcen PYP domain [51].

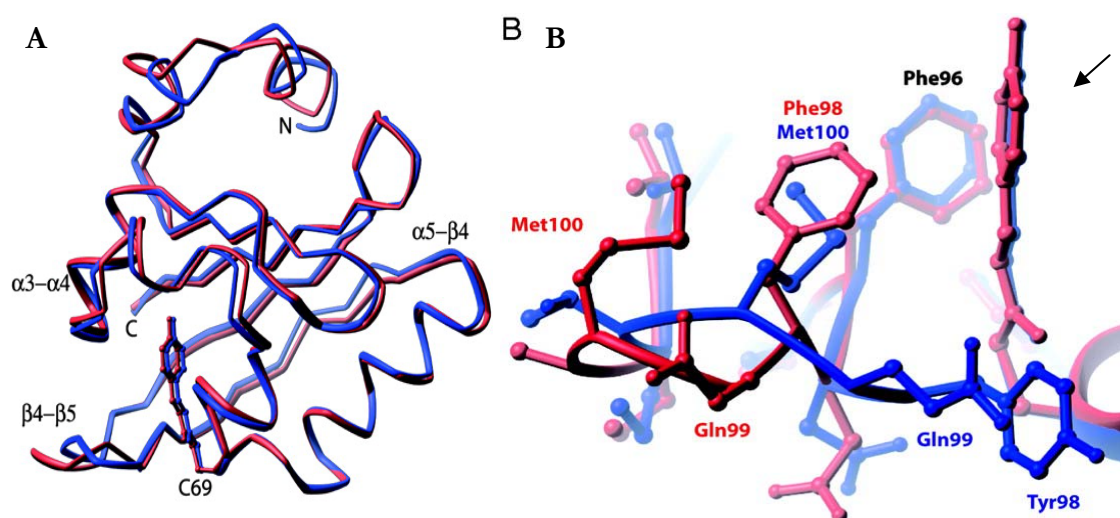


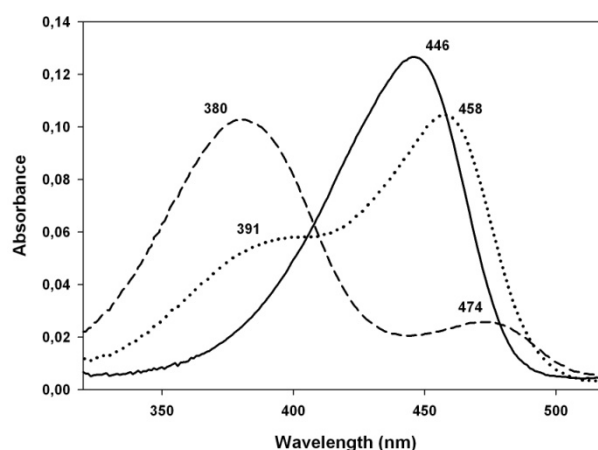
Figure 3.4

(A) Superposition of the C α chain of Ppr-PYP (red) and Hhal PYP (blue). The N- and C-termini, the C69 required for chromophore attachment, and the three loops that have statistically significant differences between Ppr-PYP and Hhal PYP are labeled. (B) Side view of the $\beta 4$ - $\beta 5$ loop of Ppr-PYP (red) and Hhal PYP (blue), after superposition as in (A). The pHCA chromophore is indicated by the arrow. Images were taken from [43].

In addition to E46, Y42 forms a direct hydrogen bond with the phenolate oxygen of the chromophore, and mutations have major outcome on the spectral properties and stability. Mutant Y42F contains a shorter wavelength shoulder (391 nm) on the 458 nm absorption maximum, that becomes dominant in the single mutants Y42A (374-450 nm) and Y42W (364-455 nm), and the double mutant Y42A/T50V (380-474 nm) [35, 37, 48, 52], as shown in **Figure 3.5**. Both the relative intensities and wavelength maxima of the shorter wavelength forms, referred to as ‘intermediate spectral forms’, are dependent on solvent and temperature, but not on pH or ambient light [35, 48].

Figure 3.5

UV-Vis absorption spectra of Hhal PYP wild-type (solid line), Y42F (dotted line) and Y42F/T50V (dashed line) at pH 7.0.



Kosmotropes, such as $(\text{NH}_4)_2\text{SO}_4$, and chaotropes, such as NH_4Cl , have opposite effects on the absorption spectrum of Y42 mutations, in which the intermediate spectral form is disfavored when the stability of the protein increases [48]. Therefore, the intermediate spectral form is believed to represent a more open but less stable conformation, which involves a change in the hydrogen bond between E46 and the chromophore, since the Y42F/E46Q double mutant has a single absorption maximum and behaves similarly as E46Q [35, 37]. Moreover, wild-type Hhal PYP and virtually all mutants tested, except those containing substitutions at E46, are capable of forming an intermediate species, which is in equilibrium with the native and unfolded protein, with a wavelength maximum between 370 and 390 nm, dependent on the concentration of denaturant [35]. These effects can be understood as an increased solvent access in the vicinity of the chromophore, either through mutation or denaturant, which raises the dielectric constant around pHCA. The more proximal solvent is thought to donate a hydrogen bond to E46, thus weakening the interaction between E46 and the chromophore.

The effect of Y42F on photocycle kinetics is much less pronounced, as shown by the respective increase and decrease of about two-fold for the bleach and recovery reaction in Y42F, but is still consistent with the reduced stability.

Although the **T50** hydroxyl donates a hydrogen bond to Y42 in Hhal PYP, its role is restricted to fine-tuning the chromophore's absorption maximum, as the T50V mutant shows only a small red-shift (to 457 nm) in the absorption spectrum and has a minimal effect on the photocycle kinetics [48]. However, the T50V/Y42F double mutant has a greater proportion of the intermediate spectral form (see above) than the Y42F single mutant (**Figure 3.5**), suggesting that Y42 and T50 mainly stabilize the chromophore in the 446 nm form [25].

The pHCA chromophore in Hhal PYP is separated from the solvent by **R52** in the ground state, which is tethered by hydrogen bonds to T50 and Y98 [46, 53]. Upon photobleaching, R52 repositions and forms a new hydrogen bond with the chromophore. A modest 6-fold decrease in the dark state recovery and the small red-shift (to 452 nm) of the R52A

mutant suggests that electrostatic interactions between R52 and the chromophore are not important for charge stabilization, in contrast to what was originally thought [30]. On the other hand, the recovery kinetics of the R52A/M100A double mutant shows a sigmoidal pH dependence ($pK_{a1} = 6.1$; $pK_{a2} = 10.0$) similar to M100A, but recovery is about 2 times slower at pH 7 and 2 times faster at pH 10 [44]. Thus, the photocycle kinetics of R52A/M100A indicates that R52 has an effect on the photocycle distinct from the catalysis of reisomerization by M100. Moreover, a third pK_a value of 7.6 is observed [44], indicating that there are additional electrostatic factors facilitating isomerization, but the nature of these interactions have not yet been identified.

Y98 is located in the $\beta 4$ - $\beta 5$ loop and interacts with R52 in the $\alpha 3$ - $\alpha 4$ loop, possibly to stabilize both loop conformations in the dark-state [53]. Moreover, Hhal PYP requires an aromatic residue at position 98 to sustain wild-type recovery kinetics, since the latter is similar in mutants Y98F and Y98W, about 4-fold slower in Y98A, and respectively 40- and 70-fold slower in Y98Q and Y98L [44]. The crystal structure of Y98Q demonstrates a conformational change of the $\beta 4$ - $\beta 5$ loop relative to wild-type PYP, and includes repositioning of M100. As dark recovery of the Y98Q/M100A double mutant is similar to the M100A mutant, slower recovery kinetics in Y98Q are thus most likely due to repositioning of M100. Consequently, it suggests that the effect on dark recovery correlates with the degree of distortion of the $\beta 4$ - $\beta 5$ loop, which would then be expected to increase in the mutants Y98A, Y98Q and Y98L respectively. Moreover, it reflects a loss in efficiency of the catalysis of reisomerization when the optimal distance between M100 and the chromophore is changed.

The PYP domains from *Rb. centenum* (Rcen) and *Thermochromatium tepidum* (Ttep) (see Section 3.4) have a natural Y98F substitution, and respectively show 300- and 1500-fold slower recovery. As already mentioned above, the Y98F mutation in Hhal PYP has no significant effect on the photocycle kinetics, most probably because there is no significant conformational change of the $\beta 4$ - $\beta 5$ loop upon mutation. On the other hand, the crystal structure of Rcen PYP shows that F98 is oriented towards the protein interior, causing repositioning of M100, as opposed to Y98 in Hhal PYP which is facing outwards (**Figure 3.4**) [44].

The absorption spectra of the Y98 mutants remain relatively unaltered, which is to be expected since this residue does not directly interact with the chromophore. However, the effect on fluorescence is more significant (see below).

In the high-resolution X-ray structure of the dark state P, Y98 and **P68** were observed to form a gate with ratchet-like properties which would sterically interfere with the *cis/trans* isomerization [53, 54], and are accordingly called ‘gateway residues’. Concerted motions of Y98,

P68, and the chromophore are thought to be necessary to open and close this gateway, leading to the initiation of the photocycle [54]. However, the rate constant for recovery of mutant P68A was only two-fold slower compared to WT PYP [44], which suggests a minimal role for P68 in the recovery to the ground state. On the other hand, P68A, Y98Q and Y98A mutations have a large effect on fluorescence quantum yields, showing 3- to 4-fold larger amplitudes of their excitation and emission spectra relative to WT [44]. Based on structural data from Y98Q, this effect on fluorescence is suggested to originate from an opening of the gateway, allowing the chromophore to obtain a more planar conformation [44]. This would be similar to the Y42F mutant, in which reversal bowing of the chromophore relative to the wild type is also associated with a marked increase in the fluorescence quantum yield [54].

Truncation of the **N-terminal cap** of Hhal PYP by 6, 15 and 23 residues has a dramatic effect on the recovery kinetics by prolonging the lifetimes of the photobleached state by about 140-, 2,300-, and 4,500-fold, respectively [55]. Such massive deletions (by as much as 20% of the total protein length) are unlikely to benefit the stability of the protein, unless the N-terminus is only weakly associated with the remainder of the protein or adopts a separate fold. The structure of the Δ 1-25 Hhal PYP dark state shows minimal changes in conformation relative to the complete protein [56]. Moreover, the N-terminal segment (residues 1-28) forms a separate subdomain that is packed against the central β -sheet through hydrophobic and electrostatic interactions [9, 53, 57], which contributes to the stabilization of the native form. However, upon deletion, the equilibrium is shifted towards the signaling state, as indicated by the slowed recovery. In addition, various solution structural studies, including NMR [58], FTIR and CD, indicate that the N-terminal cap, which consists of the first two helices, is disordered in the presumed signaling intermediate I_2' . Consequently, the N-terminus is proposed to swing away or rearrange when the native protein is photobleached [37, 59]. However, destabilization of the N-terminal cap must arise from the photoisomerization of the chromophore which is located at the opposite side of the β -scaffold. One model attributes this long-range interaction to a hydrophobic collapse of the chromophore binding pocket which is vacant after isomerization [25]. As the hydrophobic residues are drawn into the pocket, the central β -scaffold becomes distorted, weakening its interaction with the N-terminal domain. This leads to exposure of a hydrophobic surface at the N-terminus/central β -sheet interface, which provides a binding site for interaction partners [53]. Consequently, through this model, the faster recovery in the *Rhodobacter* PYPs and the slower recovery in Ppr-PYP relative to Hhal PYP is, in addition to differences in β 4- β 5 loop conformations, suggested to arise from a relatively stronger and weaker interaction, respectively, between the N-terminus and the remainder of the protein, *i.e.* the β -scaffold [37].

3.4 Phylogenetic distribution

Since its initial discovery in 1985, only two additional examples of PYP proteins have been purified from other phototrophic purple bacteria, *i.e.* from *Halochromatium salexigens* [60] and *Rhodospirillum salexigens* [61]. However, a total of twenty-one photoactive yellow protein genes have been reported to date, originating in eight species of purple phototrophic bacteria, in six species of non-photosynthetic aerobic bacteria, and in five unidentified bacteria from seawater samples (Table 3-1 and Figure 3.7).

Table 3-1 Pyp gene distribution

Name	Organism	Accession number ^a	Ref.
HhalPYPBN9626 ^{(*)b}	<i>Halorhodospira halophila</i> BN9626	AAB28014	[5, 8]
HhalPYP SL-1	<i>Halorhodospira halophila</i> SL-1	YP_001003384	JGI ^c
HhalPYP(B) ^{(**)b}	<i>Halorhodospira halophila</i> SL-1	YP_001002902	[12], JGI
HsalPYP ^(*)	<i>Halochromatium salexigens</i>	AAB36386	[60]
RsalPYP ^(*)	<i>Rhodothallasium salexigens</i>	AAB36387	[60]
IloiPYP ^(**)	<i>Idiomarina loihiensis</i> L2TR [#]	YP_156766	[62]
RcapPYP ^(**)	<i>Rhodobacter capsulatus</i>	AAC17427	[63]
RsphPYP ^(**)	<i>Rhodobacter sphaeroides</i> ATTC 17029	YP_001045536	[10]
SrubPYP ^(**)	<i>Salinibacter ruber</i> DSM 13855 [#]	YP_446329	[64]
RcenPpr ^(**)	<i>Rhodospirillum centenum</i>	AAD22391	[51]
Msp Ppr	<i>Methylobacterium sp.</i> 4-46 [#]	ZP_01845331	JGI
TtepPpd ^(**)	<i>Thermochromatium tepidum</i>	-	[47], IG ^d
RpalPYP	<i>Rheodopseudomonas palustris</i> BisB5	YP_570463	JGI
SaurPYP(A)	<i>Stigmatella aurantiaca</i> DW4/3-1 [#]	ZP_01461006	TIGR ^e
SaurPYP(B)	<i>Stigmatella aurantiaca</i> DW4/3-1 [#]	ZP_01464165	TIGR
BphyPYP	<i>Burkholderia phytofirmans</i> PsJN [#]	ZP_01510366	JGI
ScelPYP	<i>Sorangium cellulosum</i> 'So ce 56' [#]	YP_001611644	[65]
MarinePYP1	hypothetical protein GOS_1708710	EDJ36333	[66]
MarinePYP2	hypothetical protein GOS_1678089	EDJ53704	[66]
MarinePYP3	hypothetical protein GOS_3497256	ECJ65175	[66]
MarinePYP4	hypothetical protein GOS_4955130	ECM80370	[66]
MarinePYP5	hypothetical protein GOS_9643753	EBF15616	[66]

^aProtein entry code of NCBI (National Center for Biotechnology Information):

<http://www.ncbi.nlm.nih.gov>, ^b(*) Isolated *in vivo*, ^(**) Reconstituted *in vitro*, ^cJoint Genome Institute: <http://www.jgi.doe.gov>, ^dIntegrated Genomics: <http://www.integratedgenomics.com>, ^eThe Institute for Genomic Research: www.tigr.org, [#]Non-photosynthetic aerobic bacterium

So far, the photochemical properties of ten PYP proteins have been studied, either after *in vivo* isolation (3 species) or when produced *in vitro* after the gene was cloned and expressed in

E. coli (7 species) (**Table 3.1**). Based upon their homology, absorption spectra and kinetics of dark recovery following photoexcitation, the characterized Photoactive Yellow Proteins can be classified into five groups, which are further discussed below.

The **first group** comprises the PYPs found in the halophilic and phototrophic organisms *H. halophila*, *H. salexigens* and *R. salexigens*. Their physico-chemical properties, *i.e.* absorption spectra and kinetics of photobleaching and dark recovery, are strikingly similar, although they were isolated from three different families of bacteria. The PYP sequences all consist of 125 amino acids, which show a very large 68 - 76% sequence identity and require no insertion or deletion for alignment [60], as shown in **Figure 3.7**. This is a remarkable result considering that *e.g.* the electron transfer proteins of similar length are only 25 - 40% identical, with gaps in the alignment [2, 61]. Therefore, the PYP structure was considered to be highly conserved in order to perform similar essential functions within these organisms. As mentioned before, Hhal PYP is proposed to regulate negative phototaxis away from harmful UV-light [6], but an interaction of the PYP signaling state with the corresponding response regulator to mediate flagellar motion has not been demonstrated to date.

A fourth member of this PYP subgroup was discovered in the completed genome sequence of the aerobic deep-sea bacterium *Idiomarina loihiensis* [67]. When the PYP encoding gene was cloned and expressed in *E. coli*, along with the two biosynthetic enzyme genes from *Rhodobacter capsulatus*, *i.e.* *pcl* and *tal* (as described in Section 3.5), the purified Iloi PYP showed a similar absorption spectrum ($\lambda_{\max} = 446$ nm, **Figure 3.6**) as the Hhal PYP (Kyndt J. and Meyer T.E., unpublished results). Also the kinetics of recovery following photoactivation with 450 nm laser light is virtually the same as for Hhal PYP. The rate constant is 4.4 s^{-1} for Iloi PYP at pH 7.5

vs. 6.0 s^{-1} for Hhal PYP at the same pH, which is expected considering that they share 76% sequence identity.

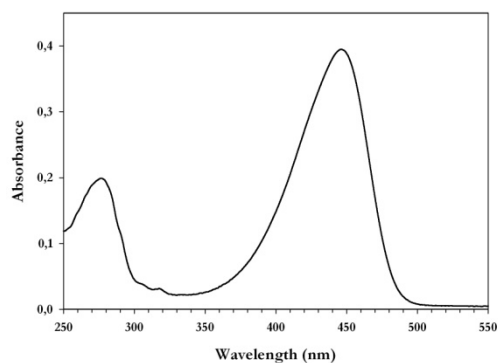


Figure 3.6

UV-Vis absorption spectrum of *I. loihiensis* PYP after *in vivo* reconstitution in *E. coli*. Spectrum from Kyndt J. and Meyer T.E. (unpublished).

However, the Iloi PYP is not necessarily expressed under the conditions of isolation, which was from an undersea volcano at 1300 meters depth where there is virtually no light. If one takes into account that the optimum salt concentration for growth is 8-10% [68], it is more likely that the normal habitat of the bacterium is in salt evaporation ponds rather than the open ocean

(2.5% salt). In shallow ponds, there would be an excess of light which would necessitate mechanisms for repair of UV-damage and periodic adjustment of the osmotic pressure. It is in this environment that Iloi PYP is most likely to be functional.

Finally, the protein product of the second *pyp* gene from *H. halophila*, PYP(B), may also be part of this subgroup, as it shows 60% sequence identity with Hhal PYP, including all key residues that control the chromophore's properties studied to date (**Figure 3.7**), and it has a similar absorption maximum ($\lambda_{\max} = 443$ nm). However, Hhal PYP(B) contains a small C-terminal extension of five amino acids and the rate constant for recovery is reported to be much lower ($1.3 \times 10^{-2} \text{ s}^{-1}$, [12]), which indicates a different functional role.

The **second group** is represented by two PYP homologues from *Rhodobacter sphaeroides* (Rsph) [10, 69, 70] and *Rhodobacter capsulatus* (Rcap) [50, 63], and three marine PYPs identified from extracted DNA samples obtained by the Craig Venter Institute's Sorcerer II Global Sampling expedition (GOS) [66] (**Figure 3.7**). The *Rhodobacter* PYPs have been cloned and expressed in *E. coli*, but not yet isolated from the natural host, presumably due to low abundance. Rsph PYP and Rcap PYP respectively show 46% and 38% identity with the above discussed PYP sequences, but are most closely related to each other having 76% identical amino acids. Their 124 amino acid sequence contains two cysteine residues at positions 69 and 118 (numbering is equivalent with the PYP sequence of *H. halophila*). However, mass spectrometry demonstrated that the single chromophore is covalently attached to C69 and not the cysteine residue at position 118 [11, 69]. These PYP proteins are further characterized by two wavelength maxima in the UV-visible absorption spectrum at neutral pH, *i.e.* 360-446 nm and 375-440 nm in Rsph PYP and Rcap PYP (**Figure 3.8**) respectively. Although the ratio of the peaks differs between Rsph and Rcap PYP, they show a significant temperature and pH-dependence in both species, where the shorter wavelength forms are favored at lower temperature and pH. The half-life for dark recovery in these species is 1.2 ms, or about 130-fold faster than in Hh PYP. Faster recovery kinetics suggests that higher light intensity is necessary to obtain the same amount of steady-state bleach as in *H. halophila* and other halophilic PYPs [50]. Thus, the properties of the *Rhodobacter* PYPs suggest a different functional role than in the halophiles, as further indicated by the genetic context described in Section 3.7.

Figure 3.7 (next page)

Alignment of identified PYP protein sequences. The conserved pHCA-binding C69 is marked in blue. Key amino acids affecting the properties of the chromophore are colored red in Hhal PYP and marked yellow when accordingly conserved in the PYP homologues. Abbreviations are as given in Table 3.1, except that marine PYPs are indicated as MPYP.

Hhal	-----MEHVGFGSDDIENTLAKMD	19
Hsal	-----MDIVHFGSDDIENSLANMS	19
Rsal	-----MEMIKFGQDDIENAMADM	19
Iloi	-----MEIVQFGSDDIENTLSKMS	19
Hhal (B)	-----MGTLIIFGRQDLENRLAAMT	19
Rcap	-----MEIIPFGTNDIDNILARE-	18
Rsph	-----MEIIPFGSADLDNILARE-	18
MPYP4	-----MEIIPFGSKDLDNILSRE-	18
MPYP1	MARSAASTTPPGRATTASSPIRRTPTAERRPDQRLPREDRTMEIIPFGSQDIDNILQRE-	59
MPYP2	-----IR-----AMEIIPFGSNDIDNILARE-	21
Sruber	-----MADSQNPYSYLREDDPDSAPGDSGDADEPEPPATDLAFDDEGVGEELRHVD	51
Rcen	-----MP-DRTTDDFGPFTEQIRGTIDGMG	24
Msp4-46	-----MS-DRALA-----AEAAR--LDALS	17
Ttep	-----MNFEDAID-----IHAPRR-LDALT	19
Saur (A)	-----MRHGILEAESLTEDRLGQLS	20
Saur (B)	-----MAPPSTSLALSNAAPPKTTPTDILLRQ--VETLS	32
Rpal	-----MNTVDFHSDSLARTIEQLA	19
Scel	-----MGSEERS-----TAGEFFFDIG--VFNLD	22
Bphy	-----MDNEFESVRI-AELAML	17
MPYP5	-----MNRHVDCAWCGKHMHGDLDSAVLSHGICGTCVAGTGLARVDELHGLD	47
MPYP3	-----GVTASTVKRWADDGSLACERTAGGHRRFLASEVARFRQHEADTTV-SHLSTLS	52
Hhal	DSQLDNLAFGAIQLDGDGTILQYNAEAGDITGRNPKEVIGKNFFKDVAECTDSPE-FSGK	78
Hsal	DQDLQDLAFGAIQLDASGKVLQYNAEAGDITGRDPKSVIGKNFFEDVAPCTKSQE-FQGR	78
Rsal	DAQIDDLAFGAIQLDETGTILAYNAEAGELTGRSPQDVIGKNFFKDIAPECTDTEE-FGGR	78
Iloi	DDKLNDAIFGAIQLDASGKI IQYNAEAGDITGRDPGAVVGKNFFNEVAPCTNSPE-FKGR	78
Hhal (B)	PEEIDDLFPFGVIQIDQHGRIILYNATEGAI TGRDPEAMIGRDFFNVDVAPCGHTEA-FYGR	78
Rcap	PARAESLFPFGAVLLDRMGRIAKYNKAEGLIAGRDPSTVIGRDFFNIEIAPCAKGR-FHGE	77
Rsph	PQRAEYLPFGAVLLDRGTILKYNRAEGGIANRNPADVIGKNFFNEIAPCAKGR-FHGE	77
MPYP4	PQRAEYLPFGAVLLDRNGKIQYNKAEGLIASRTPEDMIGKDFNEVAPCAKGR-FHGE	77
MPYP1	PKRAEYLPFGAVLLDRGTGKILKYNKAEGLIAGRDPQSVIGKSFNDIAPCAKGR-FHGE	118
MPYP2	PARAEYLPFGAVLLDRSGSIVKYNKAEGLIAGRDPGSMIGKNFFNDVAPCAKGR-FHGE	80
Sruber	EDELNAAPFGIIQIDDAGVVQFYNRYESNLSGIDPADAVGANFFTELA PCSNN-PLFFGR	110
Rcen	TAEFDALPFGAIQVDSGVIHRYNRTE SRLSGRI PERVIGRNFTEVAPCTNIPA-FSGR	83
Msp4-46	TGEIDALDLGVVQVDSGTILLYNRAESVFSGRSAERVVGRNFFRDVAPCTRLPA-FYGR	76
Ttep	PDELNRLPFGAIRVDAEGRILFYSRALVDLANRQVDSVLGRNFFSEIAPCTVVPE-FYGR	78
Saur (A)	PEEFDALPFGAIKLDAGRVL IYNAE SAFSRKRPVSVLGRRFFEEVAPCTNVA-SFRGR	79
Saur (B)	ASELDALPFGIQLDRGTGRILKFNQTEAKLARINRERQLGRNFFDDVAPCTKVRE-FYGR	91
Rpal	PEQIDALPFGVIKLDGNGIVTVFNRTAEI ESGYKSRPALGLDFFLQVAPCMGQPE-FRGR	78
Scel	ERGLDAQPFGI IRLDREGTVLSYNLYERQARRNRQDVIGKNFFTDIAPCSRVA-FHGR	81
Bphy	ADRLDGVPFGVIGFTSDALVTVYNATESKNAGLRPKMVLGKHHFGEVAPCMNN-FMVAQR	76
MPYP5	PEDADRLPFGLLHLDHDCRVVKYNFPEAERAGLDREWVIGKDFQDVAPCTRVQE-FEGR	106
MPYP3	DEELDALPYGVIGIDDEGTI IRYNATESNFSNHAVNQVLGKSFFTQVAPCTNN-RLVYGA	111
Hhal	FKEGVAS-GNLNTMFEYTFDYQMTPTKVKVHMKKAL----	125
Hsal	FKEGVAN-GNLATMFEYVFDYQMKPTKVKVHMKKAL-----VDDSYWIFVKRL-----	125
Rsal	FREGVAN-GDLNAMFEYVFDYQMQPTKVKVHMKRAI-----TGDSYWIFVKRV-----	125
Iloi	FDEGVKN-GNLNTMFEYVFDYEMQPTKVKVHMKKAL-----TGDTYWVFKRL-----	125
Hhal (B)	FQEGVRH-GDLNEIFDYTFDYRMAPTKVRVHMKKRAL-----SGDTYWIFVKRISAPAA-----	130
Rcap	FLKFNRT-GQANVMDYKFNKGAEVAVKIHLKSQP-----DGQFCWLVFKRA-----	124
Rsph	FLRFHQ-TGQVNVMFYKFAKGANVGVKIHMSQP-----DGQSCWLVFKRV-----	124
MPYP4	FLKFHNT-GQVNVIFDYKFAKYGADVGVKIHLSQP-----DGQHCWMLVKRV-----	124
MPYP1	FLKFHKT-GHVNTLFDYEFYKGANVKVRIHLKSQP-----DGQSCWMLVKRV-----	165
MPYP2	FLKFHKT-GQVNTMFDYEFYKGANVKVRIHLKAQP-----DGQNCWLF-----	123
Sruber	FKDGVRE-GGLDEYFTYFTYQMRPTLVDRVLYRD-----EAENNWILIQKR-----	156
Rcen	FMDGVTS-GTLDARFDFVFDYQMAPVRVQIRMQNA-----VPDRYWIFVRKL-----	130
Msp4-46	FREGVRR-GVLDEVFSFAYGFDPPQLRVRVALRGS-----TPGRYWIIVTRPVGQ-----	125
Ttep	FRQGVLT-GQLHTTFEFVFDYDMQPVQVRIAMHTSE-----RPGEFWILVQPLA-----	126
Saur_A	FDTLVER-GHGTESFDFQFRFRWGTRNVRIRLMVLG-----DGSRWVFTAVLTALIPLEG	135
Saur_B	FLNGLSQ-RSLYETFGFIKFDHGWNRVAITMFYS-----EKTDSVWVLSQTSVTPPPAR--	146
Rpal	IEQARQL-GRVDIELGWVGD FSDINRSLQVRIQSAS-----DG-----	115
Scel	FLAGVEQ-RELKATFGVFVHFPHKTRHVDVSLFYKAAARQQDDAVVVFIRG-----	131
Bphy	FED---E-DVLDDIVPVVLTLMRPTPVRLRLKAT-----DCATRFVLIERRATN-----	123
MPYP5	LRGLQDAGVPGREEFSFVQFRGGSRLVHVLMSHS-----PKAGTVILVEDQG-----	154
MPYP3	FKEGMAS-GSLDIKIPYTFYVMKPTNVVIMVRCQ-----DSRSNWLLIHHNTDSNGSLIV-	167

Figure 3.7

The **third group** is made up by a single PYP protein originating from a chemorganotrophic and extremely halophilic bacterium, *i.e.* *Salinibacter ruber*. The species occupies the same habitat as *Halobacterium* and *Halorhodospira* species and was recently isolated from salt evaporation ponds in Spain. To date, it is the only example of a *pyp* gene being discovered outside the proteobacteria, as the 16S rRNA sequence indicates that the organism is related to the *Cytophaga-Flavobacterium* branch of bacteria [71]. As part of this work, the PYP from *Salinibacter ruber* was studied and characterized, as presented in Chapter four. Although it has interesting differences that allow adaptation to the specific physiology of the organism, there are also similarities to the prototypic Hh PYP.

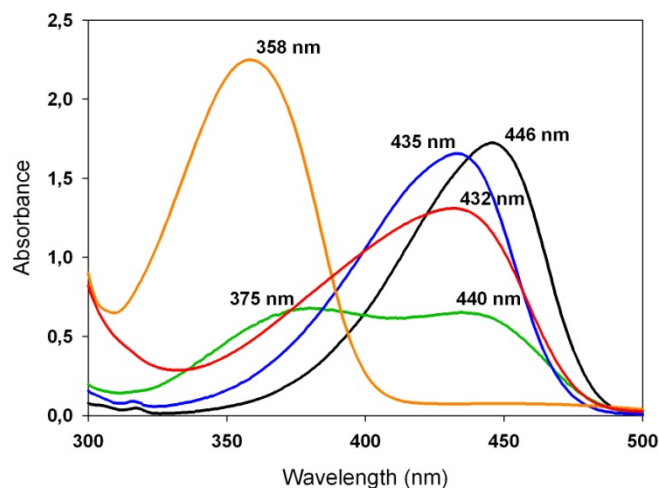
In the **fourth group**, with two representatives from *Rhodospirillum centenum* (Rcen) [51, 72] and *Methylobacterium* sp. 4-46 (Msp), the PYP is actually the N-terminal domain of a larger protein called Ppr (PYP-phytochrome related), which also contains a central domain similar to bacteriophytochromes and a C-terminal histidine kinase domain. The sequences of Ppr-PYP is as divergent from the Hhal PYP as are the *Rhodobacter* PYPs, but most of the essential residues are conserved. The spectral properties of Rcen Ppr and its proposed functional role are discussed in more detail in Chapter five and six, respectively.

A **fifth type** of PYP was identified in the genome of *Thermochromatium tepidum* (Ttep) (Integrated Genomics) as a multi-domain photoreceptor gene similar to *Rb. centenum ppr*. The gene encodes a PYP-homologue that is fused to a central bacteriophytochrome domain like Ppr, but the C-terminal domain shows about 38% homology to the GGDEF/EAL family of diguanylate cyclases and phosphodiesterases instead of the histidine kinases [37]. The *Tc. tepidum* hybrid was therefore named Ppd (PYP-bacteriophytochrome-diguanylate cyclase/phosphodiesterases) to reflect its multidomain origin. The *Tc. tepidum* PYP is the only homologue containing a substitution of Leu (**Figure 3.7**) for the color-tuning Glu46 found in the prototypic Hhal PYP. Following illumination, it has a photocycle that is initiated from a dark state with a protonated chromophore, absorbing at 358 nm at physiological pH [73], which is unique among the PYPs studied to date, as shown in **Figure 3.8**. The recovery to the dark adapted state is approximately 1500 times slower than for Hhal PYP, and shows a sigmoidal pH dependence (pK_a of 8.8) due to a pH dependent equilibrium between the I_2 intermediate and a red-shifted 440 nm intermediate [73]. The functional role of Ttep Ppd most likely involves the regulation of the level of cyclic dinucleotides (such as cyclic AMP, cyclic-GMP or cyclic di-GMP), which are second messenger molecules in all kingdoms of life and mediate a broad spectrum of cellular processes, such as c-di-GMP-mediated cellulose production in *Acetobacter xylinum* [74]. Alternatively, two major pathogens, *Salmonella typhimurium* and *Pseudomonas aeruginosa*, have been

shown to direct their transition between a sessile and motile phenotype through regulated expression of GGDEF- and EAL-domain proteins and according c-di-GMP levels [75]. However, which process(es) might be regulated by Ppd remains to be determined.

Figure 3.8

UV-Vis absorption spectra of the five PYP subtypes at pH 7.0. Hhal PYP in black, Rcap PYP in green, Rcen PYP in blue and Ttep PYP domain in orange. The absorption spectrum of Srub PYP (red) was added to the image modified from [73].



Finally, the remaining **uncharacterized** *yyp* gene products from *S. aurantiaca*, *Rb. palustris*, *S. cellulosum*, *B. phytofirmans* and, marine PYP5 and PYP3 are expected to show significant variation both in their spectral properties and photocycle kinetics compared to the prototypic PYP from *H. halophila*. As shown in **Figure 3.7**, E46 is present in all cases, consistent with its important role of lowering the pK_a for ionization of the chromophore (see Section 3.3.2), while T50 and R52 are much less conserved and natural Y42F substitutions occur in Rpal PYP and Saur PYP(B). Moreover, differences in the amino acid composition of the $\beta 4$ - $\beta 5$ loop may have interesting implications on photocycle kinetics, such as natural Y98QF/M100W, Y98QF/M100H, Y98QF/M100D, Y98F/M100G and Y98QL substitutions in Saur(A) PYP, Saur(B) PYP and Scel PYP, Rpal PYP, MPYP5 and Bphy PYP, respectively.

3.5 Biosynthesis

Before it was demonstrated to serve as a cofactor for the synthesis of PYPs, pHCA was known in plants to be an important intermediate for the production of a diverse array of secondary metabolites, such as lignin and isoflavonoids. Therefore, pHCA is formed from L-Phe in a two-step process, in which a phenylalanine ammonia-lyase (PAL) first catalyzes the non-oxidative deamination of L-Phe to yield *trans*-cinnamic acid (CA) [76, 77]. In the next step, a cytochrome P450 enzyme system hydroxylates CA to produce pHCA. Alternatively, pHCA can be synthesized directly from L-Tyr through the tyrosine ammonia-lyase (TAL) activity of PAL, which, in some cases, accepts both L-Phe and L-Tyr as a substrate. However, most natural

PAL/TAL enzymes, from either plant or microbial sources, prefer to use L-Phe rather than L-Tyr as their primary substrate.

The origin of pHCA for holo-PYP formation was elucidated upon completion of the *Rb. capsulatus* genome project (www.Integratedgenomics.com) [78, 79]. An open reading frame (Integrated Genomics accession number: RRC01844), whose sequence is homologous to the *pal* sequences in plants, was found in close proximity and upstream of a *pyp* gene, and is therefore presumed to perform the *in vivo* biosynthesis of the PYP chromophore [79]. When expressed in *E. coli*, the purified gene product was shown to possess a catalytic efficiency for tyrosine nearly 150 times larger than for phenylalanine, representing the first report of a genuine TAL enzyme, [79]. In addition, about 1 kb downstream of *pyp*, a gene encoding a *p*-hydroxy-cinnamyl:CoA ligase (pCL) was detected, which, at that time, had also been encountered downstream of the gene for PYP in *H. halophila* and *Rb. sphaeroides* [10, 80]. Since *p*-coumaryl:CoA ligase was known to be of central importance in pHCA metabolism in plants [81], pHCA was likewise believed to be activated for binding to the apoprotein through formation of a thioester with Coenzyme A (CoA) [10]. Moreover, both TAL and pCL from *Rb. capsulatus* were shown to be necessary and sufficient for the *in vivo* synthesis of holo-PYP in *E. coli* (**Figure 3.9**) [11], although it is not yet proven that this indeed occurs through a CoA-activated pHCA.

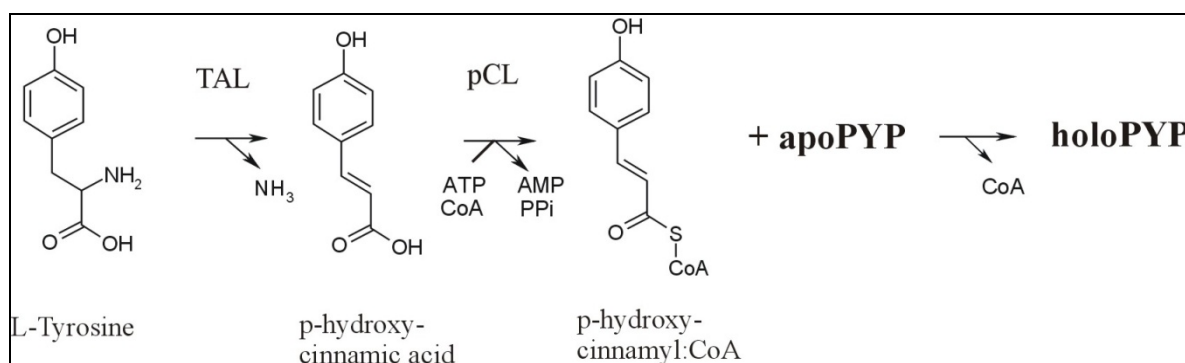


Figure 3.9

Proposed biosynthesis of holo-PYP. Tyrosine ammonia lyase (TAL) converts L-Tyrosine to *p*-coumaric acid, which is subsequently activated by a presumed *p*-coumaryl:CoA ligase (pCL) through binding to CoA at the expense of ATP. The activated chromophore is then chemically attached to the apoprotein without the help of any additional enzymes. Image taken from [11].

Consequently, by using a dual plasmid system, one containing the PYP apoprotein and the other expressing the biosynthetic enzymes TAL and pCL from *Rb. capsulatus*, holo-PYP could be successfully produced in *E. coli* in sufficient amounts for structural and photokinetic studies [11, 44, 50, 73]. This heterologous expression system was also used to characterize the *pyp* gene

product from *Salinibacter ruber*, as described in Chapter four. Until then, the only way to synthesize recombinant holo-PYP in *E. coli* was to reconstitute the apoprotein with a chemically activated chromophore, such as described in [82], although this method suffers from a highly variable yield.

The *H. halophila* SL-1 genome shows that the *pyp*, *pcl* and *tal* genes are organized in an operon, which is also observed in *H. halophila* BN9626 through walking PCR experiments (Kyndt J. and Meyer T.E., manuscript in preparation). In *H. halophila*, PYP is constitutively expressed, irrespective of cultivation in altered light conditions or NaCl concentrations (author, unpublished results). However, the enzymatic properties of TAL and pCl from *H. halophila* have not yet been characterized.

3.6 *Pyp* genes as molecular scouts in search of potential TAL biocatalysts?

An interesting feature about the *pyp* gene operon in *H. halophila* is the finding of a new TAL member of the aromatic amino acid lyase family, which also includes PAL (see 3.5) and histidine ammonia-lyases (HAL). All enzymes in the HAL/PAL/TAL family contain a unique modified amino acid cofactor, *i.e.* 3,5-dihydro-5-methylidene-4H-imidazol-4-one (MIO), which is formed autocatalytically during peptide folding from a highly conserved Ala-Ser-Gly motif [83]. The exact mechanism of ammonia elimination *via* the highly electrophilic MIO group is currently unknown, but is suggested to proceed through an E₁cB-like elimination of ammonia and a non-acidic β -proton from the substrate, and is based on structural data from the *Pseudomonas putida* HAL [84], the *Rhototorula glutinis* PAL [85], as well as the parsley PAL [86] enzymes.

PALs deaminate Phe to cinnamate (CA), while HALs convert His to urocanic acid [87], which is the first step in the degradation of His to Glu. As mentioned before, some PAL enzymes also accept Tyr as substrate, and are therefore called PAL/TAL or TAL enzymes, depending on their relative activity towards these substrates [88]. However, TALs are not omnipresent as HALs and PALs, but enzyme activity has thus far only been identified in the photosynthetic bacteria *Rb. capsulatus* (see above) and *Rb. spaeroides* (GenBank accession number: YP_355075) [89], and in the actinomycete *Saccharothrix espanaensis* (GenBank accession number: ABC88669) [90]. This rarity may originate from its specialized function in pHCA biosynthesis, which in bacteria so far is only known to be used as chromophore for PYP, and which in *S. espanaensis* represents the first step in the conversion of tyrosine to the N-(m,p-dihydroxycinnamoyl)-taurine moiety of saccharomicin antibiotics [90].

pHCA is of biotechnological interest, serving as a starting material for either the chemical or enzymatic conversion to a wide array of commercially valuable chemicals, including flavors, fragrances, pharmaceuticals, biocosmetics, and health and nutrition products [88]. Hence,

PAL/TAL enzymes with high TAL activity are attractive candidates for their potential use as biocatalyst, enabling a more direct and desirable route in biological pHCA production relative to the PAL/hydroxylase enzyme system known from plants [91].

Various bacteria and eukaryotic microorganisms have been screened, with limited success, for their ability to produce PAL/TAL enzymes with high TAL activity [91]. Hence, the expanding access to whole genome information creates new expectations to find potential TAL enzymes through sequence analysis. However, it is still not evident to accurately predict whether an enzyme will have TAL, PAL or HAL activity based on sequence information alone. Only recently, Watts *et al.* [92] defined a small sequence motif which could be used to predict enzyme function upon sequence identity. After a comparative sequence alignment and protein modeling of TAL from *Rh. sphaeroides*, a single active site residue was identified (His89, as shown in **Figure 3.10**) which, when mutated, converts the enzyme's major substrate affinity from Tyr to Phe [92]. Consequently, the following selectivity region was proposed which would define the enzyme's function: enzymes with HAL activity contain a Ser-His motif at the switch position, while PAL/TAL activity would require a Phe-Leu and a His-Leu motif, respectively.

When we performed a blast search with the TALs from *Rh. sphaeroides* and *Rb. capsulatus* as the query sequence against bacterial genomes, only 2 additional HAL/PAL/TAL homologues matched the proposed TAL key motif within the first 100 hits, *i.e.* TALs from *H. halophila* (GenBank accession number: YP_001003386) and *S. ruber* (GenBank accession number: YP_444855). This number would be expected to be higher, at least partially, considering the number of *pyp* genes (21) found in bacterial genomes to date and the knowledge about the role of TAL role in the biosynthesis of the PYP chromophore. Therefore, we analyzed all ammonia-lyase coding entries from the released genomes containing a *pyp* gene for their potential substrate specificity using the proposed key motif. However, as shown in the alignment in **Figure 3.10**, only four TAL enzymes (two of which remain to be characterized, *i.e.* TALs from *H. halophila* and *S. ruber*) could be retrieved in addition to a *pyp* gene from the same genome, at least according to the substrate selectivity switch proposed in [92]. Furthermore, the genomes of *S. cellulosum* and *S. aurantiaca* only contain a single ammonia-lyase with a predicted specificity for histidine. From the genomes of *B. phytofirmans*, *I. loihiensis* and *Methylobacterium* sp4-46, two ammonia-lyases could be identified, one of which matching the HAL key motif while the other has an unknown selectivity region (**Figure 3.10**). The latter may have affinity for both phenylalanine and tyrosine, and subsequently, the TAL activity might be sufficient to supply the required chromophore for PYP biosynthesis, as photosensors proteins are not expected to be abundantly expressed. Although at

first sight, the correlation between *pyp* and *tal* seems rather low, there is still much to learn about the enzyme's mechanism and conditions of substrate selection.

Rsph	TAL	NRLISGENVR-----TLQAN-LVHHIASGVG-----PVLDTTARAMVLARLVSIA	115
Rcap	TAL	NRLIGADQGA-----ELQONNLIYHLATGVG-----PKLSWAEARALMLARLNSIL	117
Hhal	TAL	TSRIDPSASR-----TLQRN-LVY HL CSGVG-----EPLSRCHTRATLGARIASVT	108
Srub	TAL	DEAVESDEESASAHGPSPEGDRGRKLI HL GAGAG-----SFAPPPLVRATMIARLQTLV	129
Sesp	TAL	LFDADSELE-----QGGSLISHLGTGQG-----APLAPEVSRLILWLRIQNMR	113
Srub	HAL	QKRVPEDDLE-----TLQRNLV SH AVGVG-----DLVPKALSRLILHLKIHALG	97
Scel	HAL	ETRIADHDIR-----ALQRNLV SH ACGVG-----PELGEAEVRAMIVLRAQVIA	108
Saur	HAL	EVRIEKKDLR-----ELQRNLIL SH AAGVG-----SPLPLPEARVLLLLRCNVLA	111
Bphy	HAL	STHIPHDQLE-----LLQRNLV SH AVGVG-----EPMSRPVVRLIALKLSSLG	107
Iloi	HAL	NTRIPPERLT-----DLQRRIV SH AAGTG-----DLMEDSVVRLMLLLKINSLS	109
Msp	HAL	TVRIAPDDLA-----TLQRNIV SH AAGVG-----APVPAGIVRLMMALKLASLA	108
Bphy	HAL (B)	VVDVPMELVE-----ALPLQL TR Y H GCGMG-----QYLDDAQTAVIAARLNSLA	128
Iloi	HAL (B)	TVSVPENLVN-----ELPIHL TR FH GCGLG-----DTFDEQETRAILATRLSSLA	113
Msp	HAL (B)	NQVLSLNEVE-----DLQONLI W GL KCGVG-----KKLPAAQVRSAMFIRANMLA	114
Pcri	PAL	TSHRRTKQGG-----ALQKELIRFLNAGIFGNGSDNTLPHSATRAAMLVRINTLL	168
MIO			
Rsph	TAL	QGASGASEGTIARLIDLLNSELAPAVPSRGTVGASGDLTPLAHMVLCLQGRGDFLDRDGT	175
Rcap	TAL	QGASGASPETIDRIVAVLNAGFAPEVPAQGTVGASGDLTPLAHMVLALQGRGRMIDPSGR	177
Hhal	TAL	RGHSGVTPAVVERLLAWLEHDVVPEVPAIGTVGASGDLT PLAHVARALM GEGRVCINGGE	168
Srub	TAL	QGHSAVRPALVDEVIEVFESGLIPAVPEVGS L GASGDLT PLAH IARVCTGDGAVVTS D GE	189
Sesp	TAL	KGYSAVSPVFWQKLADLWNKGFTPAIPRHGTVSASGDLQPLAHAALAFTGVGEAWTRDAD	173
Srub	HAL	LGHSGVSRET F DRLLLFAERDLVPAIPSRG S VGASGDLAPLAHLALPLL G EGRF W TEDGS	157
Scel	HAL	LGHSGVRTEVLDLLAALLERRVSPRI PA QGS V GASGDLAPLAHLALTL I GEGEAR F E G --	166
Saur	HAL	KGYSGIRPETLALALEMLNRDVVPVPERGS V GASGDLAPLAHLALV F IGEGEAF Y Q G --	169
Bphy	HAL	RGHSGIRREVMEALITLYNADVLPV IP VKGS V GASGDLAPLAHMSATLL G VGEV F AK G --	165
Iloi	HAL	RGFSGVRQVLVDALIKLLNAEVYPC I PEKGS V GASGDLAPLAH M VL PL VGE G TVRH N G--	167
Msp	HAL	QGASGVRPETVALLDAMLARGVTPV V PQGS V GASGDLAPLAH M T A AMIG V GE C L D AG G --	167
Bphy	HAL (B)	YFGSGVRPVLLERLADLVNHRVLP RI PSEGS V GASGDLT PL SY V AAALAGER D VM F E G --	186
Iloi	HAL (B)	QGYSGVSWELLERLVMLNENML PL IPKES V GASGDLT PL SY I AGALIGER D VR F RN--	171
Msp	HAL (B)	KGVSGARAELIERYLVFLNAGIT P VVRDLGS I GASGDLV PL AQ I AGCL I GL G PS F RV E R D	174
Pcri	PAL	QGYSGIRFEILEAITKFLNQNITPCLPLRGTITASGDLVPLSYIAGLLTGRPNSKAVGPT	228

Figure 3.10

Partial sequence alignment of HAL/PAL/TAL enzymes retrieved from whole genome databases containing *pyp*. PAL from *P. crispum* is added for comparison. The arrow indicates the location of the active site residue (His89) in Rsph TAL which has been shown to be critical in substrate selection [92]. Marked in green are the three residues that comprise the post-translationally modified MIO cofactor. The key motif for predicting enzyme function is shaded red for TAL, yellow for HAL and blue for PAL. Enzymes for which the substrate preference has been verified are indicated in bold. Sequences were aligned using ClustalW2 (<http://www.ebi.ac.uk/Tools/clustalw2/index.html>). Abbreviations and GenBank accession numbers are: Rsph, *Rb. sphaeroides* TAL (acc. nr.: YP_355075), Rcap, *Rb. capsulatus* TAL (acc. nr.: RRC01844), Hhal, *H. halophila SL-1* TAL (acc. nr.:), Srub, *S. ruber* TAL (acc. nr.: YP_444855) and HAL (acc. nr.: YP_444860), Sesp, *S. espanaensis* TAL (acc. nr.: ABC88669), Scel, *S. cellulosum* HAL (acc. nr.: YP_001616726), Saur, *S. aurantiaca* HAL (acc. nr.: ZP_01466821), Iloi, *I. loihiensis* HAL (acc. nr.: YP_156831) and HAL(B) (acc. nr.: YP_154526), Bphy, *B. phytofirmans* HAL (acc. nr.: ZP_01510410) and HAL(B) (acc. nr.: ZP_01512371), Pcri, *P. crispum* PAL (acc. nr.: CAA68938), Msp, *Methylobacterium* sp4-46 HAL (acc. nr.: ZP_01845061) and HAL(B) (acc. nr.: ZP_01846502).

Nevertheless, the completion of new genomes including additional PYP's will provide interesting targets to find suitable TAL biocatalysts. Accordingly, the two TAL enzymes from the extreme halophiles deserve further characterization, as they contain interesting features for a potential application as biocatalyst in the production of *p*-hydroxycinnamic acid (pHCA). Moreover, *H. halophila* and *S. ruber* thrive in habitats that are characterized by extreme heat and osmotic stress, and their PYP photoreceptors have been demonstrated to be stable at high temperatures, having a T_m of 82°C [35] and 74°C [93], respectively. Thermostability allows for an increase in reaction temperature which, in addition to accelerating the reaction rate, improves the solubility of the tyrosine substrate, and thus allows production of significantly higher amounts of pHCA.

3.7 Genetic context

Although twenty-one examples of *pyp* genes have been discovered to date, there still exists a veil of mystery about their potential role(s) in the bacterial cell. There is little doubt that they are involved in perceiving light signals, as all PYPs studied to date show characteristic features for a photosensory function, *i.e.* a light-inducible photocycle with high quantum yield and a long-living photointermediate that undergoes a concomitant conformational change. However, their mutual differences also indicate that each species of PYP is likely to perform a different functional role. In *Rb. centenum* exclusively, there is evidence that PYP is involved in a light-dependent expression of a chalcone synthase-related polyketide synthase of which the function in bacteria is still unclear. A more detailed discussion about Ppr-PYP and its participation in *Rb. centenum*s photoresponses will be presented in Chapter five and six.

Genes that encode for functionally related proteins are often clustered on the chromosome [94], and in some cases the genetic context can provide important clues to function. For example, a SRII gene has been found in *T. tepidum* near its associated signal transducer *htrII* and a cluster of chemotaxis genes, *i.e.* *cheA*, *cheW* and two *cheY*s [37], which also function in phototaxis in *Halobacterium* [95]. Through analogy with SRII from *H. salinarum*, SRII from *T. tepidum* is suggested to function as a receptor for negative phototaxis in this species [37]. Similarly, a gene for SRI is followed by a Htr1 transducer in *S. ruber*, and these are associated with flagellar genes. With new genome sequences being completed and with the discovery of additional PYPs, the genetic context of PYP can be analyzed for common features, which in the *Rhodobacter* species has provided interesting clues about PYP's potential function in the cell, such as cell buoyancy as described below.

3.7.1 *Rhodobacter* gene context

The genes for PYP and its two biosynthetic enzymes, TAL and pCL (see Section 3.5), are associated with those for gas vesicle formation in *Rh. capsulatus* [50], as shown in **Figure 3.11**. Gas vesicles are gas-filled organelles functioning as flotation devices by lowering the density of the cells. They allow aerophilic bacteria to float into oxygenated surface waters, and enable cyanobacteria and photosynthetic bacteria to float up towards the light, forming stratified layers below the water surface [96]. The genome sequence of the closely related *Rh. sphaeroides* strain 2.4.1 (JGI) indicates that the gas vesicle genes (*gvp*) are present in the same orientation, but the *pyp* and *pcl* genes are apparently absent, as shown in **Figure 3.11**. On the other hand, *Rh. sphaeroides* strain 2.4.9 (ATCC 17029) has a nearly identical *gvp* gene cluster, but the *pyp/pcl* cluster of five genes is located on a putative plasmid (Meyer T.E., pers. comm.). In an extreme case, *Rh. sphaeroides* strain 2.4.3 (ATCC 17025) apparently has neither *gvp* nor *pyp* genes. The *Rh. sphaeroides* *pyp* gene was originally cloned from strain NCIB 8253 [10], which was derived from Van Niels' strain 2.4.1, but deposited in the culture collection at a different time than that which was used for genome sequencing. It is thus likely that the NCIB 8253 *pyp/pcl* gene cluster was rearranged to another location from the *gvp/tal* cluster in strain 2.4.1, which has subsequently lost the *pyp/pcl* cluster through years of non-selective cultivation in the laboratory [37, 50]. In addition, at least one if not all marine PYPs related to *Rhodobacter* (see section 3.4) could be associated with *gvp* genes, as Orf A and Orf C, which are normally adjacent to the *Rhodobacter* PYPs, were found in two of the GOS PYP clones, and a *gvpA* gene was found in one (Meyer T.E., pers. comm.).

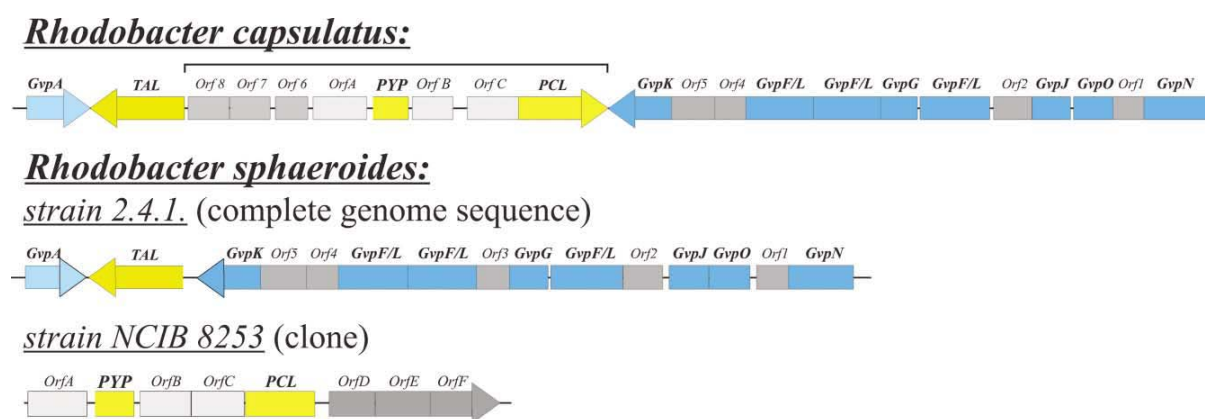


Figure 3.11

Genetic organization of PYP and presumed gas vesicles in *Rh. capsulatus* and *Rh. sphaeroides*. PYP and its biosynthetic genes are yellow, gas vesicles are blue and orf with the same designation have amino acid sequence homology. The line above the figure indicates the segment missing in the *Rh. sphaeroides* 2.4.1 genome. Image taken from [37].

In halobacteria, gas vesicles are induced by low light intensity, low oxygen, high salt concentrations, and the stationary phase of growth [97]. Although gas vesicles have not been observed before neither in *Rh. capsulatus* or in *Rh. sphaeroides*, they are similarly expected to be activated at very low light intensity and/or low oxygen conditions. As a light sensor, PYP has been hypothesized to repress the synthesis of gas vesicles at very high light intensities, when the cells have floated to the surface of the water [37, 50]. PYP may thus repress its own synthesis as well as that of the gas vesicles under these conditions, although no obvious regulatory genes could be identified in the vicinity of the *gvp* gene cluster in the two *Rhodobacter* species. The latter have only a limited capacity for fermentation and are stressed by lack of light and/or oxygen. Photosynthetic genes are activated by anaerobic conditions, but *gvp* genes may require a stepdown of light intensity or oxygen concentration for their activation.

In summary, the genetic context suggests that PYP may be widespread in the *Rhodobacter* species where it may regulate cell buoyancy, in part by repressing gas vesicle synthesis. However, similar functional implications based on genomic information for other PYP species remain highly speculative, as exemplified by the *Srub pyp* gene context described in Chapter four, and are therefore not further discussed.

3.8 References

1. Imhoff, J.F. and Suling, J., The phylogenetic relationship among *Ectothiorhodospiraceae*: A reevaluation of their taxonomy on the basis of 16S rDNA analyses. *Archives of Microbiology*, 1996. **165**(2): p. 106-113.
2. Meyer, T.E., Isolation and characterization of soluble cytochromes, ferredoxins and other chromophoric proteins from the halophilic phototrophic bacterium *Ectothiorhodospira halophila*. *Biochimica et Biophysica Acta*, 1985. **806**(1): p. 175-83.
3. Meyer, T.E., Yakali, E., Cusanovich, M.A., and Tollin, G., Properties of a water-soluble, yellow protein isolated from a halophilic phototrophic bacterium that has photochemical activity analogous to sensory rhodopsin. *Biochemistry*, 1987. **26**(2): p. 418-23.
4. Bogomolni, R.A. and Spudich, J.L., Identification of a third rhodopsin-like pigment in phototactic *Halobacterium Halobium*. *Proceedings of the National Academy of Sciences of the United States of America-Biological Sciences*, 1982. **79**(20): p. 6250-6254.
5. Van Beeumen, J.J., Devreese, B.V., Van Bun, S.M., Hoff, W.D., Hellingwerf, K.J., Meyer, T.E., McRee, D.E., and Cusanovich, M.A., Primary structure of a photoactive yellow protein from the phototrophic bacterium *Ectothiorhodospira halophila*, with evidence for the mass and the binding site of the chromophore. *Protein Science*, 1993. **2**(7): p. 1114-25.
6. Sprenger, W.W., Hoff, W.D., Armitage, J.P., and Hellingwerf, K.J., The eubacterium *Ectothiorhodospira halophila* is negatively phototactic, with a wavelength dependence that fits the absorption spectrum of the photoactive yellow protein. *Journal of Bacteriology*, 1993. **175**(10): p. 3096-104.
7. Hoff, W.D., Dux, P., Hard, K., Devreese, B., Nugteren-Roodzant, I.M., Crielaard, W., Boelens, R., Kaptein, R., van Beeumen, J., and Hellingwerf, K.J., Thiol ester-linked p-coumaric acid as a new photoactive prosthetic group in a protein with rhodopsin-like photochemistry. *Biochemistry*, 1994. **33**(47): p. 13959-62.
8. Baca, M., Borgstahl, G.E., Boissinot, M., Burke, P.M., Williams, D.R., Slater, K.A., and Getzoff, E.D., Complete chemical structure of photoactive yellow protein: novel thioester-linked 4-hydroxycinnamyl chromophore and photocycle chemistry. *Biochemistry*, 1994. **33**(48): p. 14369-77.
9. Borgstahl, G.E., Williams, D.R., and Getzoff, E.D., 1.4 Å structure of photoactive yellow protein, a cytosolic photoreceptor: unusual fold, active site, and chromophore. *Biochemistry*, 1995. **34**(19): p. 6278-87.
10. Kort, R., Hoff, W.D., Van West, M., Kroon, A.R., Hoffer, S.M., Vlieg, K.H., Crielaard, W., Van Beeumen, J.J., and Hellingwerf, K.J., The xanthopsins: a new family of eubacterial blue-light photoreceptors. *EMBO Journal*, 1996. **15**(13): p. 3209-18.
11. Kyndt, J.A., Vanrobaeys, F., Fitch, J.C., Devreese, B.V., Meyer, T.E., Cusanovich, M.A., and Van Beeumen, J.J., Heterologous production of *Halorhodospira halophila* holophotoactive yellow protein through tandem expression of the postulated biosynthetic genes. *Biochemistry*, 2003. **42**(4): p. 965-70.
12. van der Horst, M.A., Laan, W., Yeremenko, S., Wende, A., Palm, P., Oesterhelt, D., and Hellingwerf, K.J., From primary photochemistry to biological function in the blue-light photoreceptors PYP and AppA. *Photochemical & Photobiological Sciences*, 2005. **4**(9): p. 688-93.
13. Devanathan, S., Brudler, R., Hessling, B., Woo, T.T., Gerwert, K., Getzoff, E.D., Cusanovich, M.A., and Tollin, G., Dual photoactive species in Glu46Asp and Glu46Ala mutants of photoactive yellow protein: a pH-driven color transition. *Biochemistry*, 1999. **38**(41): p. 13766-72.
14. Ujj, L., Devanathan, S., Meyer, T.E., Cusanovich, M.A., Tollin, G., and Atkinson, G.H., New photocycle intermediates in the photoactive yellow protein from *Ectothiorhodospira halophila*: picosecond transient absorption spectroscopy. *Biophysical Journal*, 1998. **75**(1): p. 406-12.

15. Genick, U.K., Soltis, S.M., Kuhn, P., Canestrelli, I.L., and Getzoff, E.D., Structure at 0.85 Å resolution of an early protein photocycle intermediate. *Nature*, 1998. **392**(6672): p. 206-9.
16. Brudler, R., Rammelsberg, R., Woo, T.T., Getzoff, E.D., and Gerwert, K., Structure of the I1 early intermediate of photoactive yellow protein by FTIR spectroscopy. *Nature Structural Biology*, 2001. **8**(3): p. 265-70.
17. Borucki, B., Otto, H., Joshi, C.P., Gasperi, C., Cusanovich, M.A., Devanathan, S., Tollin, G., and Heyn, M.P., pH Dependence of the photocycle kinetics of the E46Q mutant of photoactive yellow protein: protonation equilibrium between I1 and I2 intermediates, chromophore deprotonation by hydroxyl uptake, and protonation relaxation of the dark state. *Biochemistry*, 2003. **42**(29): p. 8780-90.
18. Joshi, C.P., Borucki, B., Otto, H., Meyer, T.E., Cusanovich, M.A., and Heyn, M.P., Photoreversal kinetics of the I1 and I2 intermediates in the photocycle of photoactive yellow protein by double flash experiments with variable time delay. *Biochemistry*, 2005. **44**(2): p. 656-65.
19. Otto, H., Hoersch, D., Meyer, T.E., Cusanovich, M.A., and Heyn, M.P., Time-resolved single tryptophan fluorescence in photoactive yellow protein monitors changes in the chromophore structure during the photocycle via energy transfer. *Biochemistry*, 2005. **44**(51): p. 16804-16.
20. Shimizu, N., Imamoto, Y., Harigai, M., Kamikubo, H., Yamazaki, Y., and Kataoka, M., pH-dependent equilibrium between long lived near-UV intermediates of photoactive yellow protein. *Journal of Biological Chemistry*, 2006. **281**(7): p. 4318-25.
21. Borucki, B., Devanathan, S., Otto, H., Cusanovich, M.A., Tollin, G., and Heyn, M.P., Kinetics of proton uptake and dye binding by photoactive yellow protein in wild type and in the E46Q and E46A mutants. *Biochemistry*, 2002. **41**(31): p. 10026-37.
22. Ng, K., Getzoff, E.D., and Moffat, K., Optical studies of a bacterial photoreceptor protein, Photoactive Yellow Protein, in single crystals. *Biochemistry*, 1995. **34**(3): p. 879-890.
23. Hoff, W.D., Kwa, S.L.S., Vangrondelle, R., and Hellingwerf, K.J., Low temperature absorbency and fluorescence spectroscopy of the Photoactive Yellow Protein from *Ectothiorhodospira halophila*. *Photochemistry and Photobiology*, 1992. **56**(4): p. 529-539.
24. Imamoto, Y., Kataoka, M., and Tokunaga, F., Photoreaction cycle of photoactive yellow protein from *Ectothiorhodospira halophila* studied by low-temperature spectroscopy. *Biochemistry*, 1996. **35**(45): p. 14047-53.
25. Cusanovich, M.A. and Meyer, T.E., Photoactive yellow protein: a prototypic PAS domain sensory protein and development of a common signaling mechanism. *Biochemistry*, 2003. **42**(17): p. 4759-70.
26. Meyer, T.E., Tollin, G., Hazzard, J.H., and Cusanovich, M.A., Photoactive yellow protein from the purple phototrophic bacterium, *Ectothiorhodospira halophila*. Quantum yield of photobleaching and effects of temperature, alcohols, glycerol, and sucrose on kinetics of photobleaching and recovery. *Biophysical Journal*, 1989. **56**(3): p. 559-64.
27. Devanathan, S., Pacheco, A., Ujj, L., Cusanovich, M., Tollin, G., Lin, S., and Woodbury, N., Femtosecond spectroscopic observations of initial intermediates in the photocycle of the photoactive yellow protein from *Ectothiorhodospira halophila*. *Biophysical Journal*, 1999. **77**(2): p. 1017-23.
28. van Brederode, M.E., Gensch, T., Hoff, W.D., Hellingwerf, K.J., and Braslavsky, S.E., Photoinduced volume change and energy storage associated with the early transformations of the photoactive yellow protein from *Ectothiorhodospira halophila*. *Biophysical Journal*, 1995. **68**(3): p. 1101-9.
29. Meyer, T.E., Tollin, G., Causgrove, T.P., Cheng, P., and Blankenship, R.E., Picosecond Decay Kinetics and Quantum Yield of Fluorescence of the Photoactive Yellow Protein

- from the Halophilic Purple Phototrophic Bacterium, *Ectothiorhodospira halophila*. *Biophysical Journal*, 1991. **59**(5): p. 988-991.
30. Genick, U.K., Devanathan, S., Meyer, T.E., Canestrelli, I.L., Williams, E., Cusanovich, M.A., Tollin, G., and Getzoff, E.D., Active site mutants implicate key residues for control of color and light cycle kinetics of photoactive yellow protein. *Biochemistry*, 1997. **36**(1): p. 8-14.
 31. Van Brederode, M.E., Hoff, W.D., Van Stokkum, I.H., Groot, M.L., and Hellingwerf, K.J., Protein folding thermodynamics applied to the photocycle of the photoactive yellow protein. *Biophysical Journal*, 1996. **71**(1): p. 365-80.
 32. Salamon, Z., Meyer, T.E., and Tollin, G., Photobleaching of the Photoactive Yellow Protein from *Ectothiorhodospira halophila* promotes binding to lipid bilayers - Evidence from surface plasmon resonance spectroscopy. *Biophysical Journal*, 1995. **68**(2): p. 648-654.
 33. Hoersch, D., Otto, H., Joshi, C.P., Borucki, B., Cusanovich, M.A., and Heyn, M.P., Role of a conserved salt bridge between the PAS core and the N-terminal domain in the activation of the photoreceptor photoactive yellow protein. *Biophysical Journal*, 2007. **93**(5): p. 1687-1699.
 34. Demchuk, E., Genick, U.K., Woo, T.T., Getzoff, E.D., and Bashford, D., Protonation states and pH titration in the photocycle of photoactive yellow protein. *Biochemistry*, 2000. **39**(5): p. 1100-13.
 35. Meyer, T.E., Devanathan, S., Woo, T., Getzoff, E.D., Tollin, G., and Cusanovich, M.A., Site-specific mutations provide new insights into the origin of pH effects and alternative spectral forms in the photoactive yellow protein from *Halorhodospira halophila*. *Biochemistry*, 2003. **42**(11): p. 3319-25.
 36. Xie, A., Hoff, W.D., Kroon, A.R., and Hellingwerf, K.J., Glu46 donates a proton to the 4-hydroxycinnamate anion chromophore during the photocycle of photoactive yellow protein. *Biochemistry*, 1996. **35**(47): p. 14671-8.
 37. Kyndt, J.A., Meyer, T.E., and Cusanovich, M.A., Photoactive yellow protein, bacteriophytochrome, and sensory rhodopsin in purple phototrophic bacteria. *Photochemical & Photobiological Sciences*, 2004. **3**(6): p. 519-30.
 38. Genick, U.K., Borgstahl, G.E., Ng, K., Ren, Z., Pradervand, C., Burke, P.M., Srajer, V., Teng, T.Y., Schildkamp, W., McRee, D.E., Moffat, K., and Getzoff, E.D., Structure of a protein photocycle intermediate by millisecond time-resolved crystallography. *Science*, 1997. **275**(5305): p. 1471-5.
 39. Perman, B., Srajer, V., Ren, Z., Teng, T., Pradervand, C., Ursby, T., Bourgeois, D., Schotte, F., Wulff, M., Kort, R., Hellingwerf, K., and Moffat, K., Energy transduction on the nanosecond time scale: early structural events in a xanthopsin photocycle. *Science*, 1998. **279**(5358): p. 1946-50.
 40. Devanathan, S., Genick, U.K., Canestrelli, I.L., Meyer, T.E., Cusanovich, M.A., Getzoff, E.D., and Tollin, G., New insights into the photocycle of *Ectothiorhodospira halophila* photoactive yellow protein: photorecovery of the long-lived photobleached intermediate in the Met100Ala mutant. *Biochemistry*, 1998. **37**(33): p. 11563-8.
 41. Devanathan, S., Genick, U.K., Getzoff, E.D., Meyer, T.E., Cusanovich, M.A., and Tollin, G., Preparation and properties of a 3,4-dihydroxycinnamic acid chromophore variant of the photoactive yellow protein. *Archives of Biochemistry and Biophysics*, 1997. **340**(1): p. 83-9.
 42. Kroon, A.R., Hoff, W.D., Fennema, H.P., Gijzen, J., Koomen, G.J., Verhoeven, J.W., Crielaard, W., and Hellingwerf, K.J., Spectral tuning, fluorescence, and photoactivity in hybrids of photoactive yellow protein, reconstituted with native or modified chromophores. *Journal of Biological Chemistry*, 1996. **271**(50): p. 31949-56.
 43. Rajagopal, S. and Moffat, K., Crystal structure of a photoactive yellow protein from a sensor histidine kinase: conformational variability and signal transduction. *Proceedings of the National Academy of Sciences of the United States of America*, 2003. **100**(4): p. 1649-54.

44. Kyndt, J.A., Savvides, S.N., Memmi, S., Koh, M., Fitch, J.C., Meyer, T.E., Heyn, M.P., Van Beeumen, J.J., and Cusanovich, M.A., Structural role of tyrosine 98 in photoactive yellow protein: effects on fluorescence, gateway, and photocycle recovery. *Biochemistry*, 2007. **46**(1): p. 95-105.
45. Rajagopal, S., Anderson, S., Srajer, V., Schmidt, M., Pahl, R., and Moffat, K., A structural pathway for signaling in the E46Q mutant of photoactive yellow protein. *Structure*, 2005. **13**(1): p. 55-63.
46. Dux, P., Rubinstenn, G., Vuister, G.W., Boelens, R., Mulder, F.A., Hard, K., Hoff, W.D., Kroon, A.R., Crielaard, W., Hellingwerf, K.J., and Kaptein, R., Solution structure and backbone dynamics of the photoactive yellow protein. *Biochemistry*, 1998. **37**(37): p. 12689-99.
47. Kyndt, J.A., Biosynthesis and characterization of the photoactive yellow protein (PYP), a bacterial photoreceptor, PhD Thesis, University of Ghent, Belgium. 2003.
48. Brudler, R., Meyer, T.E., Genick, U.K., Devanathan, S., Woo, T.T., Millar, D.P., Gerwert, K., Cusanovich, M.A., Tollin, G., and Getzoff, E.D., Coupling of hydrogen bonding to chromophore conformation and function in photoactive yellow protein. *Biochemistry*, 2000. **39**(44): p. 13478-86.
49. Kumauchi, M., Hamada, N., Sasaki, J., and Tokunaga, F., A role of methionine 100 in facilitating PYP(M)-decay process in the photocycle of photoactive yellow protein. *Journal of Biochemistry (Tokyo)*, 2002. **132**(2): p. 205-10.
50. Kyndt, J.A., Hurley, J.K., Devreese, B., Meyer, T.E., Cusanovich, M.A., Tollin, G., and Van Beeumen, J.J., *Rhodobacter capsulatus* photoactive yellow protein: genetic context, spectral and kinetics characterization, and mutagenesis. *Biochemistry*, 2004. **43**(7): p. 1809-20.
51. Jiang, Z.Y., Swem, L.R., Rushing, B.G., Devanathan, S., Tollin, G., and Bauer, C.E., Bacterial photoreceptor with similarity to photoactive yellow protein and plant phytochromes. *Science*, 1999. **285**(5426): p. 406-409.
52. Imamoto, Y., Koshimizu, H., Mihara, K., Hisatomi, O., Mizukami, T., Tsujimoto, K., Kataoka, M., and Tokunaga, F., Roles of amino acid residues near the chromophore of photoactive yellow protein. *Biochemistry*, 2001. **40**(15): p. 4679-85.
53. Borucki, B., Kyndt, J.A., Joshi, C.P., Otto, H., Meyer, T.E., Cusanovich, M.A., and Heyn, M.P., Effect of salt and pH on the activation of photoactive yellow protein and gateway mutants Y98Q and Y98F. *Biochemistry*, 2005. **44**(42): p. 13650-63.
54. Getzoff, E.D., Gutwin, K.N., and Genick, U.K., Anticipatory active-site motions and chromophore distortion prime photoreceptor PYP for light activation. *Nat Struct Biol*, 2003. **10**(8): p. 663-8.
55. Harigai, M., Yasuda, S., Imamoto, Y., Yoshihara, K., Tokunaga, F., and Kataoka, M., Amino acids in the N-terminal region regulate the photocycle of photoactive yellow protein. *Journal of Biochemistry (Tokyo)*, 2001. **130**(1): p. 51-6.
56. Vreede, J., van der Horst, M.A., Hellingwerf, K.J., Crielaard, W., and van Aalten, D.M., PAS domains. Common structure and common flexibility. *Journal of Biological Chemistry*, 2003. **278**(20): p. 18434-9.
57. Harigai, M., Imamoto, Y., Kamikubo, H., Yamazaki, Y., and Kataoka, M., Role of an N-terminal loop in the secondary structural change of photoactive yellow protein. *Biochemistry*, 2003. **42**(47): p. 13893-900.
58. Rubinstenn, G., Vuister, G.W., Mulder, F.A., Dux, P.E., Boelens, R., Hellingwerf, K.J., and Kaptein, R., Structural and dynamic changes of photoactive yellow protein during its photocycle in solution. *Nature Structural Biology*, 1998. **5**(7): p. 568-70.
59. Craven, C.J., Derix, N.M., Hendriks, J., Boelens, R., Hellingwerf, K.J., and Kaptein, R., Probing the nature of the blue-shifted intermediate of photoactive yellow protein in

- solution by NMR: hydrogen-deuterium exchange data and pH studies. *Biochemistry*, 2000. **39**(47): p. 14392-9.
60. Koh, M., Van Driessche, G., Samyn, B., Hoff, W.D., Meyer, T.E., Cusanovich, M.A., and Van Beeumen, J.J., Sequence evidence for strong conservation of the photoactive yellow proteins from the halophilic phototrophic bacteria *Chromatium salexigens* and *Rhodospirillum salexigens*. *Biochemistry*, 1996. **35**(8): p. 2526-34.
 61. Meyer, T.E., Fitch, J.C., Bartsch, R.G., Tollin, G., and Cusanovich, M.A., Soluble cytochromes and a photoactive yellow protein isolated from the moderately halophilic purple phototrophic bacterium, *Rhodospirillum salexigens*. *Biochimica et Biophysica Acta*, 1990. **1016**(3): p. 364-70.
 62. Hou, S., Saw, J.H., Lee, K.S., Freitas, T.A., Belisle, C., Kawarabayasi, Y., Donachie, S.P., Pikina, A., Galperin, M.Y., Koonin, E.V., Makarova, K.S., Omelchenko, M.V., Sorokin, A., Wolf, Y.I., Li, Q.X., Keum, Y.S., Campbell, S., Denery, J., Aizawa, S., Shibata, S., Malahoff, A., and Alam, M., Genome sequence of the deep-sea gamma-proteobacterium *Idiomarina loihiensis* reveals amino acid fermentation as a source of carbon and energy. *Proc Natl Acad Sci U S A*, 2004. **101**(52): p. 18036-41.
 63. Jiang, Z.a.B., E.C., Genetic characterization of photoactive yellow protein from *Rhodobacter capsulatus*. 1998(Unpublished).
 64. Mongodin, E.F., Nelson, K.E., Daugherty, S., Deboy, R.T., Wister, J., Khouri, H., Weidman, J., Walsh, D.A., Papke, R.T., Sanchez Perez, G., Sharma, A.K., Nesbo, C.L., MacLeod, D., Bapteste, E., Doolittle, W.F., Charlebois, R.L., Legault, B., and Rodriguez-Valera, F., The genome of *Salinibacter ruber*: convergence and gene exchange among hyperhalophilic bacteria and archaea. *Proceedings of the National Academy of Sciences of the United States of America*, 2005. **102**(50): p. 18147-52.
 65. Schneiker, S., Perlova, O., Kaiser, O., Gerth, K., Alici, A., Altmeyer, M.O., Bartels, D., Bekel, T., Beyer, S., Bode, E., Bode, H.B., Bolten, C.J., Choudhuri, J.V., Doss, S., Elnakady, Y.A., Frank, B., Gaigalat, L., Goesmann, A., Groeger, C., Gross, F., Jelsbak, L., Jelsbak, L., Kalinowski, J., Kegler, C., Knauber, T., Konietzny, S., Kopp, M., Krause, L., Krug, D., Linke, B., Mahmud, T., Martinez-Arias, R., McHardy, A.C., Merai, M., Meyer, F., Mormann, S., Munoz-Dorado, J., Perez, J., Pradella, S., Rachid, S., Raddatz, G., Rosenau, F., Rueckert, C., Sasse, F., Scharfe, M., Schuster, S.C., Suen, G., Treuner-Lange, A., Velicer, G.J., Vorholter, F.J., Weissman, K.J., DWelch, R., Wenzel, S.C., Whitworth, D.E., Wilhelm, S., Wittmann, C., Blocker, H., Puhler, A., and Mueller, R., Complete genome sequence of the myxobacterium *Sorangium cellulosum*. *Nature Biotechnology*, 2007. **25**(11): p. 1281-1289.
 66. Yooseph, S., Sutton, G., Rusch, D.B., Halpern, A.L., Williamson, S.J., Remington, K., Eisen, J.A., Heidelberg, K.B., Manning, G., Li, W.Z., Jaroszewski, L., Cieplak, P., Miller, C.S., Li, H.Y., Mashiyama, S.T., Joachimiak, M.P., van Belle, C., Chandonia, J.M., Soergel, D.A., Zhai, Y.F., Natarajan, K., Lee, S., Raphael, B.J., Bafna, V., Friedman, R., Brenner, S.E., Godzik, A., Eisenberg, D., Dixon, J.E., Taylor, S.S., Strausberg, R.L., Frazier, M., and Venter, J.C., The Sorcerer II Global Ocean Sampling expedition: Expanding the universe of protein families. *Plos Biology*, 2007. **5**(3): p. 432-466.
 67. Hou, S., Saw, J.H., Lee, K.S., Freitas, T.A., Belisle, C., Kawarabayasi, Y., Donachie, S.P., Pikina, A., Galperin, M.Y., Koonin, E.V., Makarova, K.S., Omelchenko, M.V., Sorokin, A., Wolf, Y.I., Li, Q.X., Keum, Y.S., Campbell, S., Denery, J., Aizawa, S., Shibata, S., Malahoff, A., and Alam, M., Genome sequence of the deep-sea gamma-proteobacterium *Idiomarina loihiensis* reveals amino acid fermentation as a source of carbon and energy. *Proceedings of the National Academy of Sciences of the United States of America*, 2004. **101**(52): p. 18036-41.

68. Donachie, S.P., Hou, S., Gregory, T.S., Malahoff, A., and Alam, M., *Idiomarina loihiensis* sp. nov., a halophilic gamma-Proteobacterium from the Lo'ihi submarine volcano, Hawai'i. *International Journal of Systematic and Evolutionary Microbiology*, 2003. **53**(Pt 6): p. 1873-9.
69. Haker, A., Hendriks, J., Gensch, T., Hellingwerf, K., and Crielgaard, W., Isolation, reconstitution and functional characterisation of the *Rhodobacter sphaeroides* photoactive yellow protein. *FEBS Letters*, 2000. **486**(1): p. 52-6.
70. Haker, A., Hendriks, J., van Stokkum, I.H., Heberle, J., Hellingwerf, K.J., Crielgaard, W., and Gensch, T., The two photocycles of photoactive yellow protein from *Rhodobacter sphaeroides*. *Journal of Biological Chemistry*, 2003. **278**(10): p. 8442-51.
71. Anton, J., Oren, A., Benlloch, S., Rodriguez-Valera, F., Amann, R., and Rossello-Mora, R., *Salinibacter ruber* gen. nov., sp. nov., a novel, extremely halophilic member of the Bacteria from saltern crystallizer ponds. *International Journal of Systematic and Evolutionary Microbiology*, 2002. **52**(Pt 2): p. 485-91.
72. Kyndt, J.A., Fitch, J.C., Meyer, T.E., and Cusanovich, M.A., The photoactivated PYP domain of *Rhodospirillum centenum* Ppr accelerates recovery of the bacteriophytochrome domain after white light illumination. *Biochemistry*, 2007. **46**: p. 8256-8262.
73. Kyndt, J.A., Fitch, J.C., Meyer, T.E., and Cusanovich, M.A., *Thermochromatium tepidum* photoactive yellow protein/bacteriophytochrome/diguanylate cyclase: characterization of the PYP domain. *Biochemistry*, 2005. **44**(12): p. 4755-64.
74. Tal, R., Wong, H.C., Calhoon, R., Gelfand, D., Fear, A.L., Volman, G., Mayer, R., Ross, P., Amikam, D., Weinhouse, H., Cohen, A., Sapir, S., Ohana, P., and Benziman, M., Three cdg operons control cellular turnover of cyclic di-GMP in *Acetobacter xylinum*: Genetic organization and occurrence of conserved domains in isoenzymes. *Journal of Bacteriology*, 1998. **180**(17): p. 4416-4425.
75. Simm, R., Morr, M., Kader, A., Nimtz, M., and Romling, U., GGDEF and EAL domains inversely regulate cyclic di-GMP levels and transition from sessility to motility. *Molecular Microbiology*, 2004. **53**(4): p. 1123-1134.
76. Koukol, J. and Conn, E.E., Metabolism of aromatic compounds in higher plants .4. Purification and properties of phenylalanine deaminase of *Hordeum Vulgare*. *Journal of Biological Chemistry*, 1961. **236**(10): p. 2692-&.
77. Parkhurst, J.R. and Hodgins, D.S., Yeast phenylalanine ammonia-lyase: properties of enzyme from *Sporobolomyces Pararoseus* and its catalytic site. *Archives of Biochemistry and Biophysics*, 1972. **152**(2): p. 597-&.
78. Haselkorn, R., Lapidus, A., Kogan, Y., Vlcek, C., Paces, J., Paces, V., Ulbrich, P., Pecenkova, T., Rebrekov, D., Milgram, A., Mazur, M., Cox, R., Kyrpidis, N., Ivanova, N., Kapatral, V., Los, T., Lykidis, A., Mikhailova, N., Reznik, G., Vasieva, O., and Fonstein, M., The *Rhodobacter capsulatus* genome. *Photosynthesis Research*, 2001. **70**(1): p. 43-52.
79. Kyndt, J.A., Meyer, T.E., Cusanovich, M.A., and Van Beeumen, J.J., Characterization of a bacterial tyrosine ammonia lyase, a biosynthetic enzyme for the photoactive yellow protein. *FEBS Letters*, 2002. **512**(1-3): p. 240-4.
80. Kort, R., Phillips-Jones, M.K., van Aalten, D.M., Haker, A., Hoffer, S.M., Hellingwerf, K.J., and Crielgaard, W., Sequence, chromophore extraction and 3-D model of the photoactive yellow protein from *Rhodobacter sphaeroides*. *Biochim Biophys Acta*, 1998. **1385**(1): p. 1-6.
81. Hahlbrock, K. and Scheel, D., Physiology and molecular biology of phenylpropanoid metabolism. *Annual Review of Plant Physiology and Plant Molecular Biology*, 1989. **40**: p. 347-369.
82. Imamoto, Y., Ito, T., Kataoka, M., and Tokunaga, F., Reconstitution photoactive yellow protein from apoprotein and p-coumaric acid derivatives. *FEBS Letters*, 1995. **374**(2): p. 157-60.

83. Baedeker, M. and Schulz, G.E., Autocatalytic peptide cyclization during chain folding of histidine ammonia-lyase. *Structure*, 2002. **10**(1): p. 61-67.
84. Schwede, T.F., Retey, J., and Schulz, G.E., Crystal structure of histidine ammonia-lyase revealing a novel polypeptide modification as the catalytic electrophile. *Biochemistry*, 1999. **38**(17): p. 5355-5361.
85. Calabrese, J.C., Jordan, D.B., Boodhoo, A., Sariaslani, S., and Vannelli, T., Crystal structure of phenylalanine ammonia lyase: Multiple helix dipoles implicated in catalysis. *Biochemistry*, 2004. **43**(36): p. 11403-11416.
86. Ritter, H. and Schulz, G.E., Structural basis for the entrance into the phenylpropanoid metabolism catalyzed by phenylalanine ammonia-lyase. *Plant Cell*, 2004. **16**(12): p. 3426-3436.
87. Poppe, L. and Retey, J., Friedel-Crafts-type mechanism for the enzymatic elimination of ammonia from histidine and phenylalanine. *Angewandte Chemie-International Edition*, 2005. **44**(24): p. 3668-3688.
88. Xue, Z.X., McCluskey, M., Cantera, K., Sariaslani, F.S., and Huang, L.X., Identification, characterization and functional expression of a tyrosine ammonia-lyase and its mutants from the photosynthetic bacterium *Rhodobacter sphaeroides*. *Journal of Industrial Microbiology & Biotechnology*, 2007. **34**(9): p. 599-604.
89. Watts, K.T., Lee, P.C., and Schmidt-Dannert, C., Exploring recombinant flavonoid biosynthesis in metabolically engineered *Escherichia coli*. *Chembiochem*, 2004. **5**(4): p. 500-507.
90. Berner, M., Krug, D., Bihlmaier, C., Vente, A., Muller, R., and Bechthold, A., Genes and enzymes involved in caffeic acid biosynthesis in the actinomycete *Saccharothrix espanaensis*. *Journal of Bacteriology*, 2006. **188**(7): p. 2666-2673.
91. Vannelli, T., Qi, W.W., Sweigard, J., Gatenby, A.A., and Sariaslani, F.S., Production of p-hydroxycinnamic acid from glucose in *Saccharomyces cerevisiae* and *Escherichia coli* by expression of heterologous genes from plants and fungi. *Metabolic Engineering*, 2007. **9**(2): p. 142-151.
92. Watts, K.T., Mijts, B.N., Lee, P.C., Manning, A.J., and Schmidt-Dannert, C., Discovery of a substrate selectivity switch in tyrosine ammonia-lyase, a member of the aromatic amino acid lyase family. *Chemical Biology*, 2006. **13**(12): p. 1317-26.
93. Memmi, S., Kyndt, J.A., Meyer, T.E., Devreese, B., Cusanovich, M.A., and Van Beeumen, J., Photoactive yellow protein from the halophilic bacterium *Salinibacter ruber*. *Biochemistry*, 2008. **47**(7): p. 2014-2024.
94. Korbel, J.O., Jensen, L.J., von Mering, C., and Bork, P., Analysis of genomic context: prediction of functional associations from conserved bidirectionally transcribed gene pairs. *Nature Biotechnology*, 2004. **22**(7): p. 911-917.
95. Rudolph, J. and Oesterhelt, D., Deletion analysis of the che operon in the archaeon *Halobacterium salinarium*. *Journal of Molecular Biology*, 1996. **258**(4): p. 548-554.
96. Walsby, A.E., Gas Vesicles. *Microbiological Reviews*, 1994. **58**(1): p. 94-144.
97. Pfeifer, F., Gregor, D., Hofacker, A., Plosser, P., and Zimmermann, P., Regulation of gas vesicle formation in halophilic archaea. *Journal of Molecular Microbiology and Biotechnology*, 2002. **4**(3): p. 175-181.

Chapter four

4 Photoactive Yellow Protein from the halophilic bacterium *Salinibacter ruber*^{II}

Samy Memmi[§], John Kyndt^{§‡}, Terry Meyer[‡], Bart Devreese[§], Michael Cusanovich[‡] and Jozef Van Beeumen[§]

[§]Laboratory of Protein Biochemistry and Biomolecular Engineering, Ghent University, K.L. Ledeganckstraat 35, 9000 Ghent, Belgium.

[‡]Department of Biochemistry and Molecular Biophysics, University of Arizona, Tucson, AZ 85721 Arizona, USA

Abstract

A gene for photoactive yellow protein (PYP) was identified from the genome sequence of the extremely halophilic aerobic bacterium *Salinibacter ruber* (Sr). The sequence is distantly related to the prototypic PYP from *Halorhodospira halophila* (Hh) (37% identity) and contains most of the amino acid residues identified as necessary for function. However, the *Salinibacter ruber* *pyp* gene is not flanked by its two biosynthetic genes as in other species. To determine whether the Sr *pyp* gene encodes a functional protein, we cloned and expressed it in *E. coli*, along with the genes for chromophore biosynthesis from *Rhodobacter capsulatus* (Rc). The Sr PYP has a 31 N-terminal extension compared to other PYPs that appears to be important for dimerization, however, truncation of these extra residues did not change the spectral and photokinetic properties. Sr PYP has an absorption maximum at 431 nm, which is at shorter wavelengths than the prototypical Hh PYP (at 446 nm). It is also photoactive, being reversibly bleached by either blue or white light. The kinetics of dark recovery is slower than any of the PYPs reported to date ($4.27 \times 10^{-4} \text{ s}^{-1}$ at pH 7.5). Sr PYP appears to have a normal photocycle with the I₁ and I₂ intermediates. The presence of the I₂' intermediate is also inferred on the basis of the effects of temperature and alcohol on recovery. Sr PYP has an intermediate spectral form in equilibrium with the 431 nm form, similar to *Rhodobacter capsulatus* PYP and the Y42F mutant of Hh PYP. Increasing ionic strength stabilizes the 431 nm form at the expense of the intermediate spectral form and the kinetics of recovery is accelerated 6.4 fold between 0 and 3.5 M salt. This is observed with ions

^{II} This chapter has been published in *Biochemistry* 2008. **47**(7): p. 2014-24, and is presented here with some minor adaptations.

from both the chaotropic and kosmotropic series. Ionic strength also stabilizes PYP against thermal denaturation, as the melting temperature is increased from 74°C in buffer alone to 92°C in 2 M KCl. *S. ruber* accumulates KCl in the cytoplasm, like *Halobacterium*, to balance osmotic pressure, and has very acidic proteins. We thus believe that Sr PYP is an example of a halophilic protein that requires KCl to electrostatically screen the excess negative charge and stabilize the tertiary structure.

Introduction

Organisms are subjected to a variety of environmental stimuli to which they respond and adapt. The information from light stimuli is recorded by photosensory proteins, specially adapted to absorb particular wavelengths of the solar spectrum and transmitting the signals to intracellular response regulators. They solely function in signal transduction, monitoring the environmental light quality, quantity and direction, and have to be considered separately from the specialized photosynthetic pigments that convert solar energy to chemical energy for growth and development. Light absorption in biological signal transfer is conducted by a number of photosensory families, each characterized by the binding of a chromophore from a particular class of chemical compound: rhodopsins with retinal [1], phytochromes with tetrapyrrole [2], phototropins, cryptochrome [2, 3] and BLUF-proteins with FMN [4] and photoactive yellow proteins (PYPs) with p-hydroxy-cinnamic acid [5]. The latter family currently consists of a set of 20 homologous photoreceptors from 13 bacterial species [6] and 5 isolated from unidentified bacteria in seawater samples [7]. The prototypic photoactive yellow protein (Hh PYP), first isolated from the phototrophic bacterium *Halorhodospira* (formerly *Ectothiorhodospira*) *halophila* [8] has a wavelength maximum at 446 nm ($\epsilon = 45 \text{ mM}^{-1} \text{ cm}^{-1}$), and is a 14 kDa water-soluble, cytoplasmic blue-light photoreceptor. The PYP chromophore is covalently bound to a conserved cysteine residue via a thioester linkage. Upon blue light illumination, PYP enters a photocycle during which the chromophore undergoes *trans-cis* isomerization and the 446 nm absorption maximum is bleached and blue-shifted to $\sim 350 \text{ nm}$ within milliseconds and recovers in the dark within 1 s [9]. Several intermediates of the Hh PYP photocycle have been identified based on their spectral and temporal changes. The early intermediates I_0 and I_0^\ddagger have lifetimes in the picosecond time range and red shifted absorption maxima ($\sim 510 \text{ nm}$) [10, 11]. They decay to I_1 , which has an absorption maximum at 465 nm and has the chromophore in a *cis* orientation through a rotation of its C9 carbonyl [12]. In about 120 μs , this intermediate decays into I_2 , in which the chromophore ring has moved out towards the solvent and becomes protonated (lifetime $\sim 1.5 \text{ ms}$). A conformational change which involves exposure of a significant part of the hydrophobic protein interior, forms the I_2' intermediate. Finally, I_2' recovers back to the ground state in

milliseconds [13]. Since the I_2' intermediate is the longest living species and the only one with a significant conformational change, it is generally thought to be the signaling state of PYP.

There is only one instance where the functional role of PYP is clearly defined. In *Rhodospirillum centenum* (aka *Rhodocista centenaria*) there is evidence that the hybrid photoreceptor Ppr¹, which has a PYP domain linked to bacteriophytochrome and histidine kinase domains, is involved in regulating expression of a polyketide synthase related to chalcone synthase [14]. It has recently been shown that blue-light activated PYP, in Ppr, functions to accelerate the recovery of the red-light activated phytochrome domain to the dark-adapted state [15]. Moreover, expression of the polyketide synthase appears to be linked to the formation of desiccation-resistant cysts [16] that result from nutrient limitation and other stress, which could implicate a role for Ppr in regulating cyst formation. By way of contrast, PYP in *Halorhodospira halophila* is proposed to be involved in mediating a photophobic response to blue light to avoid UV-radiation damage. The wavelength dependence of this response coincides with the PYP absorption spectrum, suggesting that PYP is the primary photoreceptor for this behavior [17]; however, no conclusive evidence such as the existence of gene inactivation mutants has been presented yet.

As new genes encoding photoactive yellow proteins are discovered through genome sequencing, it becomes more obvious that those forms of PYP having significant differences in physico-chemical properties serve different functional roles [6]. The diversity of PYP gene distribution has increased even more by the recent observation that PYPs can originate from non-phototrophic bacteria, *i.e.* *Idiomarina loihiensis* [18], *Burkholderia phytofirmans* (Joint Genome Institute), *Stigmatella aurantiaca* (The Institute for Genome Research), and *Salinibacter ruber* [19], as well as from phototrophs.

Salinibacter ruber is a red, obligately aerobic, chemoorganotrophic, extremely halophilic bacterium. The species occupies the same habitat as *Halobacterium* and *Halorhodospira* species and was recently isolated from salt evaporation ponds in Spain [20]. It grows at an optimal salt concentration of 20-30% and a temperature of 37-47°C. The 16S rRNA sequence indicates that it is not an archaeobacterium, but that it is related to the *Cytophaga-Flavobacterium* branch of bacteria. Nevertheless *S. ruber* has remarkable physiological similarities to the extremely halophilic *Halobacterium*. Like the latter, *S. ruber* has adapted its life at high salt concentrations by accumulating KCl in molar concentrations to provide the necessary osmotic balance [21]. This greatly differs from the more common strategy used by all other known halophilic and halotolerant bacteria by which organic compatible solutes, such as ectoine, glycine betaine, and others, are produced and/or accumulated, to respond to osmotic stress following the initial response, which involves a transient moderate increase in KCl [22].

¹ PYP-phytochrome related

We present here the first characterization of PYP from *Salinibacter ruber*. Although it has interesting differences that allow adaptation to the specific physiology of the organism, there are also similarities to the prototypic Hh PYP. The genetic context and the presumed function are also discussed.

Materials and Methods

*Cloning of *Salinibacter ruber* pyp*

A polymerase chain reaction (PCR) was performed to amplify DNA encoding the *Salinibacter ruber* *pyp* (SRU_2224) using the Easy-A High Fidelity PCR cloning enzyme (Stratagene, La Jolla, CA). PCR was performed according to the manufacturer's instructions and using *S. ruber* chromosomal DNA as template. The following primers were designed based on the *S. ruber* genome sequence [19]: 5'-GGAATTCCCATATGGCTGACTCTCAGGAATCCG-3' and 5'-CATGCCTCGAGTCACCGCTTCTGAATCAGGATCC-3'. The primers were designed with restriction sites for *NdeI* and *XhoI* respectively (underlined in the sequence). The expression vector was constructed by ligating the *NdeI/XhoI* digested *pyp* fragment in pET20b (Novagen, Madison, WI, USA) digested with the same restriction enzymes. The construction of the pACYC(*tal;pcl*) plasmid that contains the two biosynthetic genes from *Rhodobacter capsulatus* for holo-PYP formation was described earlier [23].

*Overproduction and purification of *Salinibacter ruber* PYP*

All expression experiments were performed with *Escherichia coli* BL-21 (DE3). After co-transformation of pET20b(*Srppyp*) and pACYC(*tal;pcl*) to the bacterial cells, cultures were grown on carbenicillin (Cb, 100 µg/mL) and chloramphenicol (Cm, 25 µg/mL) antibiotics. An overnight culture was used to inoculate LB medium containing both antibiotics. The culture was grown at 37°C until an OD₆₀₀ of approximately 0.6. At that point, the temperature was lowered to 28°C and the cells were induced with a final concentration of 0.5 mM IPTG. The cells were pelleted by ultracentrifugation after 16h of induction. After resuspending in Tris-HCl buffer (100 mM, pH 8.0), the cells were frozen at -20°C till further purification. The cells were fractionated by sonication, followed by centrifugation to remove the cell debris. The soluble fractions were loaded onto a 10 mL Q-Sepharose Fast Flow column (Amersham Biosciences). Tris-HCl buffer (100 mM, pH 8.0) was used to apply the sample, and proteins were eluted using the same buffer supplemented with an increasing amount of NaCl (with steps of 100 mM, 250 mM, 350 mM, 500 mM and 1 M). The PYP eluted mainly with 350 mM NaCl. The yellow-colored fractions were pooled and concentrated on Vivaspin 15R centrifugal filters (5,000 MWCO, Sartorius, Goettingen, Germany). The purification was continued by size exclusion chromatography on a

Superdex 75 column (Hiload 16/60, Amersham Biosciences) with 100 mM Tris-HCl, pH 8.0, supplemented with 50 mM NaCl as running buffer using an ÄKTA Explorer FPLC system (Amersham Biosciences). During this step, the holo-protein eluted in two separate peaks, of which the ratio between the first and second peak was calculated to be 2.5 according to the absorbance at 431 nm. In fact, comparing the elution volume to a calibration curve indicated a dimeric and monomeric Sr PYP form present on the size-exclusion column. Mass spectrometry identified the monomeric peak as a PYP variant that was N-terminally truncated by 30 amino acids compared to the dimeric peak, representing full-length Sr PYP (see below). This observation suggests that the N-terminal extension induces dimerization of the native form. After this step, SDS-PAGE analysis showed that the sample was > 90% pure, but the UV-VIS absorption spectrum showed a 280 to 431 nm ratio of 1.2, as the consequence of the presence of apo-PYP, *i.e.* PYP protein lacking a chromophore. Holo- and apo-PYP were partially separated using hydrophobic interaction chromatography on a Phenyl Sepharose CL-4B column (GE Healthcare). Sr PYP was applied to the column in 50 mM Tris-HCl as binding buffer, pH 8.0, supplemented with 1.7 M $(\text{NH}_4)_2\text{SO}_4$, and elution was performed with the same buffer without salt using a linear gradient. After this step, the 280/431 ratio of holo-PYP was 0.94, with a yield of 1.5 mg per liter of culture.

Mass spectrometry

Molecular mass analysis was performed on a Q-TOF mass spectrometer (Micromass, Manchester, UK) equipped with a Nanomate 100 (Advion, Ithaca, NY) electrospray source. Approximately 5-10 pmol of protein was dissolved in 5 μL of 50% ACN/0.1% HCOOH and infused into the ESI-chip.

To localize the cleavage site of the truncated PYP-form, the holo-protein was digested with trypsin, in 50 mM NH_4HCO_3 , for 6 h at 37°C. The ratio of trypsin to holo-protein was 1/100 (w/w). The resulting peptides were analyzed by MALDI-TOF/TOF mass spectrometry on a 4700 Proteomics Analyzer (Applied Biosystems, Foster City, CA).

UV-Vis spectroscopy and 'time resolved' laser spectroscopy

Absorption spectra were obtained using a UVIKON spectrophotometer (Kontron, Herts, UK). Samples were measured using Tris buffer at varying concentrations and values of pH, as indicated. The recovery experiments with Sr PYP were carried out in universal buffer (2 mM CAPS, CHES, Bicine, HEPES, PIPES, MES and sodium citrate) or Tris buffer, as indicated. The protein was first bleached by a 0.5 to 1 minute exposure to a tungsten lamp (60 W) and the recovery was subsequently measured in the dark in the spectrophotometer. The maximum bleach

was achieved after ~ 3 min illumination. Absorbance changes were measured over a maximal 250 min time range, and the kinetic data were fit using Sigmaplot 8.0 software. The laser flash apparatus and data analysis protocol to study the μ s time recovery were as described previously [8, 24].

Fluorescence spectroscopy

Fluorescence excitation and emission spectra were recorded on a PC1 photon counting spectrofluorometer (ISS, Champaign, IL) and the data were analyzed with the VINCI software. The samples for fluorescence measurement were in 50 mM Tris-HCl (pH 7.1) and had an absorbance of 0.12 at their maximum wavelength (431 nm for Sr PYP and 446 nm for Hh PYP).

Results and discussion

*Gene context of *S. ruber* PYP*

The completed genome sequence of *S. ruber* [19] contains one gene coding for a PYP. To date, it is the only example of a *pyp* gene being discovered outside the proteobacteria and it is one out of four instances in which it has been found in a non-photosynthetic species. In none of these cases has the PYP protein been characterized. Five of the thirteen species in which PYP has been identified are halophiles, suggesting that it may be involved in the regulation of osmotic pressure. However, the gene for PYP (SRU_2224) is surrounded by a number of hypothetical proteins, which complicates inference of a possible functional role based on the nature of the genetic context. There are no obvious regulatory genes in the vicinity of PYP with which it may interact, but there are genes for transporters and porins in the near distance that may be relevant to its function. Adjacent to PYP is an operon consisting of a hypothetical protein (SRU_2223) and a membrane protein of the TerC family (SRU_2222, for Tellurite resistance) which is divergently transcribed relative to the *pyp* gene. Converging on *pyp* from the downstream side, the gene for a membrane protein (SRU_2225) is divergently transcribed with a hypothetical protein (SRU_2226) and a homolog of UbiE, an S-adenosyl methionine dependent methylase (SRU_2227). None of these nearby genes have obvious relevance to the possible function of PYP.

Further downstream, however, there are two stomatin homologs (SRU_2228 and SRU_2229) and an associated protease (SRU_2230). When cleaved by the protease, stomatin functions to open ion channels and regulate transporters [25]. More generally, these proteins function to degrade membrane proteins that are not folded properly. Six genes further downstream is an *ompA* porin homolog (SRU_2237) followed by a sulfate transporter (SRU_2239). A 19-gene hyper-salinity island including six genes for potassium uptake and five

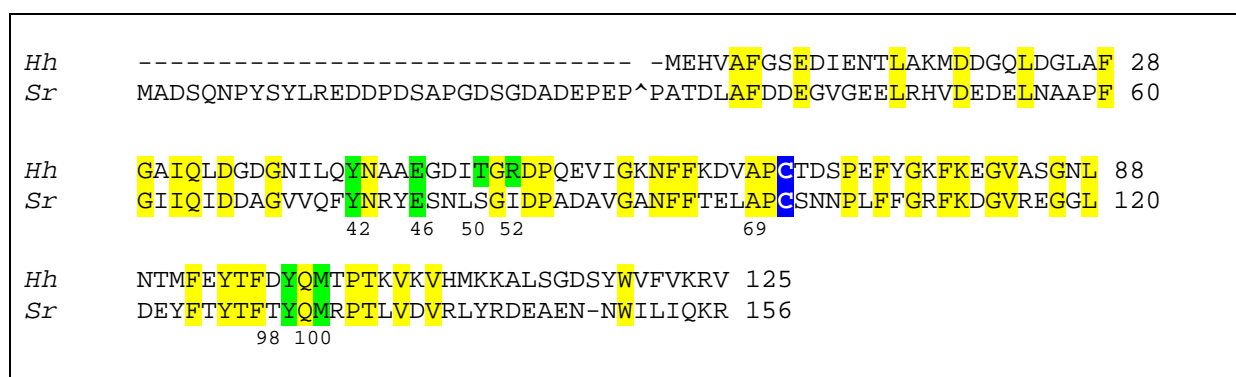
genes for cationic amino acid transporters was identified 32 genes downstream of *pyp* [19]. Immediately preceding it is a potassium/proton antiporter. All these data suggest that the hypersalinity island may be larger than thought and may include PYP and the intervening genes. Thus, the Sr PYP may be loosely associated with porin and transporter genes. Nevertheless, we were unable to locate any sensor kinase or regulator between PYP and the end of the hypersalinity island that might act as a reaction partner for PYP.

In *H. halophila*, the two biosynthetic enzyme genes, a tyrosine ammonia lyase and a p-hydroxycinnamoyl:CoA ligase [23], are located adjacent to that for PYP. In *S. ruber*, two ammonia lyase genes, SRU_717 and SRU_722, are present 1.8 Mbp from the *pyp* gene and mutually separated by 6 kbp. SRU_717 has an H103L104 sequence equivalent to the *Rhodobacter sphaeroides* active site residues H89L90 that determine tyrosine ammonia lyase specificity [26]. SRU_722, on the other hand, is consistent with having histidine ammonia lyase activity. We thus believe that SRU_717 is the biosynthetic enzyme for PYP. The second biosynthetic enzyme, p-hydroxycinnamic acid:CoA ligase, is less conserved than are the tyrosine ammonia lyases. Nevertheless, we found weak homology in SRU_1355, annotated as an o-succinyl-benzoate:CoA ligase which has most of the active site residues found in 4-chloro-benzoate:CoA ligase of which the 3D structure has been determined [27]. There is little doubt that SRU_1355 codes for a CoA ligase, but the substrate specificity is less certain.

Sequence homology

Figure 4.1 shows the sequence alignment of *S. ruber* PYP with the prototypic PYP from *H. halophila* BN9626. Sr PYP consists of 156 amino acids, shows only 37% sequence identity with 46 identical amino acids, but all amino acids previously identified as necessary for spectral tuning of the chromophore are present, except for the equivalent of Hh T50 and R52. The former is conservatively substituted by serine in Sr PYP, as in *R. centenaria* Ppr, but R52 is replaced by isoleucine, which may have functional consequences because it must move out of the way of the chromophore during isomerization [28].

S. ruber PYP has an N-terminal extension with 32 additional amino acids compared to Hh PYP and is the most acidic PYP species known to date, with a theoretical *pI* of 3.95, and it remains acidic when the 32 amino acid extension is omitted from the calculation (theoretical *pI* = 4.2). This extremely acidic nature of Sr PYP is consistent with the high intracellular potassium concentration as a mode of haloadaptation. To ensure protein solubility at such high ionic strength, *Salinibacter* proteins have a high content of acidic amino acids and a relatively low content of hydrophobic residues [19, 29].

**Figure 4.1**

Sequence alignment of the Photoactive Yellow Proteins from *H. halophila* BN9626 (*Hh*) and *S. ruber* (*Sr*). The conserved residues are marked in yellow. The residues involved in chromophore binding through a hydrogen bonding network, and Met100 are marked in green. The conserved Cys69, which forms a thioester bond with the chromophore, is marked in blue. The numbering of the important residues is according to Hh PYP. The cleavage site of $\Delta 31$ -PYP is also indicated (^).

Protein production, purification and mass spectrometry

To determine whether the *Sr pyp* gene encodes a functional protein and to study its properties, we cloned and expressed the PYP coding gene in *E. coli*, along with the two biosynthetic enzyme genes from *R. capsulatus*, *i.e.* *pcl* and *tal*. The holoprotein was successfully produced and purified, indicating that *Sr pyp* is not a pseudogene. The electrospray mass spectrum of purified *Sr* PYP yielded masses of 17402 Da and 17547 Da, corresponding to the calculated masses of apo- and holo- *Sr* PYP protein respectively, both without the N-terminal methionine (**Figure 4.2a**). During purification, it became clear that native *Sr* PYP behaved as a dimer during size-exclusion chromatography, while a second form (with a relative abundance of 40% compared to the full form) eluted as a monomer and showed molecular masses of 14210 Da and 14355 Da by ESI-MS (**Figure 4.2b**). These masses correspond to the calculated masses of apo- and holo- *Sr* PYP protein respectively, both lacking the first 31 N-terminal amino acids (including the initiator Met).

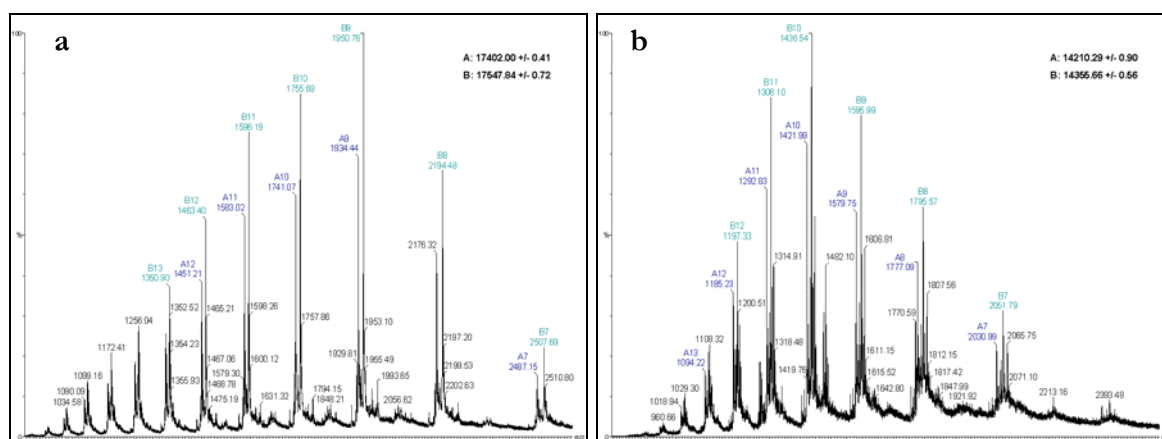


Figure 4.2

Electrospray mass spectra of heterologously produced Photoactive Yellow Protein of *S. ruber* (a) and its $\Delta 31$ N-terminally truncated form (b). The values following the letters refer to the different number of protons for each of the m/z values detected during a single scan.

The cleavage site of the truncated Sr PYP form ($\Delta 31$ -PYP) is located at the C-terminal side of proline 31, as confirmed by MALDI-MS of a tryptic digest. The peptide mass fingerprint of $\Delta 31$ -PYP showed the absence of two peaks of masses 1313.63 Da and 3729.63 Da, corresponding to the respective peptides Ala 2 – Arg 12 and Glu 13 – Arg 48. Instead, a new peak with a mass of 1833.88 Da occurred which corresponds to the theoretical mass of peptide Pro 32 – Arg 48, as shown in **Figure 4.3** and **Table 4-1**.

Table 4-1. Calculated and experimentally determined masses of tryptic peptides of heterologously produced *S. ruber* PYP.

Peptide position			Theoretical mass (Da) ^a	Experimental mass (Da)
Ala 2	–	Arg 12	1313.39	1313.64
Glu 13	–	Arg 48	3729.53	3729.63
His 49	–	Arg 76	3145.52	3145.58
Tyr 77	–	Arg 110	3633.70 ^b	3633.81
Glu 117	–	Arg 133	2121.31	2120.95
Glu 117	–	Arg 140	2901.38	2901.44
Leu 141	–	Lys 155	1904.99	1905.02
Leu 141	–	Arg 156	2061.09	2061.08
Pro 32	–	Arg 48	1833.93	1833.88

^a Calculated using monoisotopic masses of the amino acids and giving peptide masses as $[M+H]^+$
^b Mass without chromophore

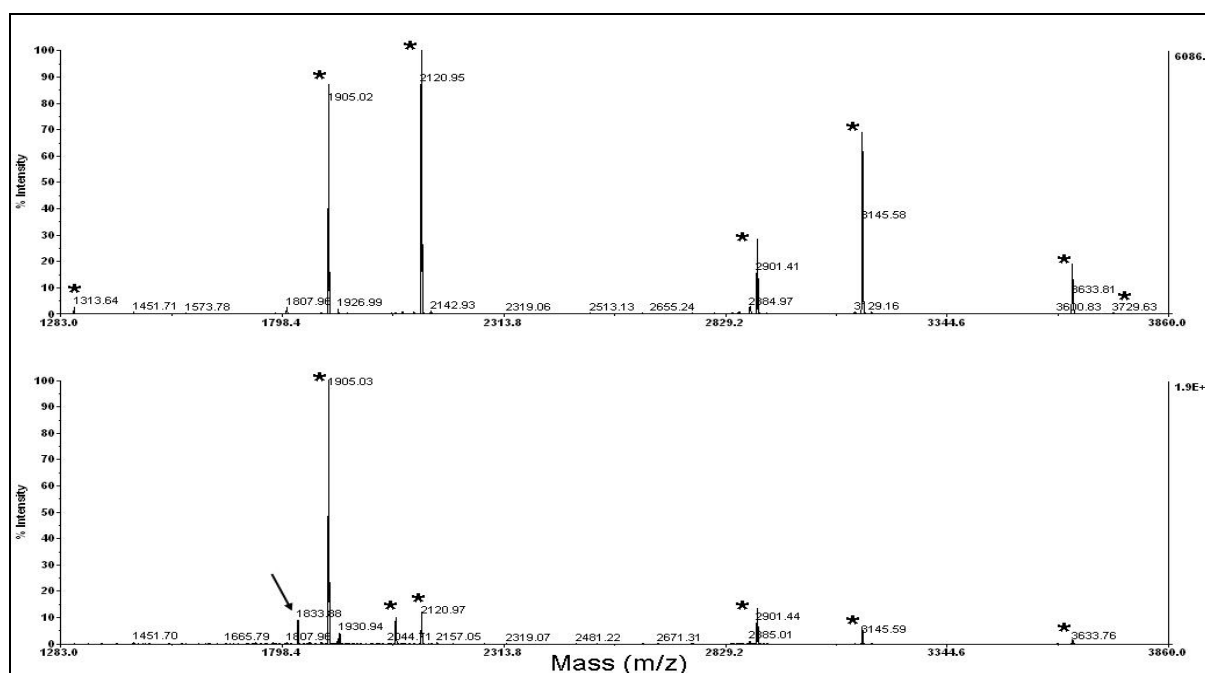


Figure 4.3

Comparative peptide mass fingerprint (PMF) of *Salinibacter ruber* PYP (upper trace) and $\Delta 31$ -PYP (lower trace) after trypsin digest. The mass peaks corresponding to tryptic peptides are marked with an asterisk (*) and listed in Table 4-1. A peak with a mass of 1833.88 Da, corresponding with the theoretical mass of peptide Pro 32 – Arg 48, is indicated by the arrow.

Since the intracellular salt concentration in *S. ruber* is unusually high to regulate osmotic balance, we performed a size-exclusion chromatography experiment with the full-length SrPYP form using 100 mM Tris-HCl, pH 8.0, supplemented with 1 M KCl as running buffer. The dimer was not interrupted and therefore is likely to be physiological. The cleavage of a Pro-Pro bond is rather unusual, with no precedent of which we are aware. It may be significant that the protein is partially cleaved by proteolysis during production and purification close to the start of homology with Hh PYP, as shown in **Figure 4.1**. It suggests that the 32-residue extension is disordered relative to the remainder of the protein and, based on its behavior during size-exclusion chromatography, induces dimerization of the full-length Sr PYP form. Dimerization of Sr PYP is unique, as no precedents with any of the other published PYPs have been described before. However, it is not uncommon for photoreceptor proteins to form functional dimers. For example, plant phytochromes exist as red-light sensing homodimers [30], which is also the case for the blue-light absorbing *Arabidopsis* cryptochrome 1 (CRY1), where homodimerization of the N-terminal domain has been shown to be essential for photoreceptor activity [31]. Another example of a dimeric photoreceptor is the blue-light sensing BLUF-domain of the transcriptional

anti-repressor AppA. In the dark state, dimerization is mediated through hydrophobic interactions between a β -sheet of two monomers, as shown by X-ray crystallography [32, 33].

In Hh PYP, the N-terminal cap, which consists of a helix-turn-helix motif, is believed to have a role in signal transduction [34, 35]. However, no structural motif could be predicted for the N-terminal extension of Sr PYP, using secondary structure prediction tools (*i.e.* Predator [36]). Moreover, a Psi-Blast with the 32 amino acid containing N-terminal sequence does not find any significant homology with protein entries in the database that would provide any hint as to function. Thus, although the truncation of the N-terminal extension does not seem to influence the photochemical properties (as further described below), its implication in signaling remains speculative as no homologous precedents are available.

UV-Vis spectroscopy: effects of chaotropic and kosmotropic agents, and temperature on full-length Sr PYP

Compared to known PYPs, *Salinibacter ruber* PYP has a blue-shifted absorption maximum at 431 nm and a broader peak as the result of a blue spectral shoulder (Figure 4.4, solid line). The absorption maximum can be partially bleached by room light and to a greater extent by white light illumination from a 60W tungsten source, as also shown in Figure 4.4.

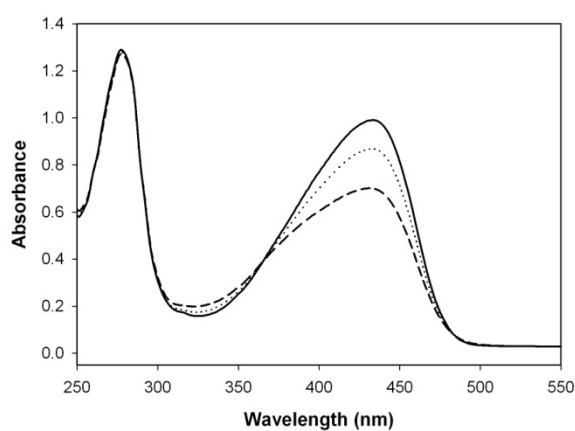


Figure 4.4

Effect of light on the spectrum of Sr PYP in 50 mM Tris pH 7.5. Dark adapted spectrum (solid line) and spectra following exposure to room light (dotted line) or 1 minute illumination from a tungsten source (dashed line).

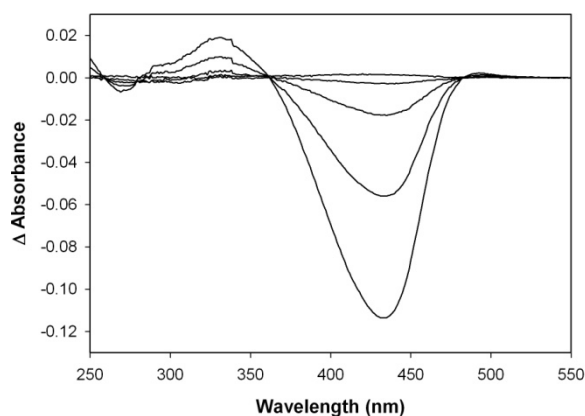


Figure 4.5

Light minus dark difference spectrum for Sr PYP recovery in 50 mM Tris-HCl, pH 8, at room temperature. Spectra were taken at different time points after illumination with a tungsten source. The isosbestic point for the 334 nm to 431 nm transition is at 361 nm.

The spectral changes are completely reversible by overnight incubation in the dark. The light minus dark difference spectrum (**Figure 4.5**) shows formation of an intermediate similar to Hh PYP I₂, with a 334 nm maximum and an isosbestic point at 361 nm, although somewhat blue-shifted as discussed below. There is also evidence for an equilibrium with a small amount of the earlier intermediate I₁, in that there is a small, but broad difference peak in the vicinity of 490 nm.

The absorption spectrum of Sr PYP suggests the presence of an intermediate spectral form similar to that of the Y42F mutant of Hh PYP [37, 38] and WT Rc PYP [39]. In the Y42F mutant, a 390 nm spectral shoulder on the 458 nm maximum, due to a second less stable chromophore conformation in the ground state, was found to be pH and temperature dependent and to be strongly affected by the opposing effects of chaotropes and kosmotropes [37]. This intermediate spectral form, the hallmark of which is a wavelength maximum that is dependent upon environmental factors, was later found in other PYP mutants, and has been ascribed to a PYP form with higher and continuously variable dielectric constant and altered hydrogen-bonding to E46 in the chromophore region [38]. Rc PYP displays a secondary peak at 375 nm that is also temperature and pH dependent, although there is an additional PYP form present that has the chromophore in a *cis* conformation (with a presumed maximum close to 350 nm) that is stabilized at low temperature, which complicates interpretation of the temperature dependence [39]. In order to investigate whether a similar behavior occurs in Sr PYP and to further characterize the spectral shoulder, we studied the effects of chaotropic and kosmotropic agents, as well as of temperature.

The effects of the kosmotrope (NH₄)₂SO₄ and the chaotrope NH₄Cl are shown in **Figure 4.6a** and **Figure 4.6b** respectively. Surprisingly, like KCl (see below), both ammonium salts stabilize the main peak at 431 nm by significantly increasing the absorption maximum while the blue shoulder decreases accordingly. Therefore, the Sr PYP appears to respond more strongly to ionic strength than to specific ion effects. We conclude that the shoulder on the short wavelength side of the absorption maximum in Sr PYP is due to a less stable conformation that is eliminated at high ionic strength. However, we have insufficient data to say whether it has the same origin as in Hh PYP Y42F or in wild type Rc PYP.

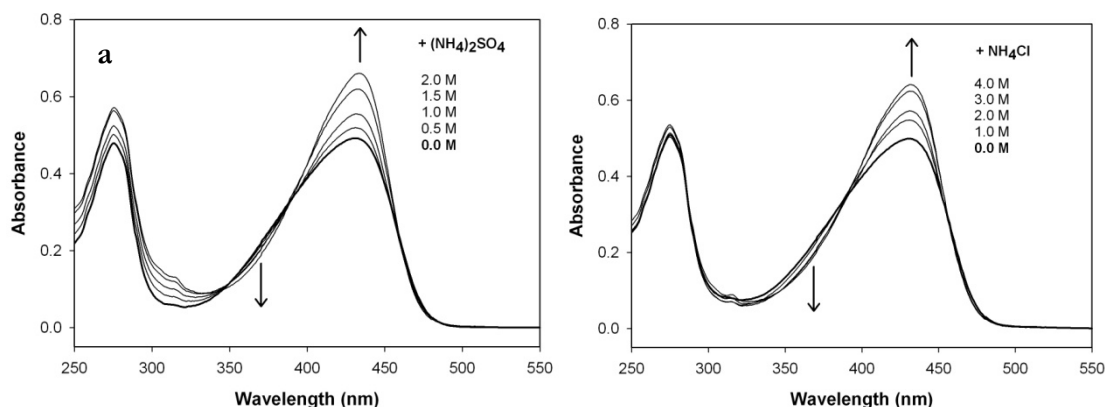


Figure 4.6

(a) Effect of increasing concentrations of the kosmotrope $(\text{NH}_4)_2\text{SO}_4$ and (b) increasing concentrations of the chaotrope NH_4Cl on the absorption spectrum of Sr PYP in 50 mM Tris-HCl buffer, pH 7.5, at room temperature. The arrows indicate the direction of increasing salt concentration.

Sr PYP can be reversibly heated to 80°C as shown in **Figure 4.7a**. However, the absorbance at 431 nm slightly drops prior to denaturation as shown by the 431 nm absorbance vs. temperature plot in **Figure 4.7b**. The 10 degrees minus 70 degrees difference spectrum (data not shown) indicates that the spectral shoulder is increased relative to the 431 nm maximum before it denatures. Under the low ionic strength conditions of measurement (50 mM Tris-HCl, pH 7.5), the melting temperature T_m is 74°C , which is intermediate between that of WT¹ Hh PYP (82°C) and the Y42F mutant (65°C) [38].

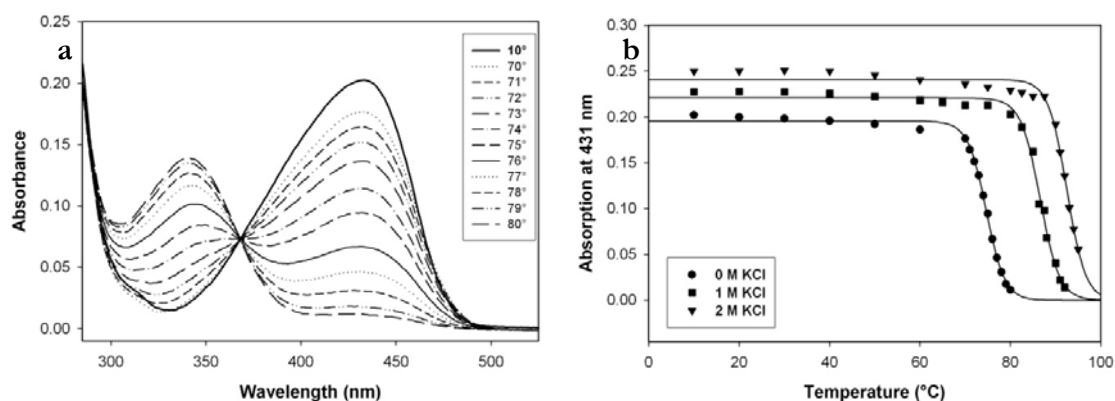


Figure 4.7

(a) Temperature dependence of the absorption spectrum of Sr PYP in 50 mM Tris-HCl, pH 7.5. Sr PYP can be reversibly heated to 80°C , at which the 431 nm peak is converted to a denatured 340 nm species with a single isosbestic point. (b) UV/VIS absorbance at the 431 nm wavelength maximum as a function of temperature in the absence (circles) and presence of 1 M (squares) and 2 M (triangles) KCl. The solid lines represent the fitted curves.

However, addition of KCl, of which *S. ruber* cells contain molar amounts to regulate osmotic balance, increases the melting temperature to 86.6 °C and 92.5 °C with 1 M and 2 M KCl, respectively, as shown in **Figure 4.7b**. This indicates a stabilizing effect of KCl on the native protein conformation. The relatively high melting temperature suggests that Sr PYP is somewhat less stable than Hh PYP under low ionic strength conditions, but may be more stable at high ionic strength (although Hh PYP was not studied under these conditions).

Fluorescence spectroscopy

We examined the fluorescence excitation spectrum (with emission monitored at 490 nm) and the emission spectrum (with excitation at 400 nm), as shown in **Figure 4.8**. As a control, we also measured the Hh PYP fluorescence spectra. It had previously been shown that the Hh PYP fluorescence quantum yield is relatively low ($\sim 0.2\%$ [40]). The excitation maximum of Sr PYP fluorescence appears to be around 400 nm, which corresponds better to the spectral shoulder in the UV-Vis absorption spectrum than to the 431 nm maximum. It is, therefore, likely that the spectral shoulder is the basis for the high Sr PYP fluorescence. The fluorescence emission maximum of Sr PYP is at 490 nm, compared to 495 nm for Hh PYP, and the intensity is about ten-fold higher than for Hh PYP when measured with the equivalent visible absorption. Taking into account that the absorption maximum of Sr PYP is blue-shifted by 15 nm (431 vs 446), the fluorescence maximum is less blue-shifted (only 5 nm), compared to the expected value. If indeed the spectral shoulder is the fluorescent form, then this ‘red shift’ would be expected to be even larger.

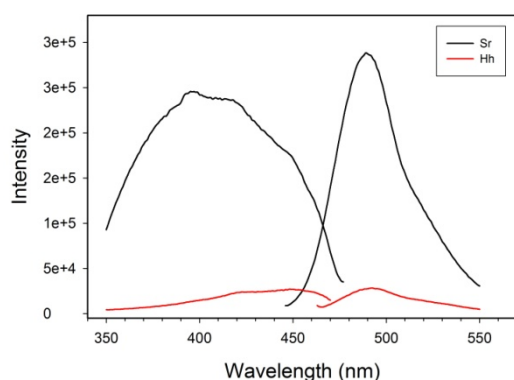


Figure 4.8

Fluorescence excitation and emission spectra of Sr PYP (black) and Hh PYP (red) in 50 mM TrisHCl (pH 7.1). Sample absorbance was 0.12 at their maximum wavelength (431 nm for Sr PYP and 446 nm for Hh PYP).

We recently showed that the Hh mutant Y98Q also has an increased and red-shifted fluorescence, [41]. Based on structural data, it was concluded that the red-shift in fluorescence was due to an increase in polarity in the chromophore environment, which was caused by a repositioning of R52 in the ground state, allowing two water molecules to come in close proximity of the chromophore. Since Sr PYP has a natural R52I substitution, it may likewise

cause a change in dielectric constant of the chromophore surroundings by making it more solvent accessible, leading to the observed ‘red shifting’ effect on the fluorescence. The excitation spectrum reveals that there is not only a shift in fluorescence of Sr PYP under UV-illumination, but also a higher intensity (**Figure 4.9**), similar to Hh mutant Y42F. Structural analysis of Y42F indicates possible chromophore bowing to be responsible for the control of chromophore fluorescence [42]. In wild-type Hh PYP, chromophore fluorescence is suppressed by the intramolecular forces in the folded protein that are responsible for spectral tuning of the chromophore. Our fluorescence results indicate that the spectral shoulder is causing the increase and shift in fluorescence and, therefore, is likely to have the chromophore in a different conformation and a more hydrophilic environment.

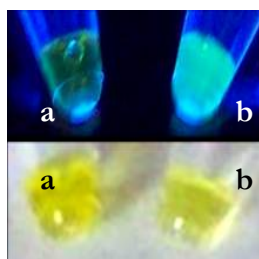


Figure 4.9

Pictures of Hh PYP (a) and Sr PYP (b) solutions taken under white light (bottom) and UV-illumination (top), showing virtual absence of fluorescence for Hh PYP and substantially enhanced fluorescence for Sr PYP.

Recovery kinetics: effects of KCl, alcohols, temperature, and pH

We determined the kinetics of recovery of Sr PYP following white light photoactivation, which is shown in **Figure 4.10**. The rate constant at pH 7.5 ($4.27 \times 10^{-4} \text{ s}^{-1}$) indicates a 14,000-fold slower recovery for Sr PYP compared to Hh PYP (6.0 s^{-1}) at the same pH. Since we could only bleach 37% of the 431 nm absorbance peak (**Figure 4.4**), we investigated the possibility of a biphasic recovery with a fast and a slow phase. However no fast recovery was observed within the limit of detection of our laser equipment (μs time range). An alternative explanation for the low amplitude of bleach is competition between photobleach and photoreversal.

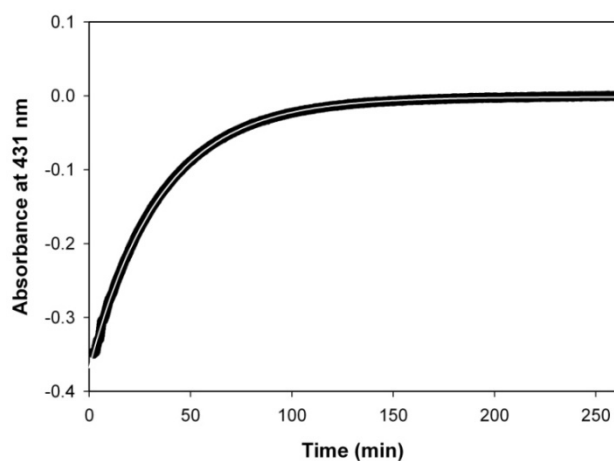


Figure 4.10

Kinetics of dark recovery of Sr PYP in 50 mM Tris-HCl, pH 7.5, after 1 minute of illumination with white light. The solid white line represents a fitted curve to the data.

However, we observed the same effect with blue light (>390 nm and <510 nm) that does not illuminate I_2 or I_2' . It is also possible that there is a significant amount of the I_1 intermediate present in equilibrium with I_2 following illumination, as suggested by the 490 nm peak in the difference spectrum (**Figure 4.5**). In Hh PYP, the absolute spectrum of I_1 is somewhat red-shifted relative to the ground state, but has about half the intensity [43] consistent with this explanation. The residual absorbance after maximum bleach has shifted to 429 nm and there is relatively more of the spectral shoulder (**Figure 4.4**, dashed line). This suggests that the contribution of I_1 is relatively small (otherwise the maximum would be red-shifted as in Hh PYP). Although there is no precedent for it, I_1 does not have to be red-shifted in Sr PYP, but could be broadened instead. Since the spectral shoulder is increasing relative to the 431 nm form, it appears as if this form is not photoactive. In addition, when the sample was bleached in 3 M KCl, where there is an increase in 431 nm absorbance due to conversion of the spectral shoulder (**Figure 4.12**), there is at least 10% more photobleach of the sample. **Figure 4.11** in comparison with **Figure 4.12** shows that the relative amount of bleach has increased from 37% to 47% by increasing the KCl concentration from 0 to 3M. As far as our data allow us to conclude, it appears that a combination of the presence of I_1 and the residual spectral shoulder is presumably the explanation for the maximum bleach of only 37% at 431 nm.

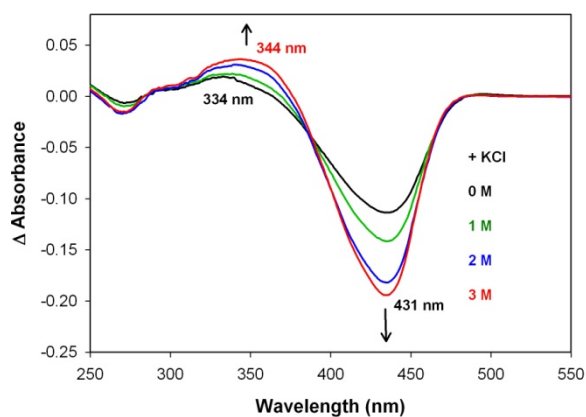


Figure 4.11

Effect of increasing concentrations of KCl on the light minus dark difference spectra, as indicated by the arrows.

As noted before, the physiological intracellular salt concentration in *S. ruber* is unusually high, as the organism maintains a high concentration of potassium inside its cytoplasm, keeping an osmotic balance against the high sodium chloride concentration outside (the species will not grow at less than 15% salt in the medium). Although procedures to establish intracellular ion concentrations suffer from certain artifacts, such as the possibility of leakage of ions from the cells during cell preparation, estimated intracellular KCl concentrations range from 1 M to 4 M [21]. Therefore, we analyzed the spectrum and kinetics of Sr PYP in high concentrations of KCl as shown in **Figure 4.12** and **Figure 4.13** respectively. An increasing amount of KCl influences the 431 nm absorption peak and the intermediate spectral form in the same manner as observed

with the kosmotrope $(\text{NH}_4)_2\text{SO}_4$ and the chaotrope NH_4Cl (see above), which further points to a general ionic strength effect.

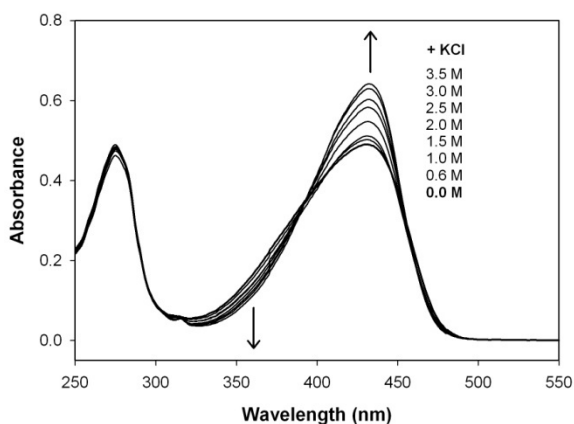


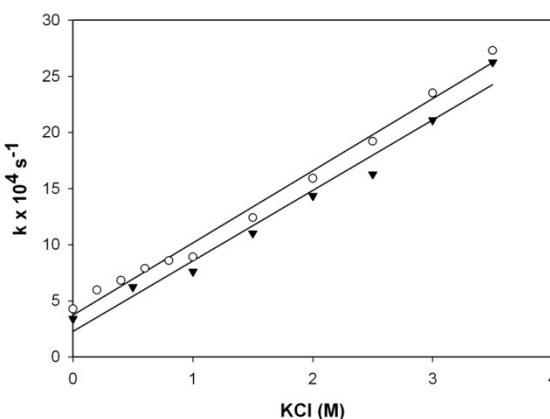
Figure 4.12

Effect of increasing concentrations of KCl on the absorption spectrum of Sr PYP in 50 mM Tris-HCl, pH 7.5 at room temperature. The arrows indicate the direction of increasing salt concentration.

In addition, the recovery rate of Sr PYP following white light photoactivation is significantly affected by KCl. The rate constant increases almost linearly with increasing amount of KCl, as shown in **Figure 4.13**. In the 0 to 3.5 M salt range, Sr PYP recovers approximately 6.4 times faster, but the maximum recovery observed (at 3.5 M KCl) is still 2200 times slower than for Hh PYP without salt and at the same pH. Although *H. halophila*, like *S. ruber*, is an extreme halophile, it accumulates ectoine and betaine rather than KCl. Recovery of Hh PYP shows a different effect of ionic strength, first decreasing due to screening of the ion pair E12/K110 (below 600 mM), and then increasing at higher ionic strength [44]. The sequence alignment shows that the ‘ion pair’ between E12 and K110 is absent in Sr PYP. This is consistent with the lack of initial decrease in the rate constant at low salt concentration.

Figure 4.13

Effect of increasing concentrations of KCl on the recovery rate of Sr PYP (open circles) and $\Delta 31$ -PYP (triangles) in 50 mM Tris-HCl, pH 7.5, at room temperature.



It is possible that the I_2/I_2' equilibrium in Sr PYP is shifted towards I_2 in high salt. A similar effect was observed in Hh PYP and was explained as the stabilizing effect on the compact and folded structure of I_2 [44]. Comparing the difference spectrum of Sr PYP after illumination in high salt with that without salt indicates that there is a less UV-shifted absorbance maximum (344 nm vs 334 nm) (**Figure 4.11**). However, the intermediate spectral form disappears at high ionic strength, which influences the apparent wavelength maximum for I_2 . Thus, based on the difference spectrum alone, we cannot say whether or not ionic strength affects the I_2/I_2' equilibrium as it does in Hh PYP.

Although we have shown that the I_1 and I_2 intermediates may be present in Sr PYP, we have not yet demonstrated the presence of I_2' , which is characterized in Hh PYP by a conformational change that exposes a hydrophobic site to solvent. Direct measurements of I_2' are complicated by its low extinction coefficient, similar to I_2 (350 nm vs 370 nm in Hh PYP), and its intrinsic instability. However, aliphatic alcohols slow Hh PYP recovery, consistent with the bleached state being more hydrophobic than the ground state, due to a conformational change upon I_2' formation [45]. We therefore studied the effect of alcohol on the recovery of Sr PYP and found that it is similar to that of Hh PYP, but only one third the magnitude, as shown in **Figure 4.14**. This suggests that the bleached state is less hydrophobic than in Hh PYP or that there is

less I_2' being formed in Sr PYP, at least at high KCl concentrations (1 M).

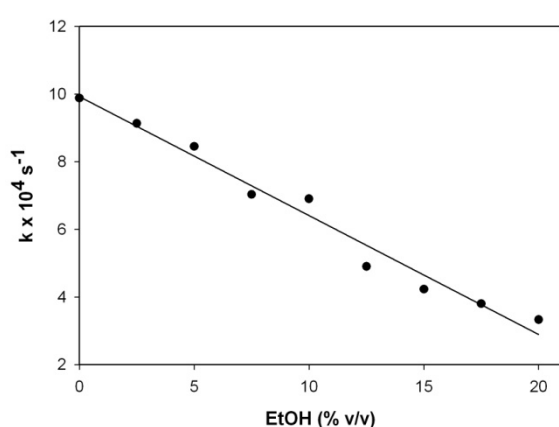


Figure 4.14

Effect of EtOH/water mixtures on recovery kinetics after white light illumination of Sr PYP in 50 mM Tris-HCl, pH 7.5, and 1 M KCl.

An alternative indirect measurement of I_2' is through temperature dependence determination. The recovery of Hh PYP has a bell-shaped dependence on temperature [45]: the reaction becomes only twice as fast between 5°C and 35°C, and then becomes threefold slower up to 62°C. This deviation is ascribed to a change in heat capacity of the protein as a result of the bleached state being more hydrophobic than the ground state [46]. Unlike Hh PYP, the effect of temperature on recovery of Sr PYP appears to show a normal Arrhenius behavior, with an activation energy of ~ 62 kJ/mol in 1 M KCl. In the absence of salt there is some curvature in the Arrhenius plot, consistent with the effect of alcohol (**Figure 4.15**) and indicative of a smaller amount of I_2' than in Hh PYP. The heat capacity change for Sr PYP (-1.53 kJ/mol·K) is only half of that in Hh PYP (-2.73 kJ/mol·K). If the two highest temperature points are ignored in the high ionic strength plot, the remaining data show a curvature which, when fit (dashed line), yields a heat capacity change of -0.75 kJ/mol·K. Whether or not there is curvature in the high ionic strength data, the conclusion remains that there is less I_2' formed than at low ionic strength.

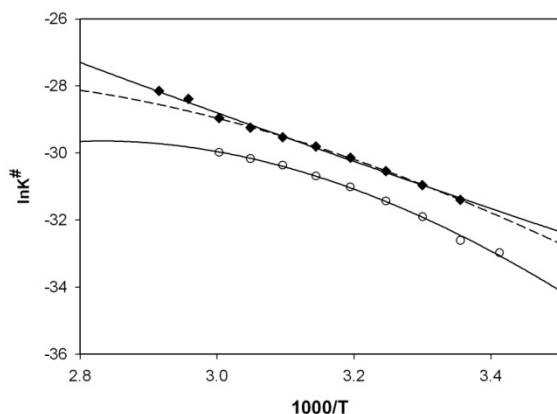


Figure 4.15

Temperature dependence of kinetics of recovery of Sr PYP in 50 mM Tris-HCl (pH 7.5) in the absence (open circles) and presence (filled diamonds) of 1 M KCl. The activation equilibrium constant K^\ddagger , calculated from the rate constant k using Van Brederode's equation 12 [46], is shown as a function of temperature. The data were fitted using Van Brederode's equation 13 [46].

Solution pH has a significant influence on the ground state recovery rate, as it is increased 17-fold between pH 4.5 and 9.0 in Sr PYP. The pH dependence is sigmoidal and has a single pK_a at 5.8, as shown in **Figure 4.16**. In contrast, the recovery of Hh PYP is optimal at pH 8 and has a bell-shaped dependence on pH governed by pK_a s of 6.4 and 9.4, presumably due to E46 and the chromophore hydroxyl [47]. Both the slow kinetics and the pH dependence of Sr PYP are more like the M100A mutant of Hh PYP [48], which indicates that the equivalent of M100 adopts a different conformation in Sr PYP, thereby preventing interaction with the chromophore and catalysis of recovery. This is similar to the *R. centenaria* PYP domain [49] and the Y98Q Hh PYP [41]. In addition, the Hh PYP M100A/R52A double mutant has a more pronounced pH dependence than the single mutant [41]. This is presumably because R52 normally acts as a counterion for the chromophore in the bleached state [28]. Because Sr PYP has a substitution of Ile for the equivalent of R52, we expected a similar pH dependence. There might still be a second

pK_a , similar to the one in M100A/R52A ($pK_a = 10$), but we were unable to measure it due to hydrolysis of the chromophore above pH 9.4.

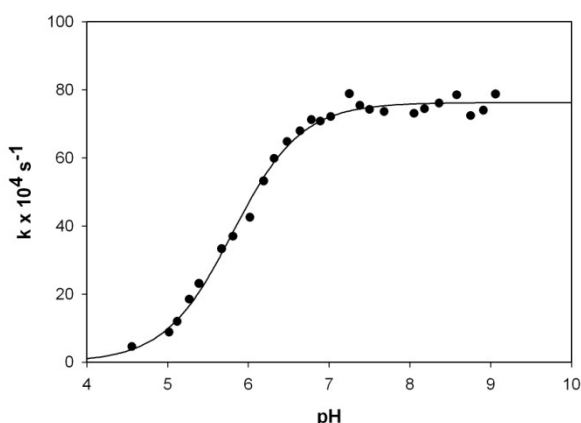


Figure 4.16

pH profile of the kinetics of recovery of Sr PYP at 37°C in universal buffer supplemented with 2.5 M KCl. The solid line represents the fitted curve with a pK_a of 5.8.

Spectrum and kinetics of $\Delta 31$ -PYP

The observed truncation of Sr PYP by 31 amino acids does not change the UV-VIS absorption spectrum and has no significant effect on the ground state recovery after white light

illumination (calculated rate constant at pH 7.5 in 50 mM Tris-HCl is $3.4 \times 10^{-4} \text{ s}^{-1}$) (data not shown). Moreover, ground state recovery of $\Delta 31$ -PYP is as strongly dependent on ionic strength as the unprocessed form, as shown in **Figure 4.13**. This argues against a functional role for the N-terminal extension, but in the absence of an interaction partner protein, a final conclusion is premature.

Other photoreceptors in S. ruber

Although *S. ruber* is a non-photosynthetic organism, its natural habitat is the same as photosynthetic organisms like *Halobacterium* and *Halorhodospira*. It is therefore likely to use similar photoreceptors for survival in these high light conditions. Besides a PYP coding gene, the *Salinibacter* genome also contains four bacterial rhodopsin genes and numerous chemotaxis genes which may point to a possible complex photobehavior for this extremely halophilic heterotroph. Three rhodopsin genes are related to *Halobacterium* rhodopsins and may have similar functions based on their genomic organization [19]. One (SRU_2780) is a possible chloride pump, another (SRU_1500) codes for a unique light harvesting complex, called xanthorhodopsin, that is shown to be a light-driven proton pump. Besides the retinal chromophore, it uses a carotenoid antenna (salinixanthin) to extend the absorption range beyond what is possible with retinal alone [50, 51]. The other two (SRU_2511 and SRU_2579) are predicted to be sensory rhodopsins (SR), distantly related to SRI. In *Halobacterium salinarum*, sensory rhodopsin I ($\sim 587 \text{ nm}$) and sensory rhodopsin II ($\sim 487 \text{ nm}$) interact with tightly bound transducer proteins to produce a color-sensitive phototactic behavior via a phosphorylation cascade modulating the cell's flagellar motor [52]. *S. ruber* is also motile and flagella have been observed through electron microscopy, although the number or localization could not be inferred [20]. It is likely that SRU_2579 has a photosensory function as it is immediately followed by an Htr1 transducer (SRU_2258) like in *Halobacterium salinarum*. The best chances are that SRU_2579 is involved in photomovement, as it is associated with a flagellar gene cluster immediately downstream and with which it is probably coregulated. A gene for SRII is presumably absent in *Salinibacter*, so it is plausible that PYP could take over its role in mediating a blue light photoresponse, although the genetic context near the hypersalinity island suggests a role in osmotic regulation.

In conclusion, Sr PYP is the first PYP characterized from a non-photosynthetic organism and is likely to be expressed and functional. The photocycle is similar to that of Hh PYP, including intermediates I_1 , I_2 , and I_2' . However, it has the slowest recovery of any PYP and is the first occasion where PYP is found as a functional dimer, which is most likely formed through the 31 amino acid N-terminal extension. Sr PYP is stabilized by ionic strength and is the first example of a truly halophilic PYP.

Acknowledgment

We thank the laboratory of Dr. Nancy Horton for the use of their PC1 photon counting spectrofluorometer.

References

1. Sharma, A.K., Spudich, J.L., and Doolittle, W.F., Microbial rhodopsins: functional versatility and genetic mobility. *Trends Microbiol*, 2006. **14**(11): p. 463-9.
2. Vierstra, R.D. and Davis, S.J., Bacteriophytochromes: new tools for understanding phytochrome signal transduction. *Seminars in Cell and Developmental Biology*, 2000. **11**(6): p. 511-21.
3. Franklin, K.A., Larner, V.S., and Whitelam, G.C., The signal transducing photoreceptors of plants. *Int J Dev Biol*, 2005. **49**(5-6): p. 653-64.
4. Gomelsky, M. and Klug, G., BLUF: a novel FAD-binding domain involved in sensory transduction in microorganisms. *Trends in Biochemical Sciences*, 2002. **27**(10): p. 497-500.
5. Cusanovich, M.A. and Meyer, T.E., Photoactive yellow protein: a prototypic PAS domain sensory protein and development of a common signaling mechanism. *Biochemistry*, 2003. **42**(17): p. 4759-70.
6. Kyndt, J.A., Meyer, T.E., and Cusanovich, M.A., Photoactive yellow protein, bacteriophytochrome, and sensory rhodopsin in purple phototrophic bacteria. *Photochemical & Photobiological Sciences*, 2004. **3**(6): p. 519-30.
7. Yooseph, S., Sutton, G., Rusch, D.B., Halpern, A.L., Williamson, S.J., Remington, K., Eisen, J.A., Heidelberg, K.B., Manning, G., Li, W., Jaroszewski, L., Cieplak, P., Miller, C.S., Li, H., Mashiyama, S.T., Joachimiak, M.P., van Belle, C., Chandonia, J.M., Soergel, D.A., Zhai, Y., Natarajan, K., Lee, S., Raphael, B.J., Bafna, V., Friedman, R., Brenner, S.E., Godzik, A., Eisenberg, D., Dixon, J.E., Taylor, S.S., Strausberg, R.L., Frazier, M., and Venter, J.C., The Sorcerer II Global Ocean Sampling Expedition: Expanding the Universe of Protein Families. *PLoS Biol*, 2007. **5**(3): p. e16.
8. Meyer, T.E., Isolation and characterization of soluble cytochromes, ferredoxins and other chromophoric proteins from the halophilic phototrophic bacterium *Ectothiorhodospira halophila*. *Biochimica et Biophysica Acta*, 1985. **806**(1): p. 175-83.
9. Meyer, T.E., Yakali, E., Cusanovich, M.A., and Tollin, G., Properties of a water-soluble, yellow protein isolated from a halophilic phototrophic bacterium that has photochemical activity analogous to sensory rhodopsin. *Biochemistry*, 1987. **26**(2): p. 418-23.
10. Devanathan, S., Brudler, R., Hessling, B., Woo, T.T., Gerwert, K., Getzoff, E.D., Cusanovich, M.A., and Tollin, G., Dual photoactive species in Glu46Asp and Glu46Ala mutants of photoactive yellow protein: a pH-driven color transition. *Biochemistry*, 1999. **38**(41): p. 13766-72.
11. Ujj, L., Devanathan, S., Meyer, T.E., Cusanovich, M.A., Tollin, G., and Atkinson, G.H., New photocycle intermediates in the photoactive yellow protein from *Ectothiorhodospira halophila*: picosecond transient absorption spectroscopy. *Biophysical Journal*, 1998. **75**(1): p. 406-12.
12. Genick, U.K., Soltis, S.M., Kuhn, P., Canestrelli, I.L., and Getzoff, E.D., Structure at 0.85 Å resolution of an early protein photocycle intermediate. *Nature*, 1998. **392**(6672): p. 206-9.
13. Borucki, B., Devanathan, S., Otto, H., Cusanovich, M.A., Tollin, G., and Heyn, M.P., Kinetics of proton uptake and dye binding by photoactive yellow protein in wild type and in the E46Q and E46A mutants. *Biochemistry*, 2002. **41**(31): p. 10026-37.

14. Jiang, Z.Y., Swem, L.R., Rushing, B.G., Devanathan, S., Tollin, G., and Bauer, C.E., Bacterial photoreceptor with similarity to photoactive yellow protein and plant phytochromes. *Science*, 1999. **285**(5426): p. 406-409.
15. Kyndt, J.A., Fitch, J.C., Meyer, T.E., and Cusanovich, M.A., The photoactivated PYP domain of *Rhodospirillum centenum* Ppr accelerates recovery of the bacteriophytochrome domain after white light illumination. *Biochemistry*, 2007. **46**: p. 8256-8262.
16. Berleman, J.E., Hasselbring, B.M., and Bauer, C.E., Hypercyst mutants in *Rhodospirillum centenum* identify regulatory loci involved in cyst cell differentiation. *Journal of Bacteriology*, 2004. **186**(17): p. 5834-41.
17. Sprenger, W.W., Hoff, W.D., Armitage, J.P., and Hellingwerf, K.J., The eubacterium *Ectothiorhodospira halophila* is negatively phototactic, with a wavelength dependence that fits the absorption spectrum of the photoactive yellow protein. *Journal of Bacteriology*, 1993. **175**(10): p. 3096-104.
18. Hou, S., Saw, J.H., Lee, K.S., Freitas, T.A., Belisle, C., Kawarabayasi, Y., Donachie, S.P., Pikina, A., Galperin, M.Y., Koonin, E.V., Makarova, K.S., Omelchenko, M.V., Sorokin, A., Wolf, Y.I., Li, Q.X., Keum, Y.S., Campbell, S., Denery, J., Aizawa, S., Shibata, S., Malahoff, A., and Alam, M., Genome sequence of the deep-sea gamma-proteobacterium *Idiomarina loihiensis* reveals amino acid fermentation as a source of carbon and energy. *Proceedings of the National Academy of Sciences of the United States of America*, 2004. **101**(52): p. 18036-41.
19. Mongodin, E.F., Nelson, K.E., Daugherty, S., Deboy, R.T., Wister, J., Khouri, H., Weidman, J., Walsh, D.A., Papke, R.T., Sanchez Perez, G., Sharma, A.K., Nesbo, C.L., MacLeod, D., Bapteste, E., Doolittle, W.F., Charlebois, R.L., Legault, B., and Rodriguez-Valera, F., The genome of *Salinibacter ruber*: convergence and gene exchange among hyperhalophilic bacteria and archaea. *Proceedings of the National Academy of Sciences of the United States of America*, 2005. **102**(50): p. 18147-52.
20. Anton, J., Oren, A., Benlloch, S., Rodriguez-Valera, F., Amann, R., and Rossello-Mora, R., *Salinibacter ruber* gen. nov., sp. nov., a novel, extremely halophilic member of the Bacteria from saltern crystallizer ponds. *International Journal of Systematic and Evolutionary Microbiology*, 2002. **52**(Pt 2): p. 485-91.
21. Oren, A., Heldal, M., Norland, S., and Galinski, E.A., Intracellular ion and organic solute concentrations of the extremely halophilic bacterium *Salinibacter ruber*. *Extremophiles*, 2002. **6**(6): p. 491-8.
22. Roessler, M. and Muller, V., Chloride dependence of glycine betaine transport in *Halobacillus halophilus*. *FEBS Letters*, 2001. **489**(2-3): p. 125-8.
23. Kyndt, J.A., Vanrobaeys, F., Fitch, J.C., Devreese, B.V., Meyer, T.E., Cusanovich, M.A., and Van Beeumen, J.J., Heterologous production of *Halorhodospira halophila* holo-photoactive yellow protein through tandem expression of the postulated biosynthetic genes. *Biochemistry*, 2003. **42**(4): p. 965-70.
24. Simonsen, R.P. and Tollin, G., Transient kinetics of redox reactions of flavodoxin: effects of chemical modification of the flavin mononucleotide prosthetic group on the dynamics of intermediate complex formation and electron transfer. *Biochemistry*, 1983. **22**(12): p. 3008-16.
25. Yokoyama, H. and Matsui, I., A novel thermostable membrane protease forming an operon with a stomatin homolog from the hyperthermophilic archaeobacterium *Pyrococcus horikoshii*. *Journal of Biological Chemistry*, 2005. **280**(8): p. 6588-94.
26. Louie, G.V., Bowman, M.E., Moffitt, M.C., Baiga, T.J., Moore, B.S., and Noel, J.P., Structural determinants and modulation of substrate specificity in phenylalanine-tyrosine ammonia-lyases. *Chemical Biology*, 2006. **13**(12): p. 1327-38.

27. Gulick, A.M., Lu, X., and Dunaway-Mariano, D., Crystal structure of 4-chlorobenzoate:CoA ligase/synthetase in the unliganded and aryl substrate-bound states. *Biochemistry*, 2004. **43**(27): p. 8670-9.
28. Genick, U.K., Borgstahl, G.E., Ng, K., Ren, Z., Pradervand, C., Burke, P.M., Srajer, V., Teng, T.Y., Schildkamp, W., McRee, D.E., Moffat, K., and Getzoff, E.D., Structure of a protein photocycle intermediate by millisecond time-resolved crystallography. *Science*, 1997. **275**(5305): p. 1471-5.
29. Oren, A. and Mana, L., Amino acid composition of bulk protein and salt relationships of selected enzymes of *Salinibacter ruber*, an extremely halophilic bacterium. *Extremophiles*, 2002. **6**(3): p. 217-23.
30. Hennig, L. and Schafer, E., Both subunits of the dimeric plant photoreceptor phytochrome require chromophore for stability of the far-red light-absorbing form. *Journal of Biological Chemistry*, 2001. **276**(11): p. 7913-7918.
31. Sang, Y., Li, Q.H., Rubio, V., Zhang, Y.C., Mao, J., Deng, X.W., and Yang, H.Q., N-terminal domain-mediated homodimerization is required for photoreceptor activity of *Arabidopsis* Cryptochrome 1. *Plant Cell*, 2005. **17**(5): p. 1569-1584.
32. Anderson, S., Dragnea, V., Masuda, S., Ybe, J., Moffat, K., and Bauer, C., Structure of a novel photoreceptor, the BLUF domain of AppA from *Rhodobacter sphaeroides*. *Biochemistry*, 2005. **44**(22): p. 7998-8005.
33. Laan, W., Gauden, M., Yeremenko, S., van Grondelle, R., Kennis, J.T.M., and Hellingwerf, K.J., On the mechanism of activation of the BLUF domain of AppA. *Biochemistry*, 2006. **45**(1): p. 51-60.
34. Bernard, C., Houben, K., Derix, N.M., Marks, D., van der Horst, M.A., Hellingwerf, K.J., Boelens, R., Kaptein, R., and van Nuland, N.A., The solution structure of a transient photoreceptor intermediate: Delta25 photoactive yellow protein. *Structure*, 2005. **13**(7): p. 953-62.
35. Vreede, J., van der Horst, M.A., Hellingwerf, K.J., Crielaard, W., and van Aalten, D.M., PAS domains. Common structure and common flexibility. *Journal of Biological Chemistry*, 2003. **278**(20): p. 18434-9.
36. Frishman, D. and Argos, P., PREDATOR : Protein secondary structure prediction from a single sequence or a set of sequences (<http://bioweb.pasteur.fr/seqanal/interfaces/predator-simple.html>).
37. Brudler, R., Meyer, T.E., Genick, U.K., Devanathan, S., Woo, T.T., Millar, D.P., Gerwert, K., Cusanovich, M.A., Tollin, G., and Getzoff, E.D., Coupling of hydrogen bonding to chromophore conformation and function in photoactive yellow protein. *Biochemistry*, 2000. **39**(44): p. 13478-86.
38. Meyer, T.E., Devanathan, S., Woo, T., Getzoff, E.D., Tollin, G., and Cusanovich, M.A., Site-specific mutations provide new insights into the origin of pH effects and alternative spectral forms in the photoactive yellow protein from *Halorhodospira halophila*. *Biochemistry*, 2003. **42**(11): p. 3319-25.
39. Kyndt, J.A., Hurley, J.K., Devreese, B., Meyer, T.E., Cusanovich, M.A., Tollin, G., and Van Beeumen, J.J., *Rhodobacter capsulatus* photoactive yellow protein: genetic context, spectral and kinetics characterization, and mutagenesis. *Biochemistry*, 2004. **43**(7): p. 1809-20.
40. Meyer, T.E., Tollin, G., Causgrove, T.P., Cheng, P., and Blankenship, R.E., Picosecond Decay Kinetics and Quantum Yield of Fluorescence of the Photoactive Yellow Protein from the Halophilic Purple Phototrophic Bacterium, *Ectothiorhodospira halophila*. *Biophysical Journal*, 1991. **59**(5): p. 988-991.
41. Kyndt, J.A., Savvides, S.N., Memmi, S., Koh, M., Fitch, J.C., Meyer, T.E., Heyn, M.P., Van Beeumen, J.J., and Cusanovich, M.A., Structural role of tyrosine 98 in photoactive

- yellow protein: effects on fluorescence, gateway, and photocycle recovery. *Biochemistry*, 2007. **46**(1): p. 95-105.
42. Getzoff, E.D., Gutwin, K.N., and Genick, U.K., Anticipatory active-site motions and chromophore distortion prime photoreceptor PYP for light activation. *Nature Structural Biology*, 2003. **10**(8): p. 663-8.
 43. Hoff, W.D., van Stokkum, I.H., van Ramesdonk, H.J., van Brederode, M.E., Brouwer, A.M., Fitch, J.C., Meyer, T.E., van Grondelle, R., and Hellingwerf, K.J., Measurement and global analysis of the absorbance changes in the photocycle of the photoactive yellow protein from *Ectothiorhodospira halophila*. *Biophysical Journal*, 1994. **67**(4): p. 1691-705.
 44. Hoersch, D., Otto, H., Joshi, C.P., Borucki, B., Cusanovich, M.A., and Heyn, M.P., Role of a conserved salt bridge between the PAS core and the N-terminal domain in the activation of the photoreceptor photoactive yellow protein. *Biophysical Journal*, 2007. **93**(5): p. 1687-1699.
 45. Meyer, T.E., Tollin, G., Hazzard, J.H., and Cusanovich, M.A., Photoactive yellow protein from the purple phototrophic bacterium, *Ectothiorhodospira halophila*. Quantum yield of photobleaching and effects of temperature, alcohols, glycerol, and sucrose on kinetics of photobleaching and recovery. *Biophysical Journal*, 1989. **56**(3): p. 559-64.
 46. Van Brederode, M.E., Hoff, W.D., Van Stokkum, I.H., Groot, M.L., and Hellingwerf, K.J., Protein folding thermodynamics applied to the photocycle of the photoactive yellow protein. *Biophysical Journal*, 1996. **71**(1): p. 365-80.
 47. Genick, U.K., Devanathan, S., Meyer, T.E., Canestrelli, I.L., Williams, E., Cusanovich, M.A., Tollin, G., and Getzoff, E.D., Active site mutants implicate key residues for control of color and light cycle kinetics of photoactive yellow protein. *Biochemistry*, 1997. **36**(1): p. 8-14.
 48. Devanathan, S., Genick, U.K., Canestrelli, I.L., Meyer, T.E., Cusanovich, M.A., Getzoff, E.D., and Tollin, G., New insights into the photocycle of *Ectothiorhodospira halophila* photoactive yellow protein: photorecovery of the long-lived photobleached intermediate in the Met100Ala mutant. *Biochemistry*, 1998. **37**(33): p. 11563-8.
 49. Rajagopal, S. and Moffat, K., Crystal structure of a photoactive yellow protein from a sensor histidine kinase: conformational variability and signal transduction. *Proceedings of the National Academy of Sciences of the United States of America*, 2003. **100**(4): p. 1649-54.
 50. Balashov, S.P., Imasheva, E.S., Boichenko, V.A., Anton, J., Wang, J.M., and Lanyi, J.K., Xanthorhodopsin: a proton pump with a light-harvesting carotenoid antenna. *Science*, 2005. **309**(5743): p. 2061-4.
 51. Boichenko, V.A., Wang, J.M., Anton, J., Lanyi, J.K., and Balashov, S.P., Functions of carotenoids in xanthorhodopsin and archaerhodopsin, from action spectra of photoinhibition of cell respiration. *Biochimica et Biophysica Acta*, 2006. **1757**(12): p. 1649-56.
 52. Spudich, J.L., The multitasking microbial sensory rhodopsins. *Trends in Microbiology*, 2006. **14**(11): p. 480-7.

Chapter five

5 PYP-phytochrome-related proteins

5.1 Introduction

A PYP-phytochrome related (Ppr) protein was originally discovered in 1999 in the non-sulfur anoxygenic purple photosynthetic bacterium *Rhodospirillum centenum* [1]. Four homologous multi-sensor domain proteins have very recently been identified in the completed genomes of the unrelated *Methylobacterium* species (JGI, <http://www.jgi.doe.gov/>) (see Section 5.2). *Rh. centenum* was isolated in 1987 from Thermopolis Hot Springs (Wyoming, USA) [2] and was named in recognition of the fact that it was discovered on the 100th anniversary of the isolation of the first pure culture of an anoxyphototroph, *i.e.* *Rhodospirillum rubrum*. However, since 1994, *R. centenum* is also referred to in the literature as *Rhodocista centenaria* [3], causing a taxonomic ambiguity and an associated debate on whether the International Code of Nomenclature of Bacteria (1990 Revision) was correctly applied [4, 5].

Rh. centenum is a nitrogen-fixing photoheterotroph with an unusual life cycle composed of swim cell, swarm cell and cyst cell differentiation, as shown in **Figure 5.1**. In liquid medium, the organism is actively motile by means of a single polar flagellum [2], while growth on solid or viscous media induces numerous peritrichous flagella, providing rapid movement of *Rh. centenum* colonies across a solid surface known as ‘swarming’ [6]. In addition, a nutritional shift-down induces differentiation into metabolically dormant cyst cells characterized by intracellular poly- β -hydroxybutyrate (PHB) storage granules and an outer-coat that envelops up to ten cells [7]. Furthermore, *R. centenum* is unusual in its ability to synthesize a functional photosynthetic apparatus regardless of the presence of molecular oxygen [8].

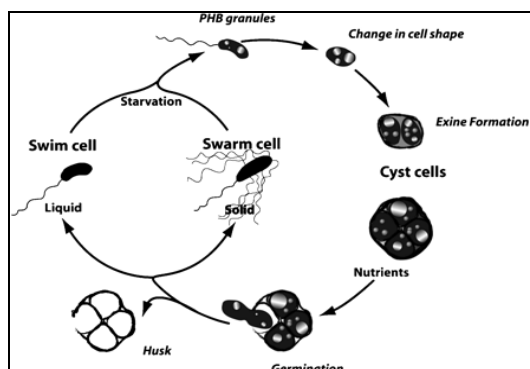


Figure 5.1

Diagram of the *Rh. centenum* life cycle, depicting swim cells, swarm cells and several stages of cyst formation. Image was taken from [7].

5.2 Properties

Ppr is a hybrid photosensor kinase consisting of an N-terminal PYP domain, a central domain similar to bacteriophytochromes (Bph) and a C-terminal histidine kinase domain. Besides the original Ppr from *Rb. centenum*, only one additional representative is currently known from *Methylobacterium* sp. 4-46 (**Figure 5.2**). However, the related *Methylobacterium* species *M. chloromethanicum* CM4, *M. extorquens* PA1 and *M. populi* BJ001 contain a gene which encodes for an unusual Ppr-like protein. Their amino acid sequences actually show a degenerate PYP domain in which the conserved chromophore binding cysteine is missing while, on the other hand, a redox sensing disulfide may be formed from C42 and C50 (Hhal PYP numbering), as shown in **Figure 5.2**. Species of the genus *Methylobacterium* are strictly aerobic facultative methylotrophs that are able to grow on one-carbon compounds, such as methanol or methylamine, as well as on a variety of C2, C3 and C4 substrates [9]. *Methylobacterium* sp 4-46 was isolated as a nitrogen-fixing symbiont of the South African legume, *Lotonis bainesii*, on which it forms root nodules like those of the *Rhizobium* species [10]. Bacteria are often pink to red, due to the presence of carotenoids, but they are not related to photosynthetic species.

Ppr from *Rb. centenum* and *Methylobacterium* sp 4-46 share 38% sequence identity, and their PYP domains contain nearly all key amino acid residues that have been identified in Hhal PYP affecting the properties of the pHCA chromophore, as shown in **Figure 5.2**. A phenylalanine replaces Y98 in both species (Hhal PYP numbering), while M100 is substituted by a proline in *Methylobacterium* sp 4-46. The partial alignment in **Figure 5.2** also shows that the Ppr-Bph domains all possess the conserved C20 of *Agrobacterium* bacteriophytochrome Agp1 which has been demonstrated to covalently bind a biliverdin (BV) cofactor [11]. Moreover, the conserved cysteine within the GAF domain serving as the phytochromobilin (PΦB) or phycocyanobilin (PCB) chromophore attachment site homologous to plant phytochromes (see Chapter two, section 2.2.1.2) is missing (data not shown), and indicates that Ppr binds BV in addition to pHCA as chromophores. BV is a linear tetrapyrrole synthesized through the oxidative cleavage of heme by heme oxygenase (HemO).

The genomic organization of neither *Rb. centenum* nor *Methylobacterium* Ppr shows any relevant genes in the immediate vicinity of *ppr* which can be related to its photoperception function, and also the biosynthetic enzymes are not located near the structural gene. Moreover, a gene for TAL is apparently absent in *Rb. centenum*, while a gene for pCL could not be found in *Methylobacterium* sp 4-46.

Rcen	-----MPDRTTDDFGPFTEQIRG-----TIDGMGTAE	27
Msp4-46	-----MSDRALAAEAAR-----LDALSTGE	20
Mchl	-----MPMADPALLNRGVAGIPAAVMVDPSQMHAVGPNGGPVLDLPVDLDALTAEQ	50
Mext	-----MAKADPALLNRGVAGIPAAVMVDPSQMHAVGPNGGPVLDLPVDLDALTAEQ	50
Mpop	MVRLFVRRKRAAGSVPALRNRTAAGIPTAIMVDPSQMHAEGPNGGPVLDLPVDLDALSPEQ	60
Agp1	-----	
	42 46 50 52 69	
Rcen	FDALPVGAIQVDGSGVIHRYNRTE SRLS GRIP ERVIGRNFFTEVA PC TNIPAF SGREMDG	87
Msp4-46	IDALDLGVVQVDS DTILLN RAESV FS GRSA ERVVGRNFFRDVA PC TRLPAFYGR FREG	80
Mchl	RDEFGVGILALDAAGIVLACNRAAGALCGLPPNTMIGRSFFRELVP SANVPSFYGRFLSG	110
Mext	RDEFGVGILALDAAGIVLACNRAAGALCGLPPNTMIGRSFFRELVP SANVPSFYGRFLSG	110
Mpop	RDEFGAGILALDPVGRVLT CNRAA GALCGLSPDAMIGRNFFRD LVSA HVPGFYGRFL SG	120
Agp1	-----	
	98 100 ▼	
Rcen	VTSGTLDARFDVFD EQMAPV RVQIR M Q NAGVPDRYWIFV RKLED LRPPGP AP EAPAAHT	147
Msp4-46	VRRGVLDEVFSFAYG FD PQ PLRVR VAL RGSAT PGR YWIVTR PV GQVTVSEAREAVR VA VD	140
Mchl	QRRSVADQAFEFVFGRI PAP LRARIGLRSGAN-GHIWLTIT PLEQ IAAGPSREAVLAAIA	169
Mext	QRRSVADQAFEFVFGRI PAP LRARIGLRSGAN-GHIWLTIT PLEQ IAAGPSREAVLAAIA	169
Mpop	QRRALTDQAFEFVFGRV PAP LRARIGLRAGAN-GCTWLTIS PLEQ IAAGPSREAVLAAIS	179
Agp1	-----MQRERLE	7
Rcen	ASVTGEVVDFSVCEQ EDIRRV GAIQ PWGAVLAVDPRDWT VCAAS DNAQALLD-CAR PPLG	206
Msp4-46	QRVRAEPI DPD LCARE PIH VP GAI Q PHAVLLACDAATLT VAA CSANA AE T LG ---AAP LG	197
Mchl	QRSRAEPVDPS LCERE PIHIPGSIQPN AV MLAADAASLEILAF SANA ADV LAP DLFPP NG	229
Mex	QRSRAEPVDPS LCERE PIHIPGSIQPN AV MLAADAASLEILAF SANA ADV LAP DLFPP NG	229
Mpop	QRSRAEPVDPS LCERE PIHIPGSIQPN AV MLAADAAT LE ILAF SANA ADV LAP ELFPP SG	239
Agp1	KVMSSHTPKLDS CGA EPIHIP GAIQ EHGALLVLSAREFSV VQAS DN L ANYIG-----VD	61

Figure 5.2

Partial sequence alignment of Ppr (bold) and Ppr-like multi-sensor domain proteins. The N-terminus of Agp1 from *Agrobacterium* is added for comparison with the BV-binding cysteine as marked in green. The conserved pHCA-binding cysteine is shaded blue, while key positions homologous to the amino acids affecting the properties of pHCA in Hh PYP are marked in red. Conserved residues across at least four sequences are shaded yellow. The arrow indicates the end of the PYP domain. The numbering of the important residues is according to Hh PYP. Abbreviations and GenBank accession numbers are: Rcen, *Rhodospirillum centenum* (acc. nr.: AAD22391), Msp4-46, *Methylobacterium* sp4-46 (acc. nr.: ZP_01845331), Mchl, *Methylobacterium chloromethanicum* CM4 (acc. nr.: ZP_02055103), Mext, *Methylobacterium extorquens* PA1 (acc. nr.: ZP_02017283), Mpop, *Methylobacterium populi* BJ001 (acc. nr.: EDO72515), Agp1, *Agrobacterium tumefaciens* Agp1 (acc. nr.: NP_354963).

The *ppr* gene product from *Rb. centenum* has been heterologously produced in *E. coli* and reconstituted with the two chromophores through co-expression with the three biosynthetic enzymes, *i.e.* TAL and pCL from *Rhodobacter capsulatus* for pHCA (see Chapter three, section 3.5) and HemO from *Rhodospseudomonas palustris* [12] for BV. The resulting green-colored holo-holo-protein shows characteristic absorption maxima at 434 nm due to the PYP domain and at 400, 642 and 701 nm due to the Bph domain [12, 13] (Figure 5.3). Illumination with white light induces a dark reversible bleach of both the PYP domain at 434 nm and the Bph at 701 nm, but both absorption maxima can also be activated separately by weak blue light or red light, respectively, as shown in Figure 5.3. This differs to typical bacteriophytochromes in which a

stable red-light absorbing form ($\lambda_{\max} \sim 700$ nm) is photoconverted to a far-red-light absorbing form ($\lambda_{\max} \sim 750$ nm) which can be rapidly reverted by subsequent illumination with far-red light in addition to the spontaneous dark recovery.

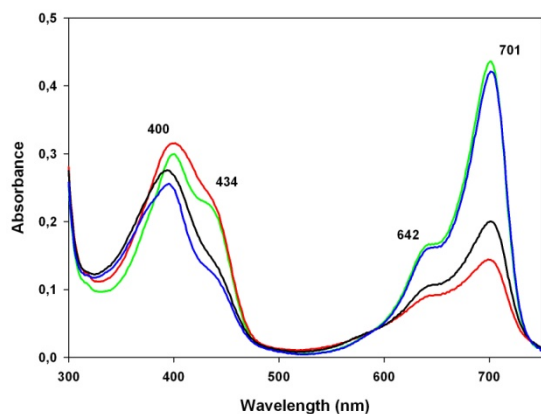


Figure 5.3

Absorption spectra of holo-holo-Ppr from *Rh. centenum* in the dark-adapted state (green), after 30 s blue-light illumination (blue), after 30 s red-light illumination (red), and after 30 s white-light illumination (black). Image was taken from [12].

When excited by blue light, the PYP domain in Ppr recovers in the dark in a biphasic fashion in which $\sim 32\%$ of the 445 nm bleach has a lifetime of 3.8 min and the remainder a lifetime of 46 min. White light primarily results in fast recovery, whereas the 130-residue PYP construct shows only the faster kinetics in both blue and white light. Furthermore, there is a slight red shift of the ground state Bph when the PYP is activated, suggesting interdomain communication [12]. Although the Bph of Ppr is not photoreversible in the same way as typical Bph (see above), its kinetics of recovery to the dark-adapted state differ markedly on prior illumination with red, blue and white light [12]. Upon illumination with red light, the Bph domain recovers with biphasic kinetics in which 57% of the 701 nm decay has a lifetime of 17 min and the remainder a lifetime of 50 min. However, when holo-holo-Ppr is illuminated by white light or by red light followed by blue light, there is a rapid recovery of Bph in a triphasic fashion, where the fastest phase is similar to that of the fast phase of the PYP domain (in white light, 25% of the 701 nm recovery has a lifetime of ~ 1 min) and the slower phases are like the recovery after red light alone, as shown in **Figure 5.4** [12].

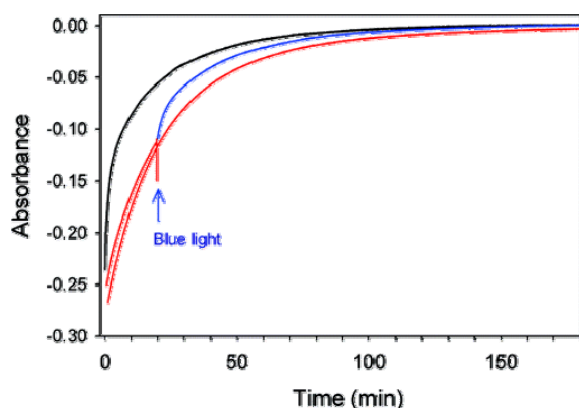


Figure 5.4

Kinetics of recovery at 701 nm following a 30 s red-light illumination (red), following a 30 s red-light illumination, a 20 min recovery, and then a 30 s blue-light illumination (red and blue), and following a 30 s white-light illumination (black). Image was taken from [12].

In addition, the kinetics for dark recovery of Bph at 701 nm following red-light activation are the same for holo-holo-Ppr and apo-holo-Ppr (with the BV chromophore only), which suggests that there is no interaction between activated Bph and ground state PYP. Thus, the photoactivated PYP domain in Ppr accelerates the recovery of the activated Bph domain, providing a unique photoswitch activated by opposing red (701 nm) and blue light (434 nm).

Subsequently, photoactivation is expected to regulate the histidine kinase domain and the concomitant phosphorylation on an unknown response regulator. *In vitro* kinase assays demonstrated that illumination with >400 nm light inhibits the dark state autophosphorylation of holo-apo-Ppr (with the pHCA chromophore only) by about two- to three-fold [1], while holo-holo-Ppr shows a differential autophosphorylation activity under red-light, blue-light and dark conditions (Kyndt J., pers. comm.). However, further studies on the kinetics of phosphorylation are ongoing.

5.3 Function

The environmental significance of a red/blue light switch in *Rh. centenum* could be related to the requirement of red light for photosynthesis or phototactic behavior. However, *Rh. centenum* Ppr was shown to be involved in a light-dependent gene expression of a type III polyketide synthase (PKS), ChsA, similar to plant chalcone synthases (CHSs) [1]. A transcriptional fusion of the *Rh. centenum chsA* promoter region to a *lacZ* reporter gene showed maximal β -galactosidase activity upon illumination with IR-light (>700 nm), which was inhibited approximately two-fold when blue (400 - 450 nm) or white light was added, as shown in **Figure 5.5**. Disruption of the *ppr* gene resulted in a low-level and light-insensitive *chsA* gene expression (**Figure 5.5**).

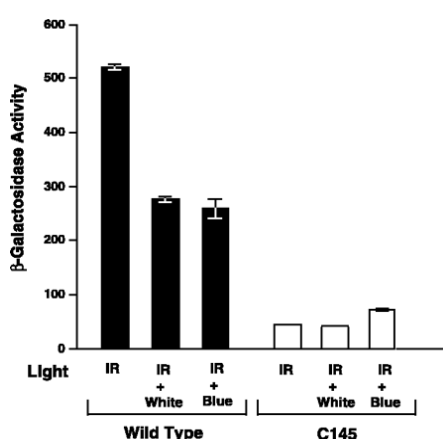


Figure 5.5

Light-regulated CHS expression of a *chsA::lacZ* fusion in wild-type *Rh. centenum* and a Δ *ppr* disrupted strain (C145). Cells were illuminated with infrared light (IR), IR + white light, or IR + blue light (400 - 450 nm) and measured for β -Gal activity. Activity units represent micromoles of *o*-nitrophenyl- β -D-galacto-pyranoside hydrolyzed $\text{min}^{-1} \text{mg}^{-1}$ protein. The image was taken from [1].

Type III PKSs are homodimeric ketosynthases that act iteratively for polyketide chain extension. Plant type III PKSs, such as chalcone synthase (CHS), stilbene synthase (STS) and *p*-

coumaroyltriacyclic acid synthase (CTAS), catalyze the sequential condensation of three malonyl-CoA molecules to 4-hydroxycinnamoyl-CoA to form an enzyme-bound tetraketide intermediate that subsequently undergoes cyclization into enzyme-specific reaction products, *i.e.* naringenin chalcone, resveratrol and *p*-coumaroyltriacyclic acid lactone, respectively (**Figure 5.6 B**). In plants, CHS is a key enzyme in the phenylpropanoid pathway leading to the biosynthesis of flavonoids, isoflavonoids, and anthocyanins [14]. Plant phenylpropanoids and flavonoids serve as antimicrobial and pigmentation agents, and as protectants from detrimental effects of UV-light [15, 16].

The role of CHS-like PKSs in bacteria is not always clear, but involves biosynthesis of a wide variety of secondary metabolites resulting from differences in the starter unit, the extension unit, the number of sequential condensation reactions and the specificity of ring closure [17]. For example, the first bacterial CHS-related type III PKS was identified in *Streptomyces griseus* and selects malonyl-CoA as the starter substrate, performs four successive extensions of malonyl-CoA and finally cyclizes the resulting pentaketide to 1,3,6,8-tetrahydroxynaphthalene (THN) as an intermediate for melanin biosynthesis [17, 18].

Alternatively, the nitrogen-fixing soil bacterium *Azotobacter vinelandii*, which is closely related to *Rh. centenum* and also able to differentiate into dormant cyst cells, contains two related PKS enzymes that produce the specialized lipid components of the enveloping cyst coat, *i.e.* 5-alkyl-resorcinol and 5-alkyl-pyrone, replacing the phospholipids in the membrane (**Figure 5.6 A**) [19, 20]. Their genes are associated with those for synthesis of the C22 fatty acid starter molecule that makes up the alkyl side chain [19]. Similarly, *chsA* gene expression in *Rh. centenum* is rapidly induced on the onset of cyst formation, as observed by high *chsA* promoter activity levels which rises up to 58-fold relative to those of the vegetative state [21]. Thus, it is possible that the product of the ChsA may be a special lipid-like that of the *Azotobacter* cysts, although the *Rh. centenum* gene does not appear to be associated with fatty acid synthase genes. Moreover, it suggests that Ppr is indirectly connected to cyst formation through a light-dependent regulation of ChsA expression.

However, *Rh. centenum* cysts are readily induced upon starvation for nutrients and so far only observed when grown in the dark (C. Bauer, pers. comm.). As bacteria use cyst formation as a strategy for surviving environmental stresses, it would therefore appear paradoxical that *chsA* gene expression, which is also related to encystment as described above, is maximal when *Rh. centenum* cells are illuminated with optimal IR-light for photosynthetic growth. Similarly, the option that ChsA initiates production of UV-absorbing compounds analogous to plant flavonoids does not correlate with a downregulation of *chsA* expression in blue light, as the latter

is expected to signal for harmful UV-light. ChsA expression shows only a two- to three-fold increase upon illumination with IR-light compared to a 58-fold upregulation in cysts, clearly indicating that ChsA is regulated on different levels and dependent on growth conditions. It is likely that the product of ChsA provides a lipid-like compound that functions as a structural component of cysts. However, the relation between ChsA expression and light, as well as a role for Ppr in encystment, remains speculative and could be clarified through identification of the ChsA enzyme product and the response regulator that modulates the phosphorylation signal of Ppr.

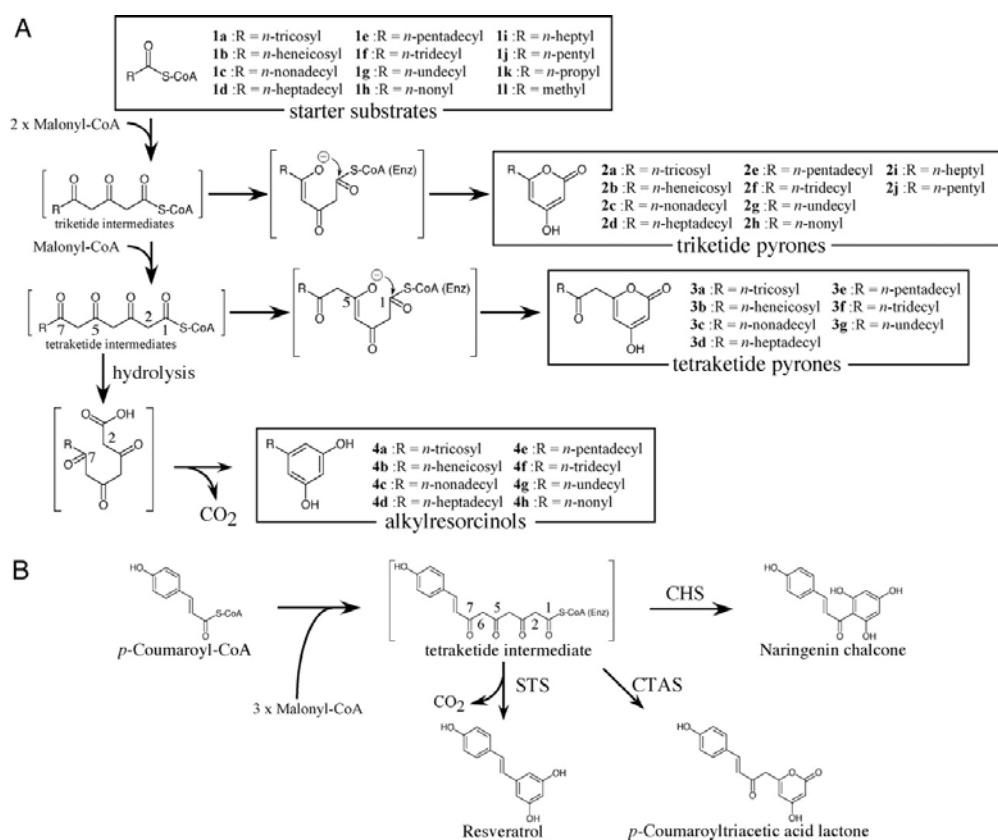


Figure 5.6

Reactions catalyzed by type III PKSs. (A) Synthesis of alkylresorcinols and alkylpyrones by *Az. vinelandii* PKSs. (B) Reactions of plant type III PKSs. CHS, STS, and CTAS use common tetraketide intermediates, which are derived from *p*-coumaroyl-CoA and malonyl-CoA. Image was taken from [19].

In Chapter six, an initial attempt is described to identify the downstream pathway and function related to the Ppr photoperception, by performing a proteomic study of the cellular photoresponse, in which comparative 2-DE is used to analyze protein expression in wild-type *Rh*.

centenum relative to a *ppr*-disrupted strain. The study indicates a shift in the lipid metabolism which could favor polyketide biosynthesis.

5.4 References

1. Jiang, Z.Y., Swem, L.R., Rushing, B.G., Devanathan, S., Tollin, G., and Bauer, C.E., Bacterial photoreceptor with similarity to photoactive yellow protein and plant phytochromes. *Science*, 1999. **285**(5426): p. 406-409.
2. Favinger, J., Stadtwald, R., and Gest, H., *Rhodospirillum centenum*, sp. nov., a thermotolerant cyst-forming anoxygenic photosynthetic bacterium. *Antonie Van Leeuwenhoek*, 1989. **55**(3): p. 291-6.
3. Kawasaki, H., Hoshino, Y., Kuraishi, H., and Yamasato, K., *Rhodocista centenaria* gen. nov., sp. nov., a cyst-forming anoxygenic photosynthetic bacterium and its phylogenetic position in the Proteobacteria alpha group. *Journal of General and Applied Microbiology*, 1992. **38**(6): p. 541-551.
4. Gest, H. and Favinger, J., Taxonomic ambiguities: a case history. *International Journal of Systematic and Evolutionary Microbiology*, 2001. **51**: p. 707-710.
5. Tindall, B.J., *Rhodocista centenaria* vs *Rhodospirillum centenum*: a reply to Gest and Favinger. *International Journal of Systematic and Evolutionary Microbiology*, 2001. **51**(Pt 2): p. 711-3.
6. Ragatz, L., Jiang, Z.Y., Bauer, C.E., and Gest, H., Macroscopic phototactic behavior of the purple photosynthetic bacterium *Rhodospirillum centenum*. *Archives of Microbiology*, 1995. **163**(1): p. 1-6.
7. Berleman, J.E. and Bauer, C.E., Characterization of cyst cell formation in the purple photosynthetic bacterium *Rhodospirillum centenum*. *Microbiology*, 2004. **150**(Pt 2): p. 383-90.
8. Yildiz, F.H., Gest, H., and Bauer, C.E., Attenuated effect of oxygen on photopigment synthesis in *Rhodospirillum centenum*. *Journal of Bacteriology*, 1991. **173**(17): p. 5502-5506.
9. Van Aken, B., Peres, C.M., Doty, S.L., Yoon, J.M., and Schnoor, J.L., *Methylobacterium populi* sp nov., a novel aerobic, pink-pigmented, facultatively methylotrophic, methane-utilizing bacterium isolated from poplar trees (*Populus deltoides* x *nigra* DN34). *International Journal of Systematic and Evolutionary Microbiology*, 2004. **54**: p. 1191-1196.
10. Jaftha, J.B., Strijdom, B.W., and Steyn, P.L., Characterization of pigmented methylotrophic bacteria which nodulate *Lotononis bainesii*. *Systematic and Applied Microbiology*, 2002. **25**(3): p. 440-449.
11. Lamparter, T., Carrascal, M., Michael, N., Martinez, E., Rottwinkel, G., and Abian, J., The biliverdin chromophore binds covalently to a conserved cysteine residue in the N-terminus of *Agrobacterium* phytochrome Agp1. *Biochemistry*, 2004. **43**(12): p. 3659-3669.
12. Kyndt, J.A., Fitch, J.C., Meyer, T.E., and Cusanovich, M.A., The photoactivated PYP domain of *Rhodospirillum centenum* Ppr accelerates recovery of the bacteriophytochrome domain after white light illumination. *Biochemistry*, 2007. **46**: p. 8256-8262.
13. Kyndt, J.A., Meyer, T.E., and Cusanovich, M.A., Photoactive yellow protein, bacteriophytochrome, and sensory rhodopsin in purple phototrophic bacteria. *Photochem Photobiol Sci*, 2004. **3**(6): p. 519-30.
14. Ferrer, J.L., Jez, J.M., Bowman, M.E., Dixon, R.A., and Noel, J.P., Structure of chalcone synthase and the molecular basis of plant polyketide biosynthesis. *Nature Structural Biology*, 1999. **6**(8): p. 775-784.
15. Austin, M.B. and Noel, A.J.P., The chalcone synthase superfamily of type III polyketide synthases. *Natural Product Reports*, 2003. **20**(1): p. 79-110.
16. Christensen, A.B., Gregersen, P.L., Schroder, J., and Collinge, D.B., A chalcone synthase with an unusual substrate preference is expressed in barley leaves in response to UV light and pathogen attack. *Plant Molecular Biology*, 1998. **37**(5): p. 849-857.

17. Funa, N., Ohnishi, Y., Ebizuka, Y., and Horinouchi, S., Properties and substrate specificity of RppA, a chalcone synthase-related polyketide synthase in *Streptomyces griseus*. *Journal of Biological Chemistry*, 2002. **277**(7): p. 4628-4635.
18. Funa, N., Ohnishi, Y., Fujii, I., Shibuya, M., Ebizuka, Y., and Horinouchi, S., A new pathway for polyketide synthesis in microorganisms. *Nature*, 1999. **400**(6747): p. 897-899.
19. Funa, N., Ozawa, H., Hirata, A., and Horinouchi, S., Phenolic lipid synthesis by type III polyketide synthases is essential for cyst formation in *Azotobacter vinelandii*. *Proceedings of the National Academy of Sciences of the United States of America*, 2006. **103**(16): p. 6356-6361.
20. Segura, D., Cruz, T., and Espin, G., Encystment and alkylresorcinol production by *Azotobacter vinelandii* strains impaired in poly- β -hydroxybutyrate synthesis. *Archives of Microbiology*, 2003. **179**(6): p. 437-443.
21. Berleman, J.E., Hasselbring, B.M., and Bauer, C.E., Hypercyst mutants in *Rhodospirillum centenum* identify regulatory loci involved in cyst cell differentiation. *Journal of Bacteriology*, 2004. **186**(17): p. 5834-41.

Chapter six

6 A proteomic study of Ppr-mediated photoresponses in *Rhodospirillum centenum* reveals a role as regulator of polyketide synthesis ^{II}

Samy Memmi[§], Fatih Mehmet Ipek[§], Carl Bauer[‡], Bart Devreese[§] and Jozef Van Beeumen[§]

[§]Laboratory of Protein Biochemistry and Biomolecular Engineering, Ghent University, K.L. Ledeganckstraat 35, 9000 Ghent, Belgium.

[‡]Department of Biology, Indiana University, Jordan Hall, Bloomington, IN 47405, USA

Abstract

Ppr from the purple phototroph *Rhodospirillum centenum* is a hybrid photoreceptor consisting of a blue light-absorbing photoactive yellow protein (PYP) domain, a red light-absorbing bacteriophytochrome (Bph) domain, and a histidine kinase (HK) domain. Ppr mediates the light-dependent regulation of a gene for a polyketide synthase related to chalcone synthase (*chsA*), which is also developmentally regulated upon transformation to metabolically resting cyst cells. Comparative proteomics of wild-type and a *ppr* gene deletion mutant revealed complex alterations in response to actinic blue- (390 - 510 nm) and red- (>600 nm) light conditions during photosynthetic growth. Differentially regulated proteins provide indications that the Ppr-mediated photoresponse involves an increased acetyl-CoA pool causing a shift in the lipid metabolism in favor of polyketide biosynthesis.

Introduction

Exposure to light can either be beneficial or harmful to living organisms. Hence, motile photosynthetic bacteria developed various behavioral responses against alterations in environmental light quality and quantity. The perceived light stimulus is relayed through a chain of reactions, leading to a different phenotype such as a change in motility or gene expression [1-3]. In the anoxygenic purple photosynthetic bacterium *Rhodospirillum centenum*, components of a chemotaxis operon, called Che₁, are essential for the control of its photophobic and phototactic behavior [4, 5]. *Rb. centenum* exists as swim cells in liquid medium, bearing a single polar flagellum

^{II} Manuscript in preparation

but differentiates into hyper-flagellated swarm cells when grown on solid surfaces [6]. A second chemotaxis operon, *Che₂*, controls synthesis of the flagella [7]. Like all motile photosynthetic bacteria, *Rb. centenum* swimmer cells undergo a tumbling response when they experience a decrease in light intensity, also referred to as the scotophobic (fear of darkness) response. In addition, swarm colonies of *Rb. centenum* are capable of rapidly migrating towards a source of infrared light (750-900 nm) even under conditions of decreasing light intensity, indicating an authentic macroscopic phototactic response [8]. On the other hand, visible wavelengths (400-600 nm) induce negative swarm motility away from the light source. However, when individual multi-flagellated cells are transferred from active swarms to liquid medium, they no longer sense the direction of light propagation but only its intensity [9]. Through a genetic screen for mutants defective in light-directed motility, it is clear that a functional photosynthetic electron transport system is required for both positive and negative phototaxes [10]. As such, it is remarkable that opposing motility responses are elicited by different wavelengths which, at the same time, drive the photosynthetic electron transport chain. It suggests an additional player(s) to be involved that would distinguish between visible and infrared light. So far, one phototransducer protein, called *Ptr*, has been identified to form a bridge between photosynthesis-dependent electron transport and light-induced motility [11]. *Ptr* contains a high degree of homology with methyl-accepting chemotaxis proteins (MCPs) and is believed to sense the redox state of a component in the cyclic electron transport chain and to subsequently transmit the signal to the chemotaxis machinery which ends up in a modulation of the flagellar motor [11].

However, the complete story on photobehavior of this phototrophic bacterium may even be more complex, as *Rb. centenum* also contains an unusual hybrid photosensor, called *Ppr*, which consists of an N-terminal photoactive yellow protein (PYP) domain, a central bacteriophytochrome (Bph) domain and a C-terminal histidine kinase (HK) domain [12, 13]. This 'PYP-phytochrome-related' protein exhibits characteristic blue (434 nm) and red (642, 701 nm) absorption maxima due to the respective PYP and Bph domains [13, 14]. Illumination of *Rb. centenum* *Ppr* with white light causes a bleach of both PYP and Bph absorbance, but both absorption maxima can also be activated separately by weak blue light or red light respectively. It has been shown that blue-light activated PYP functions to accelerate the recovery of the red-light activated phytochrome domain to the dark-adapted state [14]. Nevertheless, deletion of the *ppr* gene does not eliminate any of the previously described photobehavioral responses compared to the wild-type parent strain [12]. Thus, the *Ppr* photosensory pathway is not likely to interact with the *Che₁* signal transduction cascade that controls photosensory behavior. Instead, it has been shown to be involved in regulating expression of a polyketide synthase (*ChsA*), similar to chalcone synthase, whose product is unknown [12]. Moreover, there is a correlation between the regulation

of ChsA and the formation of bacterial resting cysts cells [15]. Upon nutrient deprivation and, possibly, exposure to other environmental stresses, *Rb. centenum* differentiates into metabolically dormant cysts which are extremely resistant to desiccation and provide protection against heat and harmful UV-light [16, 17]. Cyst cell formation is a complex developmental process controlled in part by a third Che-like signal transduction cascade, Che₃, resulting in a loss of motility, accumulation of large intracellular polyhydroxybutyrate (PHB) storage granules, and synthesis of a complex outer coat [15]. Although the role of chalcone synthase-like polyketide synthases in bacteria is not always clear, it was proposed that the polyketide synthase in *Rb. centenum* produces the membrane lipid component of the cyst, and, as such, the Ppr sensor mediates a light-dependent regulation of encystment. Unfortunately, the direct signaling partner of Ppr or a response regulator remains undetermined.

Using a proteomic approach, we investigated the cellular photoresponse of *Rb. centenum* during photosynthetic growth in red light (>600 nm) conditions supplemented with blue light (390 - 510 nm), intended to trigger possible photoresponse mechanisms initiated by the Ppr photoreceptor. By comparing the *Rb. centenum* proteome to a derivative strain in which the Ppr encoding gene has been deleted (Δppr), valuable information about the cellular photoresponse related to the Ppr photoperception function could be obtained. After separation and analysis of the total protein mixture by quantitative and qualitative 2-DE, significantly regulated proteins were identified by means of MALDI-TOF/TOF MS and nLC-coupled-ESI-Q-TRAP MS using the *Rb. centenum* protein database.

Materials and Methods

Chemicals

Urea, thiourea, ammonium persulfate, CBB G-250 and agarose were obtained from GE Healthcare (Uppsala, Sweden). Iodoacetamide, CHAPS, DTT and TEMED were from Fluka (Buchs, Switzerland). EDTA-free protease inhibitor cocktail was acquired from Roche (Mannheim, Germany). Immobilized pH gradient (IPG) strips, SDS and ampholytes were purchased from Bio-Rad (Hercules, CA, USA). The acrylamide/bisacrylamide solution was obtained from National Diagnostics (Atlanta, GA, USA). Coomassie Plus protein assay reagent, BSA and Krypton fluorescent protein stain was purchased from Pierce (Rockford, IL, USA). Ammonium sulphate, Trizma base and glycine were ordered from Sigma-Aldrich. The solvents for mass spectrometric sample preparation were obtained from Biosolve (Valkenswaard, The Netherlands).

Bacterial strains and culture conditions

Wild-type *Rhodospirillum centenum* (DSM 9894; ATCC 43720) was obtained from the DSMZ microbial collection. A *Rhodospirillum centenum* Δppr deletion mutant was constructed as described in [12]. Liquid cultures of both *Rb. centenum* strains were grown anaerobically under tungsten illumination at 30° C in medium 27 described by DSMZ. Synchronous cultures [18] were obtained by passage down a volume of sterilized glass beads (150-212 μm) (Sigma), and from this filtered fraction 5 mL was used to inoculate 100 mL anaerobically prepared medium. Cultures were grown anaerobically at 37°C in the presence of blue light (390 - 510 nm) in addition to red light (>600 nm) for photosynthetic growth. Five independent cultures were conducted for each strain. Initially, we intended to allow the cell cultures to adapt to the new light conditions for one generation before independent biological replicates were inoculated. However, second generation cell cultures showed slower cell growth and did not reach the same cell density as first generation cell cultures. Therefore, the latter cell cultures were harvested 48 hours after inoculation when the cells reached the early stationary growth phase.

Sample preparation for 2-DE

After washing with dH_2O , the cells were resuspended in lysis buffer containing 20 mM Tris-HCl (pH 7.0), 9M urea, 2M thiourea, 2% (w/v) CHAPS, 1% (w/v) DTT and Complete EDTA-free protease inhibitor cocktail (Roche, Basel, Switzerland). The proteins were released by fractionation through sonication (4 x 30 s pulses on ice), followed by centrifugation to remove the cell debris. The supernatant was treated with 0.1 volume of DNase I (0.5 mg/mL) and RNase A (0.25 mg/mL) in 50 mM MgCl_2 for 1 h on ice. Finally, the cytosolic fraction was separated from the membrane fraction by ultracentrifugation at 75.000 x g, at 4 °C for 1h, aliquotted and stored at -20°C. Protein concentrations were determined with the Coomassie Plus protein assay (Pierce, Rockford, IL) using BSA as standard according to [19].

2-DE

150 μg *Rb. centenum* total protein extract was mixed with IPG rehydration buffer (9M urea, 2M thiourea, 4% (w/v) CHAPS, 1% (w/v) DDT, 2% (v/v) Bio-Lyte 3/10 ampholytes and 0.5% (v/v) glycerol). The IPG-strips were allowed to rehydrate passively for 8h. The proteins were focused at a maximum of 10,000 V for 35,000 volt-hours using the Protean IEF cell (Bio-Rad, Hercules, CA). The temperature was kept at 20°C. After completion of the IEF program, the IPG strips were equilibrated in a 50 mM Tris-HCl solution, pH 8.8, containing 6 M urea, 30 % (v/v) glycerol, 2% (w/v) SDS and 1% (w/v) DTT, for 10 min, after which the solution was replaced with the same solution, except that DTT was exchanged by 5% (w/v) iodoacetamide. The strips

were then placed on the home-casted vertical SDS-PAGE gels (12.5% T) and sealed with 0.5% (w/v) agarose. The second dimension was performed on a Protean plus Dodeca Cell (Bio-Rad, Hercules, CA) at 10 mA/ gel for 15 min, followed by 20 mA/gel until the bromophenol blue front reached the bottom of the gel. Following electrophoresis, the protein gels were fixed in 40% (v/v) ethanol/10% acetic acid for at least 1 hour.

Protein visualization

Staining was performed using KryptonTM protein stain (Pierce, Rockford, IL) according to the manufacturer's instructions. 2-DE gel images were acquired with a Pharos FX imaging system (Bio-Rad, Hercules, CA) using a 532 nm excitation laser.

Image analysis and protein quantification

Proteomweaver 4.0 Enterprise Pro (Bio-Rad, Hercules, CA) was used to analyze 2-DE gel images. Following cropping and rotation to align the gel images, automatic image warping, spot detection, and matching were performed according to the software's instructions. Matching and spot detection were carefully reviewed and edited manually when necessary. Spot intensities given as spot volumes were normalized by Proteomweaver in a two-step process. Prior to spot matching, the absolute numeric values of every gel individually were brought into a reasonable range for the pair-matching algorithm. Therefore, the intensity of a 'normalization reference spot' was set to 1, and all other spots in the gel were adjusted accordingly. By default, the 'normalization reference spot' has an intensity higher than 95% of all spot intensities. This way, a large spot always has an intensity of about 1, huge spots have intensities larger than 1, and small spots less than 1. To allow numerical analysis, a subsequent precision normalization algorithm was performed after calculating pair matches between spot volumes from two gels. In brief, this algorithm first computes a normalization factor between all pairs of gels for which a pair match exists: for every primary or hand-match in the pair match, the quotient between the pair matched spots is calculated. The normalization factor is the median of these quotients. It then tries to compute an intensity factor for every gel, calculated by a linear equation system using 'Singular Value Decomposition' (SVD), which makes all the normalization factors as close to one as possible. As for most normalization methods, 'pair-matched-based'-normalization only works as long as the percentage of up- or down-regulated spots is less than 50%, to ensure that the median of the quotients is part of the fraction of unregulated spots.

Statistical analysis

2-DE protein maps of *Rb. centenum* containing a deletion of the Ppr encoding gene were evaluated against wild-type *Rb. centenum* 2-DE gel images. The geometric average, SD and CV were calculated for each individual protein spot across the different replicate gels in each group. The relative change of spot intensities between mutant and wild-type strain was defined as the quotient of their average group intensities, and is referred to as the regulation factor. Spots detected in at least 4 out of 5 biological replicates and showing minimal two-fold regulations were considered statistically relevant when the Mann-Whitney-Wilcoxon test indicated zero. The test is a powerful non-parametric test for comparing two populations. It is used to test the null hypothesis, *i. e.* the situation in which two populations have identical distribution functions, against the alternative hypothesis that the two distribution functions differ only with respect to the location (median). In the Mann-Whitney-Wilcoxon test, the result is exactly zero if all of the intensities in the reference group are smaller or larger than all of the intensities from the second group. Therefore, at the value of zero the test is a good indicator for significantly different spot intensities.

Mass spectrometry and protein identification

Protein spots were excised and destained by washing them twice for 20 min with 150 μ L of 200 mM NH_4CO_3 /50% ACN at 30°C. After drying them in a speed vacuum concentrator, the gel pieces were incubated with 8 μ L of freshly prepared trypsin solution (Promega, 2 μ g/mL in 50 mM NH_4CO_3) for 45 min at 0°C. The gel pieces were then covered with 20 μ L of 50 mM NH_4CO_3 and incubated at 37°C for 12-16 h. Peptides were extracted twice by treating the gel plugs with 20 μ L 60% ACN/0.1% HCOOH at 30°C. After drying the samples in a speed vacuum concentrator, the peptides were resuspended in 12 μ L 0.1% HCOOH.

A 4700 Proteomics Analyzer (Applied Biosystems) with TOF/TOF optics was used for all MALDI-MS and MS/MS applications. Samples were prepared by mixing 0.5 μ L of the sample with 0.5 μ L matrix solution (7 mg/mL alfa-cyano-4-hydroxy-cinnamic acid in 50% ACN/0.1 % TFA), and spotted on a stainless steel 192-well target plate. They were allowed to air-dry at room temperature, and were then inserted in the mass spectrometer and subjected to mass analysis. If the identification, based on MALDI TOF/TOF mass spectral data, was inconclusive, the peptide mixture was separated by nano-HPLC (Ultimate, LC Packings) and detected on-line by an ESI-Q-TRAP (Applied Biosystems/MDS SCIEX) mass spectrometer [20].

The Mascot search engine (Matrix Science, London, UK) was used to compare the MS and MS/MS data with a calculated list of all expected peptide and/or fragment masses for each sequence entry in the *Rb. centenum* protein database (unpublished). The parameters used were as follows: maximum number of missed cleavages was set at 1, and mass tolerance ranged from ± 50

to 100 ppm. The allowed modifications were carbamidomethylcysteine in fixed modification mode and oxidized methionine in variable modification mode.

Light microscopy

Wild-type and Δppr *Rb. centenum* cell cultures were grown as described above. Wet mounts were prepared at the same time interval as for preparation of the soluble protein extracts for comparative 2-DE. Individual cells were viewed with a Zeiss Axiovert 200M inverted light microscope with a differential interference contrast (DIC) on a 63 × water objective. Image capture was carried out with an AxioCam MRm cooled charge-coupled device camera and Axiovision 4.6 imaging software.

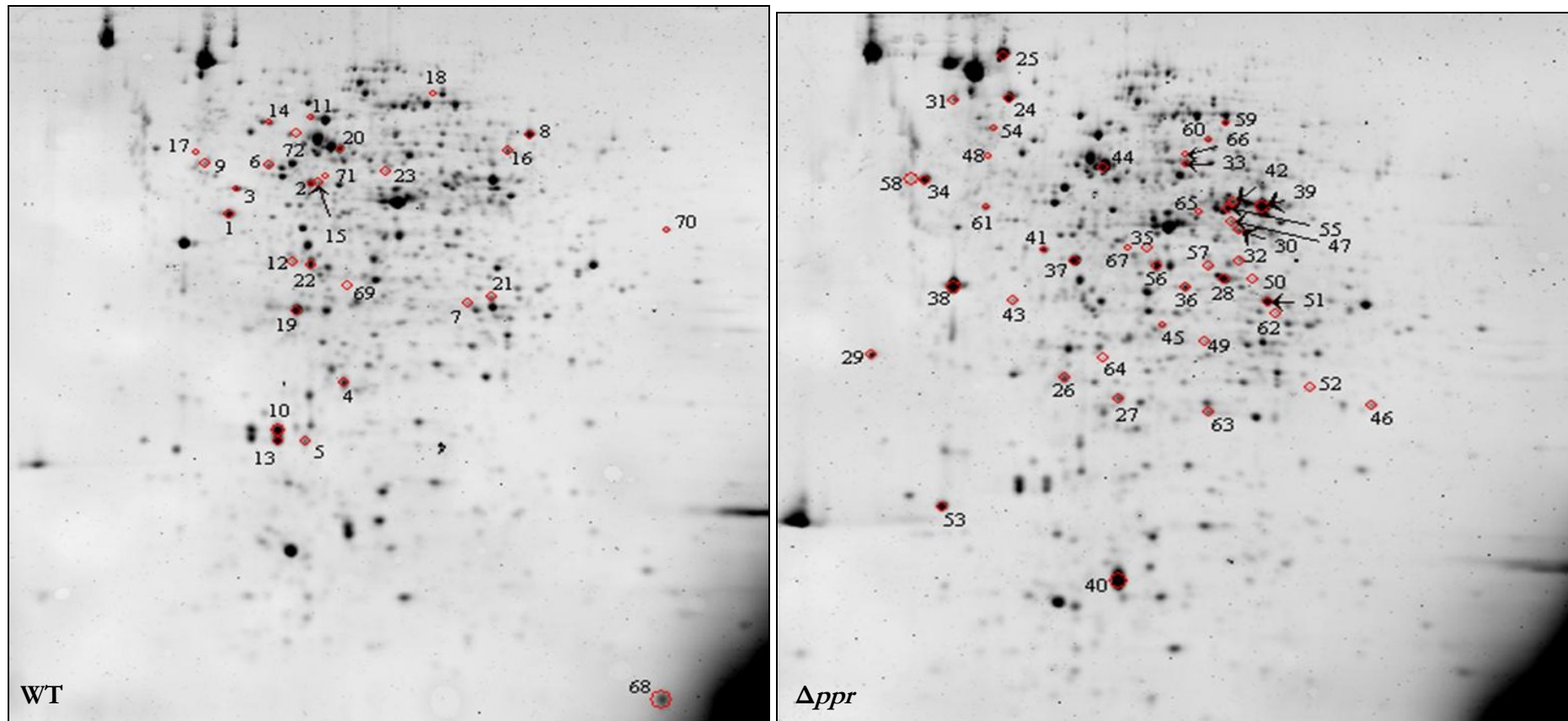
Results

Differential expression analysis

We compared the soluble subproteomes of the anoxygenic phototrophic bacterium *Rb. centenum* and a derivative mutant strain in which the *ppr* gene was deleted, after growth in red-light (>600 nm) supplemented with blue-light (390-510 nm) conditions. The objective was to unravel possible photoresponse mechanisms on the gene expression level related to the light perception function of the Ppr photosensor, which has a blue-light sensing PYP domain and a red-light absorbing bacteriophytochrome domain. Soluble protein extracts from five independently grown cultures of both strains were resolved in the first dimension by IEF using a linear pH gradient of 3-10, and subsequently separated according to their M_r in a second dimension. Using Proteomweaver 2-DE analysis software, 1215 protein spots were detected across ten 2-DE gel images. A total of 440 spots that could be found in at least 4 out of 5 biological gel replicates were selected for quantitative and qualitative analysis. Among the 440 protein spots analyzed, 5 spots appeared and 5 spots were absent in the *Rb. centenum* proteome as a result of the *ppr* gene deletion, and 62 spots showed statistically significant changes in their intensities (Mann-Whitney = 0), with at least a two-fold up- or down regulation. After growth in the described light conditions, we detected 39 upregulated protein spots in the Δppr proteome map, while 23 spots showed a decreased production. All 72 spots are presented and numbered in **Figure 6.1** and **6.2**.

Protein identification by MALDI-TOF/TOF MS and LC-MS

Mass spectrometric identification was performed on all 72 protein spots that were differentially expressed, using the *Rb. centenum* protein sequence database (unpublished), except for three protein spots (spots n° 1, 15 and 70), which had to be identified by submitting the MS data to the NCBI non-redundant database. MALDI-TOF/TOF MS resulted in the identification of 46

**Figure 6.1**

Comparative 2-DE map of the soluble proteins extracted from wild-type (left) and $\Delta pp r$ (right) *Rh. centenum* after growth in red- (>600 nm) light conditions, supplemented with blue- (390 - 510 nm) light. Differentially regulated spots are denoted by red circles and correspond to the spot numbers in Table 6-1. The presented proteome maps are average gel images of a group of 5 biological gel replicates.

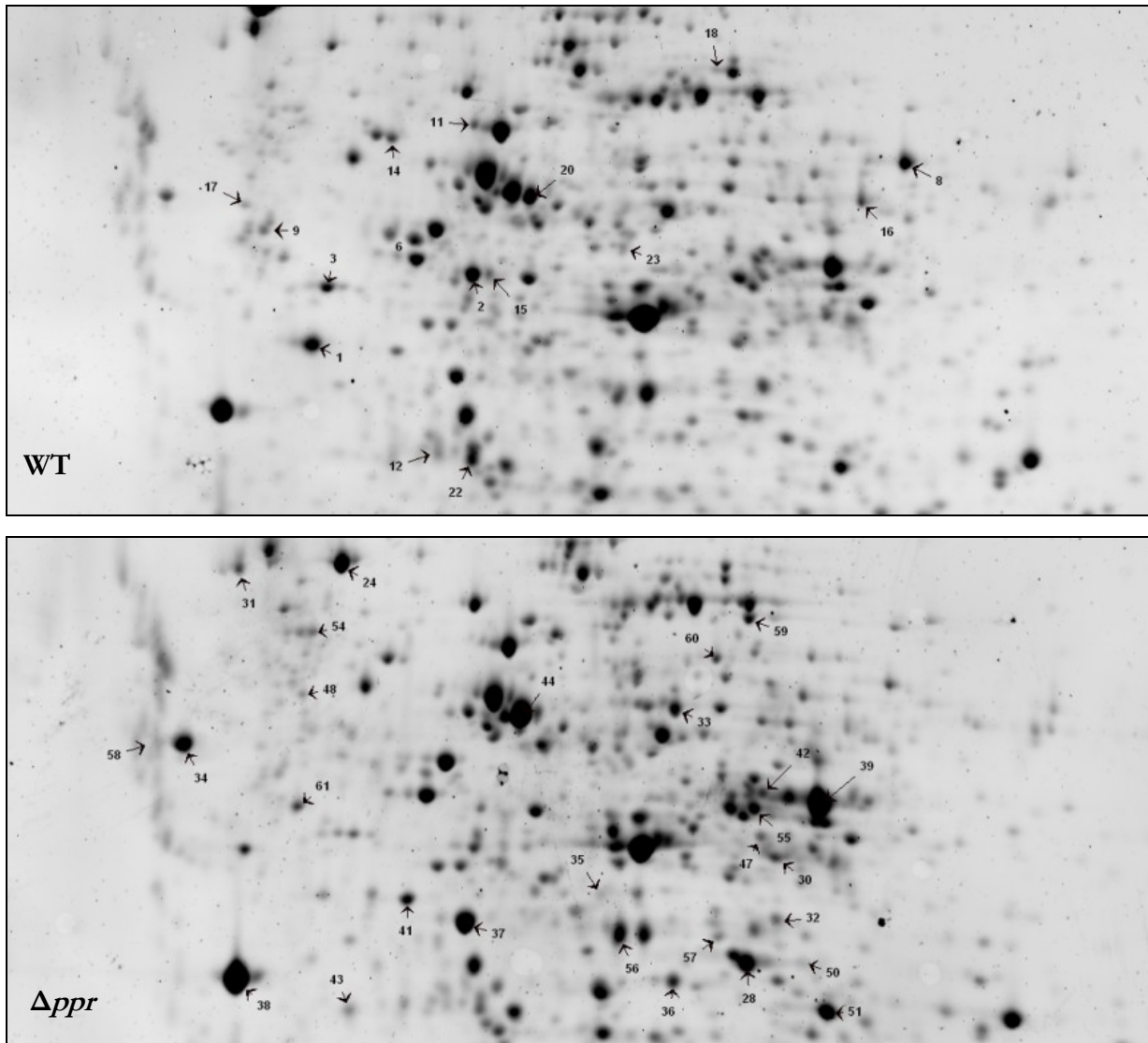


Figure 6.2

Close-up of Figure 6-1.

spots using peptide mass fingerprinting (PMF) and subsequent MS/MS analysis after collision induced dissociation. Another 19 spots were identified after separation of the peptide mixture using LC-MS. However, from the MS data of the remaining 7 spots (n° 6, 12, 67, 68, 69, 71 and 72), no conclusive identification could be achieved. Three spots (n° 33, 40 and 57) were identified as a mixture of two proteins. Subsequently, protein BLAST (<http://www.ncbi.nlm.nih.gov/blast/Blast.cgi>) was used to obtain functional information of each protein, after which the proteins were grouped according to their predicted function and listed in **Table 6-1**.

Functional annotation

Deletion of a single photoreceptor gene, *ppr*, significantly affected the levels of 72 proteins in the soluble fraction of the proteome of the anoxygenic phototroph *Rb. centenum* in response to the exposed light conditions. For 57 of the 65 proteins identified, a function could be immediately predicted *via* a protein-protein BLAST search against the annotated NCBI nr database (**Table 6-1**). The remaining proteins, of unknown function, could not be annotated, as homology was only found with hypothetical proteins (spot 26, 45, 50 and 57) or proteins that have not yet been characterized (spot 31, 43, 54 and 63). Three spots (n° 1, 15 and 70) could not be retrieved from the *Rb. centenum* protein database although clear MS/MS data were obtained. They were identified using the NCBI database, following LC-MS/MS analysis of the resulting peptide mixture after spot digestion (**Table 6-1**). A possible explanation could be that as the *Rb. centenum* protein database is not yet released to the public, it may still be incomplete. Since these four proteins all originate from the wild-type proteome (ATCC 43720), it might possibly also reflect some sequence difference with the protein entries of the *Rb. centenum* database, which was constructed from strain ATCC 51521. The latter is a motile derivative of the neotype strain (ATCC 43720), which had lost its swarm cell capability as a result of cultivation in the laboratory [8]. When both the wild-type and Δppr used in this study were grown on illuminated agar, motile cells could be observed (data not shown) and were picked for further inoculation.

Identified proteins with significant expression changes were classified into functional classes of carbon and energy metabolism, protein synthesis, signal transduction, membrane transport, cell motility and stress response, and are extensively discussed in the next section.

Microscopic analysis

The results from the comparative 2-DE indicated a shift in the acetyl-CoA metabolism in favor of polyketide synthesis in wild-type *Rb. centenum* relative to their Δppr mutants when grown phototrophically in red-light (>600 nm) supplemented with blue-light (390-510 nm), as described in the discussion. As phenolic lipid synthesis by type III polyketide synthases were demonstrated to be essential for cyst formation in the closely related species *Azotobacter vinelandii* [21], a similar correlation between enhanced polyketide metabolism through Ppr-mediated light perception and encystment in *Rb. centenum* was verified *via* microscopic observations. Thus far, *Rb. centenum* was only known to form large clusters of cyst cells upon starvation for nutrients, in which cysts typically contain four cells at the initial stage to more than 10 cells per cyst coat as the cysts mature [16]. However, in the growth conditions used for comparative 2-DE, *i.e.* mixed red/blue-light, both wild-type and Δppr mutant cells of *Rb. centenum* remained vegetative, similar to white-

light conditions as shown in **Figure 6.3**. The latter is not expected to induce metabolically resting cyst cells as it allows for full photosynthetic growth. Although the impact of mixed blue/red-light growth conditions relative to white-light on the physiology of *Rh. centenum* is not known, the similarity between wild-type and Δppr mutant cells indicates no immediate correlation between possible polyketide synthesis through Ppr-mediated light perception and cyst formation. Wet mounts of *Rh. centenum*, prepared at 48h of growth in the described light conditions, showed a mixture of single cells which were either highly motile, tumbling or immobile.'

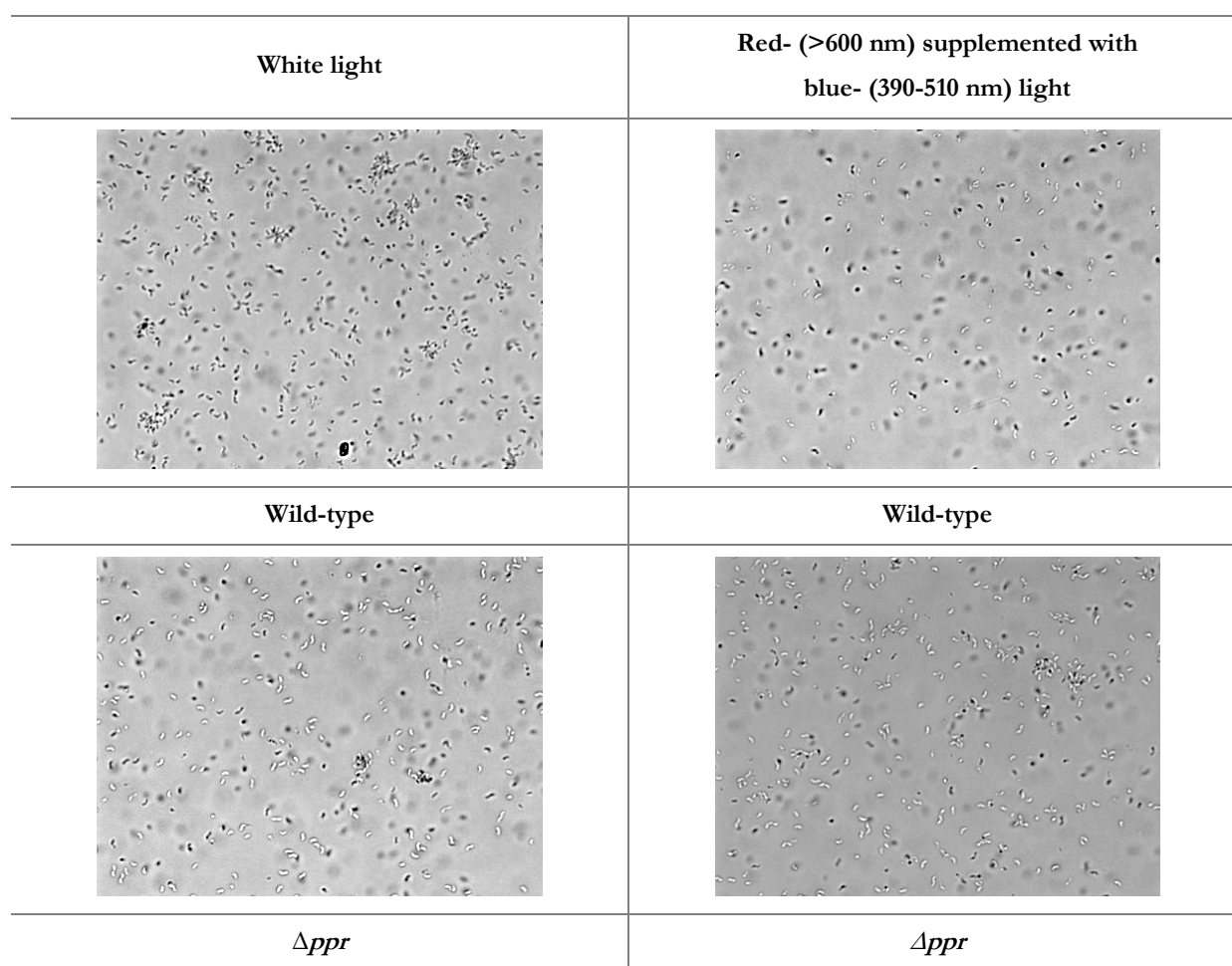


Figure 6.3

DIC microscopy of wet mounts of wild-type (top) and Δppr (bottom) *Rh. centenum* after 48h of growth in white light (left) or red-light (>600 nm) supplemented with blue-light (390 - 510 nm) (right). Both cell strains remained vegetative at all light conditions.

Discussion

In this study, the soluble proteome of the anoxygenic phototroph *Rhodospirillum centenum* was compared between wild-type and a deletion mutant of its *ppr* photoreceptor gene, after

growth in red-light (>600 nm) supplemented with actinic blue (390 - 510 nm). Ppr has been implicated to provide a basic level of phosphorylation to an unknown signal transduction pathway in the dark, as autophosphorylation levels of Ppr have been shown to decrease two- to threefold when illuminated with blue light (>400 nm). However, in that study Ppr was only reconstituted with *p*-coumaric acid as the sole chromophore [12]. Light-regulated expression of a chalcone synthase gene (*chsA*), whose product is related to the type III polyketide synthases, was found to be dependent on Ppr, as evidenced by a maximal β -galactosidase activity from the *chsA::lacZ* reporter upon illumination with IR-light (>700 nm), but inhibited approximately two-fold by blue (400 - 450 nm) or white light. Disruption of the *ppr* gene resulted in low-level and light-insensitive *chsA* gene expression [12]. However, *chsA* gene expression also increases up to 58-fold when *Rb. centenum* cells enter the cyst cell developmental pathway, indicating that *chsA* gene regulation is much more elaborate [15]. Thus, exposure to Ppr-absorbing wavelengths was expected to elicit a complex photoresponse modulating the metabolic state of the entire cell, and investigating the proteome lacking Ppr would provide us clues on which downstream signal transduction pathway(s) this unique hybrid photosensor might initiate in this light-sensitive micro-organism.

Upon deletion of *ppr*, changes to proteins with functions related to carbon metabolism include increased levels of isocitrate lyase (n° 42), malate synthase (n° 33), acetyl-CoA-acetyltransferase (n° 30), acetoacetyl-CoA reductase (n° 46) and a phasin protein (n°40), whereas levels of biotin carboxylase (n° 18) and carboxyl transferase (n° 16) decreased.

Isocitrate lyase and malate synthase are key enzymes of the glyoxylate pathway that results in the net formation of oxaloacetate from two molecules of acetyl-CoA. Acetyl-CoA-acetyltransferase (also called β -ketothiolase) catalyzes the first reaction in the poly- β -hydroxybutyrate (PHB) biosynthetic pathway, *i.e.* the condensation of two molecules of acetyl-CoA to yield acetoacetyl-CoA, which is subsequently reduced by the NADH-dependent acetoacetyl-CoA reductase to produce hydroxybutyryl-CoA, serving as a monomer in the microbial biosynthesis of PHB, a major component of cysts, as shown in **Figure 6.4** [22]. PHB is a common poly- β -hydroxyalkanoate (PHA), which is a collective term for a whole class of carbon/energy storage polymers. The length of the monomer in the polymer can vary considerably, from as short as C₄ to as long as C₁₈ in certain organisms. Phasins are a class of proteins of between 14 and 28 kDa in size that form a layer at the surface of the hydrophobic core of PHA granules [23, 24]. The soil bacterium *Ralstonia eutropha* contains four genes (*phaP1-4*) encoding for highly homologous phasin proteins [25], of which PhaP1 constitutes the predominant protein bound to the PHA granules, and is accumulated dependent on PHA

biosynthesis [26]. Note, however, that spot n° 40 was identified as a mixture of two proteins, *i.e.* phasin and a ferritin Dps family protein (**Table 6-1**).

Biotin carboxylase and carboxyltransferase make up the two catalytic subunits of the acetyl-CoA carboxylase complex that catalyzes the biotin-dependent irreversible carboxylation of acetyl-CoA to produce malonyl-CoA, as shown in **Figure 6.4**. Thus, the observed spot regulations might indicate that in the absence of Ppr, *Rb. centenum* responds to the exposed light conditions with a decreased production of malonyl-CoA, as acetyl-CoA is instead metabolized *via* the glyoxylate pathway or transformed to PHB.

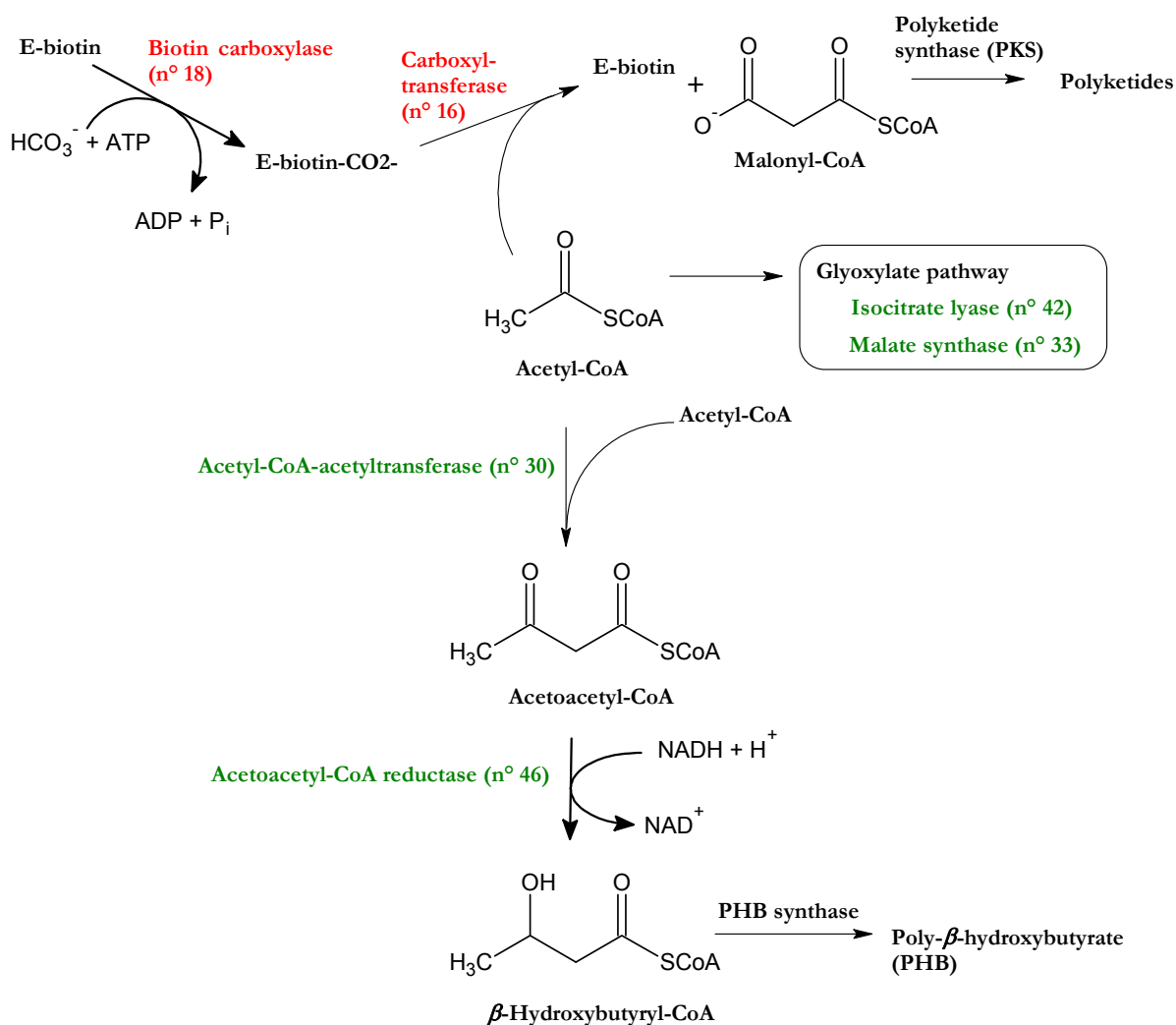


Figure 6.4

Schematic representation of the reaction pathways involving regulated proteins with related function in carbon metabolism that were identified in the comparative 2-DE protein map of wild-type and Δppr *Rh. centenum*, after photosynthetic growth in red-light supplemented with blue-light. Red-colored enzymes were found to be down-regulated upon deletion of *ppr* and growth under mixed red-blue light, while the protein levels of green-colored enzymes showed a significant increase. Enzyme names are followed by the spot number in correspondence with Table 6-1 and Figure 6.1.

Besides its role in chain elongation during fatty acid biosynthesis, malonyl-CoA is also an important building block in polyketide biosynthesis. Moreover, in the closely related species *Azotobacter vinelandii*, a nitrogen-fixing soil bacterium which is also able to differentiate into resting cyst cells, two type III polyketide synthases, ArsB and ArsC, use malonyl-CoA as an extender substrate to produce the corresponding alkylresorcinols and alkylpyrones, which constitute the major chemical components of their cyst coat [21].

Thus, the wild-type *Rb. centenum* photoresponse might involve an increased acetyl-CoA pool causing a shift in its lipid metabolism in favor of polyketide synthesis and possible cyst formation. However, two observations contradict this hypothesis. First, a polyketide synthase such as ChsA (MW = 38 kDa) was not found to be substantially regulated, although it could be one of the protein spots of which the MS data were insufficient for identification (**Table 6-1**). As *ppr*-disruption still provides a basal level of *chsA* expression [12], which in addition is developmentally regulated (see above), the change of ChsA between wild-type and Δppr might be too small to have passed our filter criteria for significant regulation. Moreover, the light-regulated fold change of *chsA* expression was observed *via* promoter activity [12] and might differ from the effective change in ChsA protein amount. Secondly, if Ppr is indeed responsible for light regulated cyst formation, stimulated PHB synthesis through the increased expression of acetyl-CoA-acetyltransferase, acetoacetyl-CoA reductase (**Figure 6.4**) and phasin, is expected to occur in the wild-type instead of the Δppr proteome, as cyst formation is characterized by the presence of intracellular PHB storage granules [16, 21]. In *A. vinelandii*, mutations in the *phbBAC* operon, coding for the enzymes of the PHB biosynthetic pathway, do not impair the capacity to form mature cysts [22]. Rather, it was postulated that lipid/polyketide metabolism may be induced from the increased acetyl-CoA and NADH pools to compensate impairment of PHB synthesis [22]. However, our microscopic analysis of wild-type *Rb. centenum* and Δppr mutant cells did not support the hypothesis of a light-regulated encystment, as only vegetative cells could be observed (**Figure 6.3**), suggesting that, if Ppr-mediated light perception favors polyketide synthesis to accommodate the cell to the exposed light conditions, it is not involved in triggering the cells to transform into dormant cysts.

Finally, our assumption that lipid metabolism in *Rb. centenum* is severely altered upon the loss of the *ppr* gene, is strengthened by another differentially expressed protein spot (n° 36), identified as a α/β -hydrolase fold-3 domain protein with high homology to the class of esterases and lipases.

Where it not that the microscopic observations indicated otherwise, the respective loss (n°64) and 3.4-fold decrease (n°34) of two flagellin proteins when comparing the proteome of

wild-type *vs.* that of Δppr , would have supported a possible role for Ppr in cyst development. In *Rb. centenum*, cyst formation can be induced in 2-3 days through growth on butyrate derivatives as a sole carbon source [17], and it has been observed that, between 24h and 36h after induction, encysting cells lose their motility and are accompanied by the accumulation of ejected flagella in the culture medium [16].

Energy metabolism is also altered upon *ppr* disruption in response to the exposed light conditions. Expression of 6-phosphofructokinase (PFK, n° 57), an important control point in the glycolytic pathway, and two enzymes of the citric acid cycle, *i.e.* succinate dehydrogenase (n° 60) and succinyl-CoA synthetase (n° 49) increased approximately two-fold, while phosphoenolpyruvate carboxykinase (PEPCK, n° 8), catalyzing a rate-controlling step of gluconeogenesis, and enolase (n° 3) decreased three- and four-fold respectively. Considering these protein changes in the wild-type proteome, the reduced expression of two enzymes of the citric acid cycle could cause a channeling of acetyl-CoA towards lipid/polyketide metabolism as it is not metabolized to PHB (see above). Secondly, the net expression changes of two key enzymes of opposing metabolic reactions, *i.e.* PFK and PEPCK, may result in an elevated glucose production, which might provide structural building blocks for the synthesis of the enveloping outer coat. In *A. vinelandii*, the glyoxylate shunt and gluconeogenic enzymes are induced upon encystment [27] and the polymer alginate is a major component of the intine and exine layer of the cyst capsule [28]. However, isocitrate lyase and malate synthase are down-regulated in the wild-type proteome, consistent with the absence of cysts during microscopic analysis (see above), and the exopolysaccharide of *Rb. centenum* cysts is not known.

Among the differentially regulated genes in protein metabolism, a glutamine synthetase was identified in both proteomes as two abundantly expressed spots (n° 20 and n° 44) with the same MW but an observed shift in *pI*, representing an altered post-translational modification state of the enzyme (**Figure 6.2**). Glutamine synthetase is an enzyme that plays an essential role in the metabolism of nitrogen by catalyzing the condensation of glutamate and ammonia to form glutamine. Glutamine is the amino group donor in the formation of many biosynthetic products, as well as being a storage form of ammonia. Glutamine synthetase is regulated by several allosteric effectors as well as by covalent modification *via* adenylation of a specific tyrosine residue. The enzyme's activity decreases with its degree of adenylation.

Other observed changes involve two enzymes (n° 55 and n° 56) that participate in methionine and cysteine metabolism, as well as an alanine dehydrogenase (n° 47), a branched-chain amino acid aminotransferase and a number of peptidases (n° 33, 59, 21 and 29) for processing and degradation of intracellular proteins. The highest regulation (more than six-fold) is

observed for a translation elongation factor, responsible for the selection and binding of the cognate aminoacyl-tRNA to the acceptor site of the ribosome.

Three signal transduction proteins had a significantly lowered expression in the Δppr proteome. Two of them (n° 23 and 4) respectively show stronger and weaker homology to methyl-accepting chemotaxis proteins, but they are not identical to the phototransducer protein Ptr nor do they originate from the three previously identified Che-like operons that regulate chemotaxis and phototaxis [4], flagella biosynthesis [7], or cyst formation [29]. However, the gene encoding the MCP-like protein from spot n° 23 is located eight genes upstream of the Che₂ gene cluster that regulates flagella biosynthesis [7]. The Che₂ may thus be larger than previously thought and may correlate to the altered flagellin production as described above. A third sensory transducer (n° 14) was identified as the sensor histidine kinase NtrY involved in nitrogen fixation.

The membrane protein composition in *Rb. centenum* is also severely altered upon deletion of the *ppr* gene. Decreased levels of an outer membrane protein with homology to porins (n° 10, 13 and 5), two TonB-dependent receptors (n° 17, 9 and 11) and two ABC-type transporters (n° 19 and 22), are compensated by increased expression of alternate TonB-dependent receptors (n° 24 and 48), extracellular solute binding proteins (n° 37 and 41), an ABC transporter (n° 28), a phosphate selective porin (n° 61) and two OmpA related proteins (n° 25 and 38). When hypercyst mutants of *Rb. centenum*, which form cysts under rich growth conditions, were generated through transposon mutagenesis, one strain contained a disruption of a gene encoding an ABC transporter [15]. However, it is not identical to one of the regulated transporters described above.

The increased appearance of a number of stress-related proteins (n° 40, 52 and 62) in the Δppr proteome, may be consistent with the fact that the Δppr mutant strain experiences the exposed light conditions as a more stressful situation compared to wild-type, as it is not able to respond accordingly through Ppr photoperception.

Finally, the most abundantly down-regulated spot (n° 1) in the *ppr*-disrupted strain could be identified as a dihydroxyacetone (Dha) kinase, using the NCBI database. Dha kinases are a sequence-conserved family of enzymes which utilize two different phosphoryldonors: ATP (in animals, plants, and some bacteria), or a multiphosphoprotein of the phosphoenolpyruvate carbohydrate phosphotransferase system (PTS) (in most bacteria). Little is known about the function of this enzyme and the metabolic origin of its substrate, Dha. Dihydroxyacetone phosphate (DhaP) can be formed by aldol cleavage of fructose-1,6-bisphosphate [30], by isomerization from glyceraldehyde-3-phosphate, and by oxidation of glycerol-3-phosphate in the mitochondrial glycerol phosphate shuttle [31]. DhaP is an obligatory precursor of glyceryl ether

phospholipid biosynthesis. In *E. coli*, two catalytic subunits of Dha kinase act antagonistically as coactivator and corepressor of the transcription activator DhaR to regulate its own transcription [32]. Which role the Dha-like protein plays in the Ppr-mediated photoresponse remains unclear.

Concluding remarks

Comparative 2-DE on soluble protein extracts from wild-type *Rb. centenum* cells and their Δppr mutants provided clues on a role for the Ppr photosensor in a light-regulated change in the lipid/polyketide metabolism. It is consistent with the light-dependent gene promoter activity of ChsA [12], a type III polyketide synthase-related protein, although the enzyme was not found to be light-regulated in this study. Protein expression changes upon *ppr* deletion were not sufficient, however, to indicate a role for Ppr in cyst formation, which is consistent with the lack of visible cyst structures during our microscopic analysis. Moreover, *Rb. centenum* has thus far only been observed to transform into metabolically resting cyst cells when grown in the dark, but never when grown photosynthetically (unpublished observations). Nevertheless, Ppr may be involved in regulating the lipid/polyketide metabolism, as suggested by the decreased malonyl-CoA biosynthetic enzymes upon *ppr* deletion and the concomitant increase of PHB synthesis. Light perception by Ppr could mediate the acetyl-CoA pool in favor of polyketide synthesis to adapt the cell against the exposed light conditions, but the nature of this response remains unclear. To further verify our conclusions, a differential and qualitative analysis of the lipid composition of wild-type and Δppr *Rb. centenum* cell membranes would be helpful, performed both on vegetative cells as on dormant cysts. Unfortunately, we were not able to perform these experiments within the time frame for this thesis work.

Acknowledgement

The authors are very grateful to Dr. John Kyndt and Dr. Terry Meyer for their critical reading and helpful suggestions. We thank Prof. Dominique Van Der Straeten and Dr. Filip Vandenbussche for their assistance with the microscopic analyses.

Table 6-1A. Down-regulated proteins upon *ppr* gene deletion in *Rh. centenum*

Spot ^(a)	Accession ^(b)	Annotation	Theo. pI	Theo. MW	Sequence coverage % (PMF ^(d))	Mascot score MS (PMF)	MASCOT peptides identified by MS/MS ^(c)	Mascot score MS/MS	RF ^(e)	MS-method
Carbon metabolism										
16	ORF_00412	Carboxyl transferase	6.3	55703	62	155	IQEGVASLGGYAEVFQR	93	0.45	MALDI
18	ORF_00406	Biotin carboxylase	5.87	72450	55	147	-	-	0.46	MALDI
Energy metabolism										
3	ORF_00116	Enolase	4.87	45079	3	72	LGANAILGVSLAVAK	72	0.23	LC-MS/MS
8	ORF_02776	Phosphoenolpyruvate carboxykinase (PEPCK)	6.41	58308	75	172	DGPLVALTGQHTGR	82	0.34	MALDI
Protein synthesis										
20	ORF_01237	Glutamine synthetase	5.23	52012	77	126	LVPGYEAPVLLAYSSR AYEGGNLAHRPAVK	80 51	0.47	MALDI
7	ORF_01862	Branched-chain amino acid aminotransferase I	6.09	32862	77	85	IPYSAAEIEK AAGLYMICTMSK + (C) IGDITYTPGEITK ALMLDYDALVNGR IPYSAAEIEKATNDVVK HAAENDGFQDALMLDYR SGEILGFRIPYSAAEIEK AISADELKDFTEVFLTGTAAEVTAVGR	37 39 78 66 10 69 39 70	0.33	LC-MS/MS
21	ORF_02214	Peptidase M24	6.21	29257	65	69	GAVPATLGYHGYR HASCISINHVVTHGVPSEDKR + (C)	56 35	0.48	MALDI
2	ORF_00684	Translation elongation factor Tu (EF-TU)	4.66	43132	6	68	NMITGAAQMDGAILVVSADGPMPQTR+(M)	68	0.16	LC-MS/MS
15	gij18311389	Translation elongation factor Tu (EF-TU)	4.94	43530	9	176	LLDEAQAGDNIGALLR KLLDEAQAGDNIGALLR ATDKPFLMPVEDVFTITGR + (M)	77 63 36	0.45	LC-MS/MS
Signal transduction and transcription regulation										
14	ORF_00129	Nitrogen regulation protein NtrY	6.62	83125	35	49	-	-	0.45	MALDI
4	ORF_01638	Methyl-accepting chemotaxis protein	4.99	89550	36	61	-	-	0.24	MALDI
23	ORF_00326	Methyl-accepting chemotaxis sensory transducer with Pas/Pac sensor	5.59	53502	96	205	NLANQAAQATSQITR EHVAGTASAIEEQSAVTR	71 26	0.50	MALDI
1	gij50119808	Dihydroxyacetone kinase	5.2	61396	1	85	GVAGDLMVFK + (M) RGVAGDLMVFK + (M)	55 31	0.15	LC-MS/MS
Membrane proteins										
5	ORF_02876	Porin	5.25	24683	68	59	-	-	0.26	MALDI
10	ORF_02876	Porin	5.25	24683	67	56	AGLLATPDTLVYGR	89	0.39	MALDI
13	ORF_02876	Porin	5.25	24683	69	70	AGLLATPDTLVYGR	93	0.44	MALDI

17	ORF_03674	TonB-dependent receptor	4.59	1E+05	18	556	TLVLVNGR YETYLGYGK NPTFGAPSISR QDFEGIEADAR YGISEEGDGIEK FFMEGTYAGTQTK FLVGADGDIPMVEGWR TSESQVSNGQVNVQSVR TNSNFQTASAGAATINLR YLFATQGDYEVNDNLR AQGCHPINLFGFGSISPEAAK + (C) NPLVPTALYDAATDTNGDGLKDLVFTR	14 35 38 59 36 52 73 54 57 56 63 20	0.46	LC-MS/MS
9	ORF_03674	TonB-dependent receptor	4.59	1E+05	46	161	YLFATQGDYEVNDNLR TNSNFQTASAGAATINLR	36 23	0.35	MALDI
11	ORF_01157	TonB-dependent copper receptor	5.24	70444	60	121	-	-	0.42	MALDI
19	ORF_03204	ABC transporter, ATPase component	5.85	36877	2	34	GISLSIPR	34	0.46	LC-MS/MS
22	ORF_03212	Phosphate ABC transporter, periplasm binding protein	5.25	36876	5	46	LFCAGVGADHPDITGASR + (C)	46	0.50	LC-MS/MS
Unidentified										
6	-								0.27	LC-MS/MS
12	-								0.43	LC-MS/MS
(a)	Spot number according to the position on the 2-DE gel image									
(b)	<i>Rhodospirillum centenum</i> gene ID or NCBI accession number									
(c)	(M), Methionine oxidized; (C), carbamidomethylcysteine									
(d)	PMF, Peptide Mass Fingerprint									
(e)	Regulation factor									

Table 6-1B. Up-regulated proteins upon *ppr* gene deletion in *Rh. centenum*

Spot ^(a)	Accession ^(b)	Annotation	Theo. pI	Theo. MW	Sequence coverage % (PMF ^(d))	Mascot score MS (PMF)	MASCOT peptides identified by MS/MS ^(c)	Mascot score MS/MS	RF ^(e)	MS-method
Carbon metabolism										
33	ORF_02644	Malate synthase A	5.73	59539	15	329	TTLPAGVTLK LMPGPNQIAR + (M) GSGPYFYLPK MIINALNSGAR TIEFTDPASGK MLADLVFTDR NAPAIGGMAAFIPIKGDEEANR + (M)	43 39 60 46 57 51 37	3.42	LC-MS/MS
39	ORF_02642	Isocitrate lyase	6.13	47531	69	147	VLIPIQQFIR MLAYNCSPSFNWK + (C)	75 68	2.54	MALDI
42	ORF_02642	Isocitrate lyase	6.13	47531	41	90	-		2.44	MALDI
30	ORF_03886	Acetyl-CoA C-acetyltransferase	6.02	40262	42	186	QAAVNAGIPVER	22	3.60	MALDI
46	ORF_03887	Acetoacetyl-CoA reductase	6.84	25306	75	76	FDVSDFEAVQAGVAR VVSDLGPVEVLVNNAGITR MTFEQWDEVIR	125 118 65	2.31	MALDI
32	ORF_03711	Glycosyl transferase (weak homology)	6.10	37298	67	52	MLEHTSILIPVLPGR	76	3.42	MALDI
36	ORF_02384	α/β hydrolase domain protein (esterase/lipase)	5.72	37274	71	115	TVVTSDLTLAGAAGPLR LAPEHPYAAAEDAVAAAYADAAAR RATDSACEWLR + (C)	107 127 73	2.82	MALDI
40	ORF_01866	Phasin	5.39	17455	87	60	NIEALTAANQLAFEGLQAVMR	65	2.52	MALDI
Energy metabolism										
60	ORF_03879	Succinate dehydrogenase flavoprotein subunit A	5.88	65398	58	97	EAIPAIIELEHYGVPFSSR LGSNSLLDLVVFGR	33 38	2.00	MALDI
49	ORF_02155	Succinyl-CoA synthetase alpha chain	5.86	29484	32	232	ESGLKPPVVGFIAGR LIGPNCPGVITPDECK + 2 (C) AAGVHVADSPASLGSTMLK + (M) GGTTHLDLPVFDTVADAVAK VICQGFTGAQGTFFHSEQAIAYGTR + (C)	19 58 49 47 58	2.22	LC-MS/MS
57	ORF_01823	6-phosphofructokinase (PFK)	5.92	38173	37	608	LLAWSNR AVDLIAEGK LLASAFGVR SQEIIGGLR VTVLGHVQR VMVLEVMGR AVDLIAEGKSDR NFALVVVSEAVK	34 42 62 51 50 49 55 55	2.06	LC-MS/MS

								IGILTSGGDCAGLNAVIR + (C)	101		
								QGGTVLGTNNKGDPPFAYPMADGSTR	22		
								QVIDVPIEEAIAAYASVDTASTLVQTAR	79		
51	ORF_04003	Phosphoribulokinase	6.09	33455	75	64		YICPQFSLTDVNFQR + (C)	107	2.12	MALDI
								VPTVDTSNPFVAR	107		
Protein synthesis											
44	ORF_01237	Glutamine synthetase	5.23	52012	38	99	-			2.35	MALDI
47	ORF_00752	Alanine dehydrogenase	5.94	39072	78	128		QLVAHGHQVIVQR	85	2.28	MALDI
								EIKNHEYR	61		
								LTHPGLAHLGDVVPAGTAIGA	66		
55	ORF_01297	O-acetylhomoserine/O-acetylserine sulfhydrylase	5.96	46017	68	133		QLYGGTLNQFANSFPR	111	2.08	MALDI
								QHPAVAWVNYAGLPDSR	81		
								AIFIESLANPGGVVLDIEAIAR	95		
								SLIIHPASTTHSQLSPEGLAAAGAGPDVVR	118		
								LFSHLANIGDTR	85		
56	ORF_02999	Cysteine synthase A (O-acetylserine(thiol)lyase)	5.57	35004	91	152		IQGIGAGFVPDVLAR	111	2.06	MALDI
								IYDSILDTVGATPLVR	117		
								VVAVEPEDSPVLSGGPLGPHK	85		
33	ORF_01542	Leucyl aminopeptidase	5.83	51890	15	380		FGAELDER	70	3.42	LC-MS/MS
								IADGVCLTR + (C)	58		
								VAVLSDEPTVAK	50		
								AGSITAAQFLQR	62		
								SGAIALTVAQDAGLGR	97		
								MPLAAAYDKDIDSDAADMK	46		
59	ORF_01825	Metallopeptidase PepO, peptidase, M13 family	6.40	77387	21	403		AIAPLLADLHR	73	2.06	LC-MS/MS
								VNGTVSNMEDFAK	68		
								MGTLEWMSPETQTK	61		
								GNLSNWWTEDDAKR	37		
								MLSMVADIQSAFHEK	33		
								ATSLDDLKTYLSWHALR	40		
								GLKPLEPVLSGIQGLKDKK	8		
								CVAATDNALGEDLGQHYVEK + (C)	45		
								IGYPDQWLDYSLLEVQPDDALGNAAR	44		
29	ORF_03337	Metalloprotease	4.27	68935	6	208		NPDVADAGIDPLR	67	4.15	LC-MS/MS
								SAVTLEATGPWGVR	71		
								LSGAATGTDVASGVELIR	70		
Cell motility											
34	ORF_03701	Flagellin protein	4.75	44832	55	142		DLGLSSLDIDAGGVR	76	3.39	MALDI

						ASDDPAVFSIAQGIR	56			
						AVQEGLAFGSAVLGTASK	63			
Membrane proteins										
24	ORF_03282	TonB-dependent receptor	4.85	87929	60	182	TNWDISTVYGR	32	6.88	MALDI
48	ORF_00397	TonB-dependent receptor	4.57	109667	6	213	FFVEGNYSK	61	2.25	LC-MS/MS
								LSSVTSLQAPVER	43	
								IVTGFSGDFDVADR	60	
								TIPLVTAGGIPLTVNSGGGSAAAITSR	56	
53	ORF_01582	Outer membrane protein W (OmpW)	4.48	23087	52	81	VDLGDVWLLPPTLTAQYHFNP	103	2.10	MALDI
								KLWLSTDVSDAGLPSR	58	
								GQVSPYIGLVNYTIFYNVDEGAAR	101	
28	ORF_03802	Sulfate ABC transporter, periplasmic	6.47	37089	57	78	SYEILNVSYPTR	28	4.52	MALDI
37	ORF_01437	Extracellular solute-binding protein	5.31	39587	77	108	KVEETMLAIRPHIK	93	2.70	MALDI
								NLDPALMALVQR	86	
41	ORF_01038	Extracellular ligand-binding receptor	5.05	38891	81	143	GGLQEVMYQAVTVGER	20	2.45	MALDI
61	ORF_03892	Phosphate-selective porin O and P	4.66	50189	69	131	LQAANIAYTGVPQWR	66	2.04	MALDI
38	ORF_00836	OmpA family protein	4.72	36992	71	163	NTATFDGAWTGVIIEGGYR	16	2.61	MALDI
25	ORF_00457	OmpA family protein	4.81	117994	64	334	YEYSSDDKPR	18	5.55	MALDI
Stress related proteins										
52	ORF_01909	Glutathione S-transferase	6.54	26040	69	107	WLETVAARPAVQR	16	2.11	MALDI
								GDQFRPEFLK	25	
								YGLVTDEYPNVR	41	
								YGLVTDEYPNVRR	21	
40	ORF_01847	Ferritin Dps family protein	5.49	18944	9	93	AMTIDIGIPEADRK	38	2.52	MALDI
								QLVAGHEAVAR	55	
62	ORF_02409	Universal stress protein (Usp)	6.32	30483	76	130			2.87	MALDI
Proteins of unknown function										
31	ORF_02332	Protein of unknown function	4.46	64959	82	265	LGIPAAIVQGW	41	3.86	MALDI
								ATDSIIEWFGGVR	70	
45	ORF_03895	Hypothetical protein	5.98	33952	70	152	KLPFDALADFR	21	2.34	MALDI
								FAELGTAPVAQER	24	
								ATPDVHAAFLKEEIER	13	
50	ORF_01769	Hypothetical protein	8.83	34210	52	85	TDFKDAPGTIQR	35	2.22	MALDI
								VNRLETELQTLR	20	
57	ORF_01898	Hypothetical protein	5.81	37932	27	400	IVQSVIR	52	2.06	LC-MS/MS
								SVTINLVALR	62	
								VTVDSVGAQANR	77	
								STDLQEQAQAQAFR	79	
								LAPTSLVFGAWDSR	56	
								GFVHVPSVNPAGGIAR	46	

54	ORF_03305	Protein of unknown function	4.67	54829	60	164	SAQYNPALDYTALGVFDETDKAK	31		
							VHGLEGWVAAAAAR	48	2.09	MALDI
							AVDQLHQSILR	54		
26	ORF_00789	Hypothetical protein	5.18	29204	88	118	QWVVLPESYR	56	5.16	MALDI
							TIEAYDGPLEQDGR	93		
							RQAAPDLIVLPVPAPEAAQ	68		
43	ORF_01684	Protein of unknown function	4.95	35453	9	112	GVGTAPPTYTTIDR	66	2.39	LC-MS/MS
							NVDPNSETPNFTLSILAHK	46		
35	ORF_03432	Crispr-associated protein, Cmr3 family	5.34	37670	68	99	DGAPLLPAPLHLHR	49	3.28	MALDI
							GGKPFAGAGTGATSGLPQPQTLGALR	46		
27	ORF_03238	Microcystin dependent protein	6.00	20749	8	59	YLTAAAGDFGGDAVTVK	59	5.07	LC-MS/MS
58	ORF_00817	Hemolysin-type calcium-binding region	4.09	107220	12	547	AAVDAGVFK	58	2.06	LC-MS/MS
							YLADNLDVK	38		
							AHFEQFGVK	26		
							SALEHYLAYGR	51		
							DVFDWYVNTGVK	53		
							SNFLAFDSTAYLK	49		
							TGVAPNAELATFDSAK	88		
							LTLVESDGGATVAAAAGTR	65		
							NNPDVLQAVLNGGFPSAR	32		
							DALAAVTVQDATGLTTVASDVLTK	86		

- (a) Spot number according to the position on the 2-DE gel image
 (b) *Rhodospirillum centenum* gene ID or NCBI accession number
 (c) (M), Methionine oxidized; (C), carbamidomethylcysteine
 (d) PMF, Peptide Mass Fingerprint
 (e) Regulation factor

Table 6-1C. Proteins appearing in *Rh. centenum* after Ppr gene deletion and growth in blue/red light

Spot ^(a)	Accession ^(b)	Annotation	Theo. pl	Theo. MW	Sequence coverage % (PMF ^(d))	Mascot score MS (PMF)	MASCOT peptides identified by MS/MS ^(c)	Mascot score MS/MS	MS-method
Motility									
64	ORF_00204	Flagellin protein	5.2	29594	67	63	ALNENISINAATVQTAR RLELQADFTSK	62 8	MALDI
Energy metabolism									
66	ORF_00245	Phosphodiesterase/alkaline phosphatase D	6.03	59170	29	111	GYHLHEVTPK	9	MALDI
Proteins of unknown function									
65	ORF_00794	TPR domain protein	7.72	50880	64	60	AAELSDNGEGFIR LAQAYLEREDWK	32 17	MALDI
63	ORF_00841	Protein of unknown function	5.89	24705	17	241	WADQMQLLR TAGALLSAGADTAGR LSELASQSTDAAMR	66 102 74	LC-MS/MS
Unidentified proteins									
67	-								MALDI

Table 6-1D. Proteins disappearing in *Rh. centenum* after Ppr gene deletion and growth in blue/red light

Spot ^(a)	Accession ^(b)	Annotation ^(c)	Theo. pl	Theo. MW	Sequence coverage % (PMF)	Mascot score MS (PMF)	MASCOT peptides identified by MS/MS	Mascot score MS/MS	MS-method
Membrane transport									
70	gij70730127	Phosphate ABC transporter, periplasmic	8.51	40468	19	247	AAFLNNDYTK LIQVPSVATSVAVPFNK ITYMSPDYAAPTLAGLDDATK + (M) DSFVTASSGLSIGNASVCNAIGRPL + (C) ITYMSPDYAAPTLAGLDDATKVK + (M)	48 47 52 66 34	LC-MS/MS
Unidentified proteins									
68	-								LC-MS/MS
69	-								LC-MS/MS
71	-								LC-MS/MS
72	-								LC-MS/MS

^(a) Spot number according to the position on the 2-DE gel image

^(b) *Rhodospirillum centenum* gene ID or NCBI accession number

^(c) (M), Methionine oxidized; (C), carbamidomethylcysteine

^(d) PMF, Peptide Mass Fingerprint

References

1. Armitage, J.P., Behavioural responses of bacteria to light and oxygen. *Archives of Microbiology*, 1997. **168**(4): p. 249-261.
2. Bauer, C., Elsen, S., Swem, L.R., Swem, D.L., and Masuda, S., Redox and light regulation of gene expression in photosynthetic prokaryotes. *Philosophical Transactions of the Royal Society of London Series B-Biological Sciences*, 2003. **358**(1429): p. 147-153.
3. Han, Y.C., Braatsch, S., Osterloh, L., and Klug, G., A eukaryotic BLUF domain mediates light-dependent gene expression in the purple bacterium *Rhodobacter sphaeroides* 2.4.1. *Proceedings of the National Academy of Sciences of the United States of America*, 2004. **101**(33): p. 12306-12311.
4. Jiang, Z.Y., Gest, H., and Bauer, C.E., Chemosensory and photosensory perception in purple photosynthetic bacteria utilize common signal transduction components. *Journal of Bacteriology*, 1997. **179**(18): p. 5720-7.
5. Jiang, Z.Y. and Bauer, C.E., Analysis of a chemotaxis operon from *Rhodospirillum centenum*. *Journal of Bacteriology*, 1997. **179**(18): p. 5712-9.
6. Nickens, D., Fry, C.J., Ragatz, L., Bauer, C.E., and Gest, H., Biotype of the purple nonsulfur photosynthetic bacterium, *Rhodospirillum centenum*. *Archives of Microbiology*, 1996. **165**(2): p. 91-96.
7. Berleman, J.E. and Bauer, C.E., A che-like signal transduction cascade involved in controlling flagella biosynthesis in *Rhodospirillum centenum*. *Molecular Microbiology*, 2005. **55**(5): p. 1390-402.
8. Ragatz, L., Jiang, Z.Y., Bauer, C.E., and Gest, H., Macroscopic phototactic behavior of the purple photosynthetic bacterium *Rhodospirillum centenum*. *Archives of Microbiology*, 1995. **163**(1): p. 1-6.
9. Sackett, M.J., Armitage, J.P., Sherwood, E.E., and Pitta, T.P., Photoresponses of the purple nonsulfur bacteria *Rhodospirillum centenum* and *Rhodobacter sphaeroides*. *Journal of Bacteriology*, 1997. **179**(21): p. 6764-8.
10. Jiang, Z.Y., Rushing, B.G., Bai, Y., Gest, H., and Bauer, C.E., Isolation of *Rhodospirillum centenum* mutants defective in phototactic colony motility by transposon mutagenesis. *Journal of Bacteriology*, 1998. **180**(5): p. 1248-55.
11. Jiang, Z.Y. and Bauer, C.E., Component of the *Rhodospirillum centenum* photosensory apparatus with structural and functional similarity to methyl-accepting chemotaxis protein chemoreceptors. *Journal of Bacteriology*, 2001. **183**(1): p. 171-7.
12. Jiang, Z.Y., Swem, L.R., Rushing, B.G., Devanathan, S., Tollin, G., and Bauer, C.E., Bacterial photoreceptor with similarity to photoactive yellow protein and plant phytochromes. *Science*, 1999. **285**(5426): p. 406-409.
13. Kyndt, J.A., Meyer, T.E., and Cusanovich, M.A., Photoactive yellow protein, bacteriophytochrome, and sensory rhodopsin in purple phototrophic bacteria. *Photochemical & Photobiological Sciences*, 2004. **3**(6): p. 519-30.
14. Kyndt, J.A., Fitch, J.C., Meyer, T.E., and Cusanovich, M.A., The photoactivated PYP domain of *Rhodospirillum centenum* Ppr accelerates recovery of the bacteriophytochrome domain after white light illumination. *Biochemistry*, 2007. **46**: p. 8256-8262.
15. Berleman, J.E., Hasselbring, B.M., and Bauer, C.E., Hypercyst mutants in *Rhodospirillum centenum* identify regulatory loci involved in cyst cell differentiation. *Journal of Bacteriology*, 2004. **186**(17): p. 5834-41.
16. Berleman, J.E. and Bauer, C.E., Characterization of cyst cell formation in the purple photosynthetic bacterium *Rhodospirillum centenum*. *Microbiology*, 2004. **150**(Pt 2): p. 383-90.
17. Favinger, J., Stadtwald, R., and Gest, H., *Rhodospirillum centenum*, sp. nov., a thermotolerant cyst-forming anoxygenic photosynthetic bacterium. *Antonie Van Leeuwenhoek*, 1989. **55**(3): p. 291-6.

18. Bates, D., Epstein, J., Boye, E., Fahrner, K., Berg, H., and Kleckner, N., The *Escherichia coli* baby cell column: a novel cell synchronization method provides new insight into the bacterial cell cycle. *Molecular Microbiology*, 2005. **57**(2): p. 380-391.
19. Bradford, M.M., A rapid and sensitive method for the quantitation of microgram quantities of protein utilizing the principle of protein-dye binding. *Analytical Biochemistry*, 1976. **72**: p. 248-54.
20. Sandra, K., Devreese, B., Van Beeumen, J., Stals, I., and Claeysens, M., The Q-trap mass spectrometer, a novel tool in the study of protein glycosylation. *Journal of the American Society for Mass Spectrometry*, 2004. **15**(3): p. 413-423.
21. Funai, N., Ozawa, H., Hirata, A., and Horinouchi, S., Phenolic lipid synthesis by type III polyketide synthases is essential for cyst formation in *Azotobacter vinelandii*. *Proceedings of the National Academy of Sciences of the United States of America*, 2006. **103**(16): p. 6356-6361.
22. Segura, D., Cruz, T., and Espin, G., Encystment and alkylresorcinol production by *Azotobacter vinelandii* strains impaired in poly- β -hydroxybutyrate synthesis. *Archives of Microbiology*, 2003. **179**(6): p. 437-443.
23. Steinbuchel, A., Aerts, K., Babel, W., Follner, C., Liebergesell, M., Madkour, M.H., Mayer, F., Pieperfurst, U., Pries, A., Valentin, H.E., and Wieczorek, R., Considerations on the structure and biochemistry of bacterial polyhydroxyalkanoic acid inclusions. *Canadian Journal of Microbiology*, 1995. **41**: p. 94-105.
24. Wieczorek, R., Pries, A., Steinbuchel, A., and Mayer, F., Analysis of a 24-kDa protein associated with the polyhydroxyalkanoic acid granules in *Alcaligenes eutrophus*. *Journal of Bacteriology*, 1995. **177**(9): p. 2425-2435.
25. Potter, M., Muller, H., Reinecke, F., Wieczorek, R., Fricke, F., Bowien, B., Friedrich, B., and Steinbuchel, A., The complex structure of polyhydroxybutyrate (PHB) granules: four orthologous and paralogous phasins occur in *Ralstonia eutropha*. *Microbiology-Sgm*, 2004. **150**: p. 3089-3089.
26. York, G.M., Junker, B.H., Stubbe, J., and Sinskey, A.J., Accumulation of the PhaP phasin of *Ralstonia eutropha* is dependent on production of polyhydroxybutyrate in cells. *Journal of Bacteriology*, 2001. **183**(14): p. 4217-4226.
27. Sadoff, H.L., Encystment and germination in *Azotobacter vinelandii*. *Bacteriological Reviews*, 1975. **39**(4): p. 516-539.
28. Campos, M.E., MartinezSalazar, J.M., Lloret, L., Moreno, S., Nunez, C., Espin, G., and SoberonChavez, G., Characterization of the gene coding for GDP-mannose dehydrogenase (algD) from *Azotobacter vinelandii*. *Journal of Bacteriology*, 1996. **178**(7): p. 1793-1799.
29. Berleman, J.E. and Bauer, C.E., Involvement of a Che-like signal transduction cascade in regulating cyst cell development in *Rhodospirillum centenum*. *Molecular Microbiology*, 2005. **56**(6): p. 1457-1466.
30. Schurmann, R. and Sprenger, G.A., Fructose-6-phosphate aldolase is a novel class I aldolase from *Escherichia coli* and is related to a novel group of bacterial transaldolases. *Journal of Biological Chemistry*, 2001. **276**(14): p. 11055-11061.
31. Daniel, R., Stuert, K., and Gottschalk, G., Biochemical and molecular characterization of the oxidative branch of glycerol utilization by *Citrobacter freundii*. *Journal of Bacteriology*, 1995. **177**(15): p. 4392-4401.
32. Bachler, C., Schneider, P., Bahler, P., Lustig, A., and Erni, B., *Escherichia coli* dihydroxyacetone kinase controls gene expression by binding to transcription factor DhaR. *EMBO Journal*, 2005. **24**(2): p. 283-293.

Abstracts of other publications

Cardol, P.; Boutaffala, L.; **Memmi, S.**; Devreese, B.; Matagne, R.F.; Remacle, C.

In *Chlamydomonas*, the loss of ND5 subunit prevents the assembly of whole mitochondrial complex I and leads to the formation of a low-abundant 700 kD subcomplex

(2008) *Biochimica et Biophysica Acta – Bioenergetics* 1777, 388-96

In the green alga *Chlamydomonas reinhardtii*, a mutant deprived of complex I enzyme activity presents a 1T deletion in the mitochondrial *nd5* gene. The loss of the ND5 subunit prevents the assembly of the 950 kDa whole complex I. Instead, a low abundant 700 kDa subcomplex, loosely associated to the inner mitochondrial membrane, is assembled. The resolution of the subcomplex by SDS-PAGE gave rise to 19 individual spots, sixteen having been identified by mass spectrometry analysis. Eleven, mainly associated to the hydrophilic part of the complex, are homologs to subunits of the bovine enzyme whereas five (including gamma-type carbonic anhydrase subunits) are specific to green plants or to plants and fungi. None of the subunits typical of the β membrane domain of complex I enzyme has been identified in the mutant. This allows us to propose that the truncated enzyme misses the membrane distal domain of complex I but retains the proximal domain associated to the matrix arm of the enzyme. A complex I topology model is presented in the light of our results. Finally, a supercomplex most probably corresponding to complex I–complex III association, was identified in mutant mitochondria, indicating that the missing part of the enzyme is not required for the formation of the supercomplex.

Kyndt, J.A.; Savvides, S.N.; **Memmi, S.**; Koh, M.; Fitch, J.C.; Meyer, T.E.; Heyn, M.P.; Van Beeumen, J.; Cusanovich, M.A.

Structural role of tyrosine 98 in Photoactive Yellow Protein: effects on fluorescence, gateway, and photocycle recovery

(2007) *Biochemistry* 46, 95-105.

We have recently shown that the Y98Q mutant of PYP has a major effect on the photocycle kinetics (similar to 40 times slower recovery). We have now determined the crystal structure of Y98Q at 2.2 Å resolution to reveal the role of residue Y98 in the PYP photocycle. Although the overall structure is very similar to that of WT, we observed two major effects of the mutation. One obvious consequence is a conformational change of the $\beta 4$ - $\beta 5$ loop, which includes a repositioning of residue M100. It had previously been shown that the photocycle is slowed by as much as 3 orders of magnitude when residue M100 is substituted or when the conformation is altered as in *Rhodospirillum rubrum* PYP. To investigate whether the altered photocycle of Y98Q is due to this repositioning of M100 or is caused by an effect unrelated to M100, we determined the dark recovery kinetics of the Y98Q/M100A mutant. We find the recovery kinetics to be very similar to the M100A single mutant kinetics and therefore conclude that the slower recovery kinetics in Y98Q is most likely due to repositioning of M100. In addition, we find that other

substitutions at position 98 (Y98W, Y98L, and Y98A) have differing effects on the photocycle recovery, presumably due to a variable distortion of the $\beta 4$ - $\beta 5$ loop. The second effect of the Y98Q mutation is a repositioning of R52, which is thought to interact with Y98 in WT PYP and now forms new interactions with residues Q99 and Q56. To determine the role of R52, we also characterized an R52A/M100A double mutant and found that the effects on the recovery kinetics (similar to the 2000-fold slower recovery than WT) are due to unrelated events in the photocycle. Since the Y98Q/M100A recovery kinetics is more similar to those of M100 than R52A/M100A, we conclude that the repositioning of R52, caused by the Y98Q mutation, does not affect the dark state recovery. In addition, it has been proposed that Y98 and P68 are gateway residues between which the chromophore must pass during isomerization. We tested the recovery kinetics of mutant P68A and found that, although the gateway may be important for photocycle initiation, its role in recovery to the ground state is minimal.

Scharlaken, B.; De Graaf, D.C.; **Memmi, S.**; Devreese, B.; Van Beeumen, J.; Jacobs, F.J.

Differential protein expression in the honey bee head after a bacterial challenge

(2007) *Archives of Insect Biochemistry and Physiology* 65, 223-37.

Insect immune proteins and peptides induced during bacterial infection are predominantly synthesized by the fat body or by haemocytes and are released into the hemolymph. However, tissues other than the immune-related ones are thought to play a role in bacteria-induced responses. Here we report a proteomic study of honey bee heads designed to identify the proteins that are differentially expressed after bacterial challenge in a major body segment not directly involved in insect immunity. The list of identified proteins includes structural proteins, an olfactory protein, proteins involved in signal transduction, energy housekeeping, and stress responses, and also two major royal jelly proteins. This study revealed a number of bacteria-induced responses in insect head tissue directly related to typical functions of the head, such as exocrine secretion, memory, and senses in general.

Samyn, B.; Sergeant, K.; **Memmi, S.**; Debysers, G.; Devreese, B.; Van Beeumen, J.

MALDI-TOF/TOF *de novo* sequence analysis of 2D-PAGE-separated proteins from *Halorhodospira halophila*, a bacterium with unsequenced genome

(2006) *Electrophoresis* 27, 2702-11.

Because protein identifications rely on matches with sequence databases, high-throughput proteomics is currently largely restricted to those species for which comprehensive sequence databases are available. The identification of proteins derived from organisms with unsequenced genomes mainly depends on homology searching. Here, we report the use of a simplified, gel-based, chemical derivatization strategy for *de novo* sequence analysis using a MALDI-TOF/TOF mass spectrometer. This approach allows the determination of *de novo* peptide sequences of up to 20 amino acid residues in length. The protocol was applied on a proteomic study of 2-D PAGE-separated proteins from *Halorhodospira halophila*, an extremophilic eubacterium with yet unsequenced genome. Using three different homology-based search algorithms, we were able to identify more than 30 proteins from this organism using subpicomole quantities of protein.

Samenvatting

Het leven op aarde is direct of indirect afhankelijk van licht dat zowel dienst doet als een bron van energie als van informatie. Licht wordt waargenomen door fotoreceptoren, eiwitten die in staat zijn specifieke golflengten te absorberen door middel van een chromofore groep. In fototrofe micro-organismen en groene planten vormen ze gespecialiseerde fotosynthetische pigmenten die lichtenergie omzetten in chemische energie voor hun groei en ontwikkeling. Daarnaast bestaan er ook fotoreceptoren die louter een signaalfunctie bezitten waarbij ze het heersende lichtklimaat waarnemen en die informatie doorgeven aan intracellulaire respons eiwitten.

Verschillende fotoreceptoren die lichtenergie omzetten naar een gepast biologisch signaal zijn ondertussen gekend en worden onderverdeeld, ondermeer, aan de hand van de identiteit van hun chromofore groep. Eén ervan is het bacteriële fotoactief geel eiwit of 'photoactive yellow protein' (PYP). Het werd voor het eerst geïsoleerd in 1985 uit de extreem halofiele en fototrofe bacterie *Halorhodospira halophila* (Hh), en absorbeert blauw licht met een maximum bij 446 nm. Lichtabsorptie leidt tot een *trans* naar *cis* isomerisatie van zijn chromofoor, *p*-coumaarzuur, waardoor het PYP een fotocyclis ondergaat. Verschillende intermediaire vormen die het tijdens zijn fotocyclis aanneemt werden reeds geïdentificeerd. Het langst levende fotointermediair wordt gekarakteriseerd door een conformationele verandering t.o.v. zijn toestand in het donker, en wordt verondersteld de signalisatietoestand te zijn die interageert met een tot op heden ongekende signaaltransductiepartner. Oorspronkelijk werden PYP-fotoreceptoren enkel teruggevonden in een aantal halofiele proteobacteriën, maar onder meer als gevolg van de exponentiële toegang tot beschikbare genomische informatie zijn ondertussen al 21 genen geïdentificeerd die coderen voor homologe PYP-eiwitten. Daarenboven blijkt dat de verspreiding van *pyp* genen niet beperkt is tot fototrofe bacteriën, maar dat *pyp* ook voorkomt in de genomen van aërobe, niet-fotosynthetische bacteriën.

In dit kader hebben we een gen dat codeert voor een unieke PYP fotoreceptor opgepikt uit het genoom van de extreem halofiele, aërobe en chemotrofe bacterie *Salinibacter ruber* (Sr). Het gen werd samen met de biosynthetische genen voor *p*-coumaarzuur afkomstig van *Rhodobacter capsulatus* heteroloog tot expressie gebracht in *E. coli*. In vergelijking met de andere PYPs bevat het gevormde Sr PYP een unieke N-terminale extensie van 31 aminozuren dat betrokken is in de vorming van een dimeer, maar de functionele relevantie hiervan is nog onduidelijk. Wanneer deze N-terminale extensie wordt afgesplitst ontstaat het monomeer, maar dit heeft echter geen invloed op het absorptiespectrum of de kinetiek van de fotocyclis. Sr PYP vertoont een

absorptiemaximum bij 431 nm en ondergaat een typische fotocycclus na belichting met blauw of wit licht. De fotocycclus verloopt echter 14.000 keer trager in vergelijking met het PYP van *H. halophila* (de 'signaaltoestand' van Sr PYP heeft een leeftijd van ongeveer 39 min, terwijl die voor Hh PYP 160 ms bedraagt), en is tot dusver de traagste fotocycclus van alle bestudeerde PYPs. Het absorptiemaximum bij 431 nm van Sr PYP bevat een schouder bij lagere golflengte dat een spectrale vorm voorstelt die intermediair is aan de grondtoestand (~431 nm) en de belichte vorm (~334 nm). Het absorptiemaximum en de spectrale schouder vormen een evenwicht gelijkaardig aan dat voor het PYP van *Rb. capsulatus* en de Y42F mutant van *H. halophila*, en wordt sterk beïnvloed door de ionaire sterkte van de oplossing. Zowel chaotrope als kosmotrope zouten stabiliseren het absorptiemaximum bij 431 nm ten koste van de intermediaire vorm, en versnellen de fotocycclus tot 6,5 keer tussen 0 en 3,5 M zout. PYP van *S. ruber* is een voorbeeld van een halofiel eiwit dat hoge zoutconcentraties nodig heeft om zijn tertiaire structuur te stabiliseren, als gevolg van hoge concentraties aan KCl die *S. ruber* opstapelt in de cel als respons op de hoge osmotische druk van hun leefomgeving.

Een andere merkwaardige PYP variant is de Ppr (PYP-phytochrome-related) fotoreceptor van de fototrofe purperbacterie *Rhodospirillum centenum*, die bestaat uit een N-terminaal PYP-domein, een centraal bacteriofytochrom-domein en een C-terminaal domein dat homoloog is aan bacteriële histidinekinasen. Fotoactivatie van het PYP-domein heeft een antagonistische werking op het effect van rood licht op het bacteriofytochromdomein. Op die manier vormt Ppr een lichtgevoelige schakelaar dat zijn kinaseactiviteit reguleert afhankelijk van het aanwezige blauw en rood licht. Het blijft echter nog onduidelijk in welke signaaltransductiepathway dit hybride fotoreceptorkinase is betrokken. Daarom hebben wij een initiële studie uitgevoerd naar de functionele pathways waarin Ppr lichtabsorptie betrokken zou kunnen zijn aan de hand van een vergelijkende proteoomanalyse via 2D-PAGE. Via een samenwerking kregen we toegang tot een mutante stam van *Rb. centenum* waarin het gen voor Ppr werd verwijderd, en het proteoom van deze mutant werd vergeleken met dat van wild-type *Rb. centenum*, na blootstelling aan blauw (390 - 510 nm) en rood (>600 nm) licht tijdens de fotosynthetische groei. In de analyse wijzen verschillende differentieel geëxprimeerde eiwitten op een regulerende rol voor het Ppr in het metabolisme van een polyketide. De functionele betekenis van deze respons is vooralsnog onduidelijk. Verder onderzoek naar de identiteit van deze polyketiden en hun licht-gereguleerde synthese is dan ook wenselijk.

De allereerste PYP-fotoreceptor werd ondertussen al meer dan twintig jaar geleden ontdekt, en hun aantal blijft groeien. Toch blijven de PYPs in vele opzichten nog een mysterieuze familie van blauw-licht receptoren waarbij het zoeken naar het mechanisme van

signaaloverdracht, de primaire signalisatiepartner(s) en hun fysiologische rol nog steeds een grote uitdaging vormt in het biochemisch onderzoek.

Dankwoord

De realisatie van dit proefschrift was niet mogelijk geweest zonder de steun van een heleboel mensen die ik hiervoor dan ook oprecht wil bedanken.

Eerst en vooral dank ik mijn promotoren Prof. Jozef Van Beeumen en Prof. Bart Devreese voor hun vertrouwen en deskundige bijstand tijdens mijn onderzoek. Ook hun toegewijde inzet bij het nalezen van dit werk wordt enorm geapprecieerd.

Een bijzonder persoon die ik uitdrukkelijk wens te bedanken is Dr. John Kyndt. Niet alleen bracht hij me de beginselen van PYP bij, zijn ideeën en kritieken betekenden een voortdurende inspiratie en motivatie voor het realiseren van dit proefschrift. Het was (en blijft) een plezier om met John samen te werken en ik koester dan ook heel veel respect en bewondering voor zijn verwezenlijkingen. Daarenboven zal de gastvrijheid die ik mocht genieten van John en zijn gezin tijdens mijn bezoek aan hun avontuur in Arizona een blijvende mooie herinnering vormen.

Verder dank ik ook Prof. Mike Cusanovich, Prof. Terry Meyer en John Fitch uit de Verenigde Staten voor hun hartelijk ontvangst tijdens mijn studieverblijf in hun laboratorium. Vooral Terry's wetenschappelijke inzichten, suggesties en kritische kanttekeningen hebben me zeer gesmaakt.

Uiteraard wil ik ook alle mensen van het L-PROBE team bedanken voor hun onschatbare praktische hulp, raad en luchtige onderbrekingen gedurende de voorbije jaren. In het bijzonder dank ik nog Jimmy, Paco, Maarten, Bart, Bert, Kenneth, Jan en Bjorn voor twee plezierige (en succesvolle!) seizoenen in het mini-voetbal.

Ook wil ik mijn ouders, broer en zus bedanken voor hun steun en geleverde inspanningen gedurende mijn ganse studieloopbaan. Tot slot dank ik mijn prachtige echtgenote Sara voor de geweldige steun en liefde, zowel tijdens de mooie als de moeilijke momenten van mijn doctoraatsonderzoek.

Gent, 14 mei 2008.